This is to certify that the

dissertation entitled
Evaluation of Ordinary Cokriging and Artificial
Neural Networks for Optimizing Rainfall Estimate
Using Stage III NEXRAD Precipitation Surfaces
and Rain Gage Measurements

presented by

Chia-Yii Yu

has been accepted towards fulfillment
of the requirements for

_____Ph. D._____ degree in __Biosystems Engineering__

William J. Northcott
Major professor

Date_ 1/16/03 _

0-12771

PLACE IN RETURN BOX to remove this checkout from your record.
TO AVOID FINES return on or before date due.
MAY BE RECALLED with earlier due date if requested.

DATE DUE	DATE DUE	DATE DUE

6/01 c:/CIRC/DateDue.p65-p.15

EVALUATION OF ORDINARY COKRIGING AND ARTIFICIAL NEURAL
NETWORKS FOR OPTIMIZING RAINFALL ESTIMATE USING STAGE III
NEXRAD PRECIPITATION SURFACES AND RAIN GAGE
MEASUREMENTS

By

Chia-Yii Yu

A DISSERTATION

Submitted to
Michigan State University
in partial fulfillment of the requirements
for the degree of

DOCTOR OF PHILOSOPHY

Department of Agricultural Engineering

2003

ABSTRACT

EVALUATION OF ORDINARY COKRIGING AND ARTIFICIAL NEURAL NETWORKS FOR IMPROVING STAGE III NEXRAD PRECIPITATION SURFACES USING RAIN GAGE MEASUREMENTS

By

Chia-Yii Yu

The deployment of the National Weather Service Weather Surveillance Radar-1988 Doppler (WSR-88D) has provided an improved tool for monitoring real-time areal mean precipitation spatial distribution (4-km resolution) for hydrometeorological modeling. Unfortunately, a number of factors introduce discrepancies between radar precipitation estimates and actual precipitation at the Earth's surface. In this project, a pilot study was performed by making two types of statistical analyses to describe the correlation between SEMCOG rain gage values and stage III NEXRAD: (1) the agreement of occurrence of precipitation between the two sources and the magnitude of error in precipitation when there is disagreement of occurrence, and (2) the error in magnitude between rain gage measurement and NEXRAD estimate when they both register a precipitation amount. These analyses provided a basis of justification for using models to improve the correlation between the two sources of precipitation measurements. Twenty-two daily precipitation events (partial and full rainfall coverage) during the months of May through September in 1999 and 2000 were selected to estimate the precipitation using Stage III NEXRAD data and SEMCOG rain gage measurements. Artificial neural network and ordinary cokriging models were evaluated by the performances of improved precipitation estimates. The best performing model, the ANN model, significantly improved the accuracy of the radar-derived precipitation surfaces

(Average correlation coefficient was improved from 0.61 to 0.76).

The ANN model was applied to improve the precipitation estimate of the entire state of Michigan. The 16-km NEXRAD grid size was used for improving the Stage III NEXRAD data for the entire state of Michigan. Six daily precipitation events (partial and full rainfall coverage) were selected to optimally estimate the precipitation by combining Stage III NEXRAD data with forty-two National Weather Service Fisher & Porter rain gages distributed around the Michigan. The results showed that the Stage III NEXRAD precipitation surfaces were fairly improved (Average correlation coefficient was improved from 0.72 to 0.87).

ACKNOWLEDGEMENTS

I like to express my sincere gratitude to my major professor, Dr. William J. Northcott for his never-ending support and guidance of this study.

My sincere thanks to my committee members, Dr. J. Andresen, Dr. J. Bartholic, Dr. F. Nurnberger, and B. Pijanowski for their insight, guidance, and support in this study.

I would like thank the faculty and staff of the Department of Agricultural Engineering for providing a challenging learning environment. Special thanks to Departmental Chairman, Dr. Ajit K. Srivastava, for his support and encouragement.

Finally, a very special thank you to my parents, parents-in-law, and wife Tsui-Ting Yang, for their never-ending love, support, encouragement, and guidance.

TABLE OF CONTENTS

LIST OF TABLES

LIST OF FIGURES

precipitation event occurred on 07/01/1999). Heavy Precipitation Event-- 115

Chapter 1 INTRODUCTION

Being able to accurately estimate the distribution of rainfall over a region is an important aspect of water resources management. Accurate estimation of rainfall over large areas allows for prudent management decisions in numerous areas such as agricultural production and irrigation timing, flood forecasting, hydrologic and water quality modeling, and groundwater recharge. Historically, accurate spatial rainfall estimation attempts have used dense networks of rain gages, incorporating spatial interpolation using such methods as Theissen Polygons and Inverse Distance Weighting (IDW) to estimate rainfall amounts between point gage locations (ASCE, 1996). Currently, the National Weather Service (NWS) operates over 8,000 daily non-recording rain gages, but with spatial distances between gages of greater than 100km, it is possible that these networks do not capture the spatial variability of rainfall events (Groisman and Legates, 1994). More recently, Next Generation Radar (NEXRAD), a weather radar system with nationwide coverage, has become a promising new tool for high spatial and temporal resolution estimation of rainfall.

Weather radar works on the premise that reflected emitted radar energy that is reflected by precipitation can be converted to precipitation rate by means of an empirical relationship (NOAA, 1991). The NEXRAD system consists of 161 individual radar stations within the United States and provides overlapping coverage of radar reflectivity. Since its deployment in 1995, NEXRAD has become a useful tool for tracking severe weather patterns in real time. Raw Stage I NEXRAD data allows 5-6 minute sweeps of an area with a radius of 230 km and can provide very high-resolution (~1km) estimates of rainfall intensity. With its Stage III data, NEXRAD offers hourly estimation of rainfall

over large areas with a 4 km resolution. While the NEXRAD system provides real-time, high-resolution relative rainfall intensity; the system is not without its faults. It has been shown that, in general, NEXRAD underestimates rainfall amounts when compared to ground gage data. There are several explanations for these underestimations and discrepancies that include rainfall missed between radar sweeps, systematic and random errors, and inaccuracy in the empirical methods to convert from radar reflectivity to rainfall. These errors and discrepancies can lead to as much as 100% differences between radar rainfall estimation and ground gage values (Matsoukas et al., 1999).

Because there is promise in developing NEXRAD as a tool for real-time spatial rainfall estimate, there have been several research attempts to develop a method for "correcting" the NEXRAD products to provide a more accurate rainfall surface. Much of this research has focused on adjusting the NEXRAD rainfall surface in smaller, local areas based on actual values from ground-based rain gage networks (Eddy, 1979; Brandes, 1975). A number of techniques have been used to adjust the NEXRAD surface. These techniques have incorporated simple methods such as linear adjustment based on Thiessen Polygons (Johnson et al., 1999), to more complex methods such as geostatistical methods that incorporate kriging (Seo et al., 1990a and 1990b; Seo et al., 1996) and ordinary cokriging (Seo et al., 1990a and 1990b; Krajewski, 1987), and more recently, artificial neural networks (ANNs) (Matsoukas et al., 1999). These have provided with varying degrees of success. This method holds promise for becoming a powerful tool in a wide range of hydrologic applications, especially in the area of quantifying regional water balances. The overall goal of this study is to improve the accuracy of NEXRAD rainfall surfaces across the state of Michigan using ground gages and computer modeling

techniques. Specifically, the objectives are to:

1. Perform a statistical analysis on hourly Stage III NEXRAD data and hourly rain gage data from rain gages in the Southeast Michigan Council of Government (SEMCOG) rain gage network.

2. Perform a pilot study using ordinary cokriging (OC) and artificial neural network (ANN) models to calibrate and validate daily NEXRAD Stage III rainfall surface in the SEMCOG rain gage network.

3. Apply an ANN-based model to adjust Stage III NEXRAD data across the State of Michigan using National Weather Service gages and evaluate its performance.

Chapter 2 LITERATURE REVIEW

2.1. Rain Gage Measurement and Spatial Estimation

Rain gage measurement dates back at least to the 4th century B.C., when a network of rain gages was established in India (Biswas, 1967). Rain gages were used in Palestine in the 1st century B.C., in China in the 13th century A.D., and in Korea in the 15th century A.D. (Biswas, 1970). The Chinese and Korean gages were cylindrical or barrel-shaped and had approximately the same characteristics and accuracy of many of the rain gages in widespread use today. Rain gages were first used in Europe in the 17th century. The 18th century was marked by the development and use of numerous designs of gages around the world. The measurement of the "exact quantity" of rainfall that falls upon a horizontal surface has been the subject of a large number of investigations in the past two hundred years. For years, rain gages have become more and more technologically advanced and are currently characterized by automated features and high temporal resolution (ASCE, 1996). However, gages producing real-time ground point measurements are not sufficiently dense to represent a larger area.

The United States meteorological network consists of about 8,000 daily rainfall non-recording stations (Groisman and Legates, 1994). Distances between rain gage stations often exceed 100km providing inadequate spatial rainfall sampling, i.e. the variance of the sample long-term mean area rainfall and mean area rainfall of a storm event becomes large (Rodriguez-Iturbe and Mejia, 1974). Therefore, the variance, a function of correlation in time, space, length of operation of the network, and the geometry of the gauging array, is an important index for the framework design of the rain gage network. In addition, rain gage measurement errors produced by wind/turbulent

losses, gage wetting, splash into and out of the gage, condensation, evaporation, and measurement correction compound the estimation problem (ASCE, 1996; Groisman and Legates, 1994). However, compared to the errors of the radar-derived rainfall surface, the errors of the rain gage measurement are small and thus rain gage measurements can be regarded as the true rainfall values.

Because of the drawbacks of point measurements in rain gage networks, many methods have been used to interpolate or extrapolate point rainfall values. These methods include the use of Thiessen polygons (Croley and Hartmann, 1985; Shih and Hamrick, 1975; Diskin, 1969), isohyetal (France, 1985; Hamlin, 1983; Linsley et al., 1949), linear and multi regression (Salas, 1993), polynomial interpolation (Tabios and Salas, 1985; Chidley and Keys, 1975; Unwin, 1969), objective analysis, and kriging methods (Seo et al., 1990, Yates and Warrick, 1986a and 1986b; Yates, 1986; Dingman et al., 1988; Tabios and Salas, 1985; Creutin and Obled, 1982; Chua and Bras, 1982; Montmollin et al., 1980). More recently, volumetric estimation of rainfall using radar technology has shown promise for real-time estimation of rainfall with high spatial resolution.

2.2. NEXRAD Measurement and Rainfall Estimation

Weather radar has been used for measuring rainfall values since the 1950's. In the 1980s, the U.S. National Weather Service (NWS) began installing the Weather Surveillance Radar-1988 Doppler (WSR-88D), Next Generation Weather Radar (NEXRAD) and finished the deployment of the NEXRAD stations in 1995. 161 NEXRAD stations are distributed throughout the U.S. and selected overseas locations to form a meteorological network for rainfall measurements (Figure 2.1). The NEXRAD network is a joint effort of the U.S. Departments of Commerce (DOC), Defense (DOD),
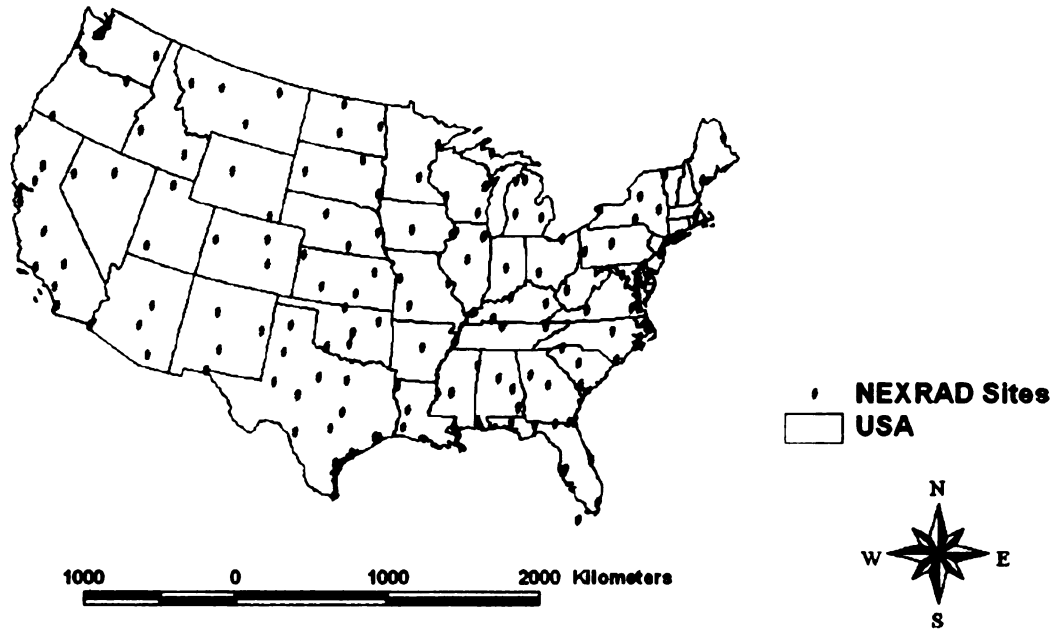
Figure 2.1. NEXRAD radar sites distributed in the United States.

and Transportation (DOT). The controlling agencies are the National Weather Service (NWS), Air Weather Service (AWS) and Federal Aviation Administration (FAA), respectively (The NEXRAD Joint System Program Office, 1986a).

The primary advantage of radar as a rainfall measurement system is that it can estimate rainfall at high spatial (in NEXRAD volumetric-averaged measurement up to 230 km from the radar site) and temporal (real-time) resolution (ASCE, 1996). The rainfall locations, boundaries, and intensities shown as the radar echoes, and their changes with time, may be accurately determined either visually or digitally. Unfortunately, a number of errors, such as systematic and random errors of the radar and Z-R relationship conversion error, may introduce over 100% discrepancies between NEXRAD rainfall estimate and actual rainfall at the Earth's surface (Matsoukas et al., 1999; Smith et al., 1996). Although the NEXRAD network provides detailed rainfall information that is readily available to the user, these data are not being used to the fullest extent. Confusion and misunderstanding about the ability of the NEXRAD to measure rainfall and about the factors that contribute to errors lead to this underutilization of the data.

Since 1970's, there has been an increasing amount of research relating to the topic of radar and rain gage data validations and comparisons. The methods used in these studies include: objective analysis (Eddy, 1979; Brandes, 1975), kriging (Krajewski, 1987; Seo et al., 1990a and 1990b; Seo, 1998a and 1998b; Matsoukas et al., 1999), and artificial neural networks (ANNs), (Matsoukas et al., 1999).

Eddy (1979) used an objective analysis model to make maximum likelihood estimates of convective storm-total rainfalls in Montana by using the High Plains

Cooperative Program (HIPLEX) radar reflectivity data combined with the optimal deployment of the rain gage network. Brandes (1975) used an objective analysis scheme to calibrate the radar rainfall surface based on rain gage observations by determining multiplicative calibration factors at each rain gage site. Rainfall estimates are improved when rain gage observations are used to calibrate quantitative radar, as well as, to estimate rainfall in areas without radar data. Estimated areal rainfall depth errors for nine rainfalls over a 3,000 km^2 watershed averaged 13% and 14% (1.5 and 1.8mm) when the radar was calibrated by rain gage networks having densities of one gage per 900 and 1,600 km^2, respectively Areal precipitation estimates derived from rainfalls observed at the gages alone produced errors of 21% and 24% (2.5 and 3.0mm). Adjusting the radar data by a single calibration factor resulted in an error reduction of 18%. Radar data added to gage observations also increased the variance in point rainfall estimates above that from gages alone, from 53% to 77% and 46% to 72% for the above gage densities. However, the objective analysis methods failed to account for the spatial autocorrelation between rain gages and radar directly.

Krajewski (1987) developed an ordinary cokriging procedure to optimally combine 245 daily rain gage observations with radar data. The covariance matrices required to perform ordinary cokriging are computed from single realization data, using the ergodicity assumption. Because the ground truth and the errors of the radar data are unknown, parameterization of the covariance between radar and the true rainfall is required. This procedure removes the bias in radar very well. Seo et al. (1990a and 1990b) evaluated the performances of ordinary, universal, and disjunctive cokriging by combining rain gage measurements and radar rainfall data. Two simulation experiments

were used to evaluate these three models. The first experiment assumed that high quality radar rainfall surfaces to be ground truth rainfall fields and the second experiment used a stochastic, space-time rainfall model to generate the assumed ground truth rainfall surfaces of various characteristics.

Matsoukas et al. (1999) developed an ANN approach that combined radar-measured a rainfall surface with rain gage measurements and evaluated the performance of the ANN method by validation and comparison to ordinary cokriging method. Four hourly storm events (two events from the summer and two events from the winter seasons) from Tulsa, Oklahoma were examined. Forty-three rain gage measurements and 4km resolution radar data were used. Three types of sample-splitting (80%-20%, 50%-50%, and 20%-80%) were used for training the neural network model and to determine the semivariograms in ordinary cokriging model, and validations of both models. The comparison of rainfall estimation using ordinary cokriging and ANN models suggests that the performance of the ANN model provides better rainfall estimations than that of the ordinary cokriging model for Oklahoma.

Because of the great variability in the intensity and structure of rainfall events, more radar-gage validations and comparisons should be made in order to cover a larger number of storms for different geographical locations. It is important to have an understanding of the physical factors impacting the NEXRAD rainfall estimate accuracy to make the best possible estimate of surface rainfall from the NEXRAD and rain gage data available for a particular event.

2.3. NEXRAD System and Data

2.3.1. NEXRAD System

The NEXRAD system consists of three functional components: Radar Data Acquisition (RDA), the Radar Product Generator (RPG), and the Principal User Processor (PUP) (Federal Coordinator for Meteorological Services and Supporting Research, 1990; The NEXRAD Joint System Program Office, 1984). To adequately sample the rainfall the RDA uses four types of Volume Coverage Patterns (VCPs): VCP 11, VCP 21, VCP 31, and VCP 32 (The NEXRAD Joint System Program Office, 1990; The NEXRAD Joint System Program Office, 1985; The NEXRAD Joint System Program Office, 1984). The VCP is the series of 360-degree sweeps of the antenna at selected elevation angles completed in a specified period of time with various microwave wavelengths. The RDA emits a beam of energy, a microwave signal, at an object and measures the reflected energy. When the energy strikes an object, the energy is scattered in all directions. A small fraction of that scattered energy is directed back toward the NEXRAD. This reflected energy is received by the RDA during its signal-receiving period and contains: reflectivity of the returned pulse, radial velocity, and spectrum width of the reflected signal.

The function of the RPG is to use computer algorithms to convert the reflectivity of the returned pulse from the RDA into various meteorological and hydrological data. The computer algorithms of the RPG convert the reflectivity, (Z, unit: dBZ), into rainfall rate, (R, unit: mm/hr) by a Z-R relationship formula, $Z = aR^b$, where a and b are coefficients. The NEXRAD products are stored on a Write Once Read Many (WORM) optical disk that is sent to the National Climatic Data Center for archive and

10

dissemination. The main function of the PUP is to display the NEXRAD products, such as reflectivity, mean radial velocity, echo-top height, and precipitation accumulation amounts, generated at the RPG by the advanced microcomputers and peripheral systems.

2.3.2. Z-R Relationship and Accuracy of Rainfall Estimations

The Z-R relationship linking rainfall rate to radar reflectivity is complex, nonlinear, and inexact. Rainfall rates are proportional to the volume of the raindrops, but also to raindrop surface area. Therefore, a raindrop size distribution must be converted from reflectivity to rainfall rate, i.e. the reflectivity is a function of the numbers and sizes of the raindrops, snow, ice, and hail; reflectivity is converted into a rainfall rate by the Z-R relationship using the formula: $Z = aR^b$, where a and b are coefficients.

A significant problem is that the Z-R relationship values vary as a function of storm types because of the differences in raindrop size distributions (Joss and Lee, 1995). For convective type storms, $Z = 300R^{1.4}$ works very well for deep convective storms but severely underestimates other types of storms. $Z = 250R^{1.2}$ is used for hurricanes, tropical storms, and small scale deep-saturated storms. $Z = 200R^{1.6}$ is used for the stratiform type of storms; for winter stratiform type of storm at sites east, $Z = 130R^{2.0}$, and sites west, $Z = 75R^{2.0}$ of the continental divide. In addition, there are additional factors complicating the Z-R relationship including: beam attenuation, range effects, temperature and vapor gradients, hail and vertical air motions, accretion and evaporation (Wilson and Brandes, 1979; Lhermitte and Gilet, 1975).

2.3.3. NEXRAD Products

The NWS has developed a set of post processing algorithms for NEXRAD rainfall estimates that are referred to as Stage I, II, and III rainfall estimates. The Stage I

11

rainfall estimate transforms the raw reflectivity data from the RDA into the rainfall rate by a reflectivity and rainfall rate relationship, i.e. a Z-R relationship. The Stage II rainfall estimate is processed by utilizing "ground truth" rain gage measurement to remove a mean field bias in the radar rainfall estimates. Since 1992, the NWS River Forecast Centers (RFCs) have been using a prototype Stage II algorithm to combine NEXRAD hourly Stage I rainfall estimates with the adjustment of the local rain gage observations. The main purpose of using Stage II products is to provide an optimal estimate of the rainfall that has fallen during a given clock hour using a combination of radar and hourly rain gage observations. The procedure is carried out on the HRAP grid which is a polar stereographic map projection with approximately 4-km resolution.

The Stage III algorithm currently used at the RFCs takes the Stage II multi-sensor rainfall estimates from multiple NEXRAD stations and mosaics them together to provide hourly rainfall estimates covering the entire RFC area of responsibility. The Stage III rainfall estimate is created specifically for the NWS RFCs which need rainfall estimates over a much larger area than covered by an individual radar station. Therefore, the Stage III algorithm mosaics together Stage II rainfall estimates from multiple NEXRAD onto a subset of the NWS Hydrologic Rainfall Analysis Project (HRAP) grid covering the RFC area of responsibility. In areas where data from two or more NEXRAD sites overlap, the mean or maximum value is used.

The NEXRAD WSR-88D rainfall algorithm generates a one-hour rainfall product that has been remapped from a local, radar-centered, polar grid into the national, quasi-rectangular HRAP grid of nominal grid size of 4 km x 4 km. The polar-to-HRAP coordinate transformation is performed within the NEXRAD WSR-88D algorithm. The

latitude-longitude grid cell locations based on the NEXRAD polar-to-HRAP transformation equations is compared with the corresponding locations determined by the equations used in the River Forecast System and Stage III Precipitation Processing operational software applications that use these HRAP rainfall products for follow-on hydrologic processing within the NWS. An error assessment is performed. These locations are also compared with those computed within the GENHRAP program. This information will serve as guidance for NWS users as well as users from other commercial or governmental organizations who wish to use high resolution NEXRAD WSR-88D HRAP rainfall estimates within GIS-based distributed hydrologic models or other applications.

The NEXRAD WSR-88D HRAP rainfall product contains mean areal rainfall over the HRAP grid box where a grid box is defined as the area enclosed by four contiguous HRAP grid points *(I, J)* where *I, J* are integers. Thus the HRAP rainfall estimates are actually centered at HRAP grid points *(I + 0.5, J + 0.5)*. All rainfall estimates on the polar grid whose cell centers lie within the boundary of an HRAP grid box are averaged to become the rainfall estimates for that HRAP box regardless of how much of the polar grid box may lay outside of the given HRAP grid box. This is a simple and efficient method of remapping the polar data into the quasi-rectangular HRAP grid within the operational rainfall algorithm.

NEXRAD reflectivity data spatial resolution at each radar site is initially 1 degree by 1-km with time steps of five, six, or ten minutes depending upon weather conditions and the applied VCP type. When rain is detected within an individual radar coverage area, radar scan intervals are five or six minutes. To compute rainfall estimates, the NWS re-

maps the original 1 degree by 1-km polar coordinate data through a series of intermediate resolutions to the HRAP grid, with an approximate resolution of 4-km in hourly time steps. This resolution is intended to meet the needs of the NWS river forecast mission, which primarily services large river systems where hourly 4-km resolution is appropriate.

2.4. Ordinary Cokriging

Kriging provides the best linear unbiased estimator (BLUE) of characteristic studies about unknown variates. Ordinary cokriging is an interpolation technique that allows one to use a more intensely sampled covariate in the estimation of values for a related variate. If the primary variate is difficult or expensive to measure and it is correlated with a more available covariate, ordinary cokriging can greatly improve interpolation estimates. (Matsoukas et al., 1999; Seo et al., 1990a and 1990b; Krajewski, 1987). Ordinary cokriging characterizes simultaneous regionalized K variables $\{z_k(x), \ k = 1 \ to \ K\}$ by a set of K spatial inter-correlated random function $\{Z_k(x), \ k = 1 \ to \ K\}$ (Deutsch and Journel, 1998; Goovaerts, 1997; Isaaks and Srivastava, 1989; Journal and Huijbregts, 1979). Ordinary cokriging assumes second-order stationarity of these random functions: (1) for each random function $Z_k(x)$, the mathematical expectation is: $E\{Z_k(x)\} = m_k = $ constant, $\forall x$, (2) for each pair of random function $Z_k(x)$ and $Z_{k'}(x)$, the cross covariance is: $E\{Z_{k'}(x+h) \cdot Z_k(x)\} - m_{k'} \cdot m_k = C_{k'k}(h)$, $\forall x$, and (3) for the cross variogram:

$$E\{[Z_{k'}(x+h) - Z_{k'}(x)][Z_k(x+h) - Z_k(x)]\} = 2\gamma_{k'k}(h), \quad \forall x.$$

2.4.1. Random Function Model and Second-Order Stationarity

The concept of the random function model is very important to ordinary cokriging. The random function model joins together two different aspects: regionalization and

randomness (Wackernagel, 1998). The regionalization aspect is that the spatial data values stem from a physical environment (time; and 1, 2, and 3D space) and are in some way dependent on their location in the region. The randomness aspect is that the regionalized sample values are continuous over an entire surface but they cannot be modeled with a simple deterministic function because of the spatial variations. Therefore, the probabilistic approach is used to regard these data values as outcomes of the random mechanism.

Stationarity is a property of the random function model meaning that characteristics of a random function stay the same when shifting a given set of n points, $\{x_1, x_2, ..., x_n\}$, from one part of the region to another (Deutsch and Journel, 1998; Wackernagel, 1998). Stationarity expresses the property of a random function that certain joint distributions or that certain moments of the random function are translation invariant. Therefore, second-order stationary assumes the stationarity of the first two moments of the variable considering only pairs of points $\{x_1, x_2\}$ in the domain and tries to characterize only the first two moments, not a full distribution.

2.4.2. Semivariogram Cloud, Semivariogram, and Cross Semivariogram

Pairs of sample values are evaluated by computing the squared difference between the values (Deutsch and Journel, 1998; Wackernagel, 1998). The resulting dissimilarities are plotted against the separation of sample pairs in geographical space and form the semivariogram cloud:

$$\gamma^*(h) = \frac{1}{2}[z(x_\alpha) - z(x_\alpha + h)]^2$$

2.1

where $\gamma^\bullet(h)$ is the dissimilarity depending on the spacing and on the orientation of the point pair described by the absolute values of the spatial separation vector, h.

The semivariogram cloud is classified according to separation in space and the average dissimilarities in each class form the sequence of values of the experimental semivariogram. The plot of the semivariogram cloud depicts the individual point-pair contributions to the final semivariogram. When comparing with the simple semivariogram it allows a subjective impression of whether the apparent pattern of spatial variation is related to systematic trends in the data (spatial dependence) or to unusual points (spatial outliers) (Bailey and Gatrell, 1995).

The empirical semivariogram depicts the semivariance among sets of pairs of points, summarized by increasing distances among points (Deutsch and Journel, 1998; Wackernagel, 1998). The directional empirical semivariogram constructs individual semivariograms arranged by estimate of anisotropy and isotropy. Anisotropy is processed when spatial dependence is a function of distance and direction; and isotropy is processed when spatial dependence is a function of distance only (direction does not matter) (Bailey and Gatrell, 1995). Two experimental measures of spatial variability or continuity are used for semivariogram model fitting in ordinary cokriging. One is the semivariogram and the other one is cross semivariogram.

The semivariogram is a measure of dissimilarity. The semivariogram is a plot of semivariance against spatial separation vector, h. It can be used to find the rate at which a regionalized variable changes along a specific direction. It is defined as half of the average squared difference between two attribute values approximately by vector h:

$$\gamma(h) = \frac{1}{2N(h)} \sum_{i=1}^{N(h)} [z(x_i) - z(x_i + h)]^2 \qquad\qquad 2.2$$

where $N(h)$ is the number of pairs, $z(x_i)$ is the value at the start of the pair i, $z(x_i + h)$ is the corresponding end value, and h is the separation vector specified with some direction and distance *(lag)* tolerance (Deutsch and Journel, 1998).

The cross semivariogram measures cross variability for the possibility of mutual correlation estimation of several interconnected data. It is defined as half of the average product of h-increments relative to two different attributes:

$$\gamma_{zy}(h) = \frac{1}{2N(h)} \sum_{i=1}^{N(h)} [w(x_i) - w(x_i + h)][y(x_i) - y(x_i + h)] \qquad\qquad 2.3$$

where $w(x_i)$ is the value of attribute w at start of the pair i and $w(x_i + h)$ is corresponding end value; the locations of the two values $w(x_i)$ and $w(x_i + h)$ are separated by vector h with specified directions and distance tolerance. $[y(x_i) - y(x_i + h)]$ is the corresponding h-increment of the other attribute y (Deutsch and Journel, 1998; Wackernagel, 1998; Goovaerts, 1997).

The constructions of the semivariogram and cross semivariogram become more complex when more reality is introduced. For example, in the simplest model the regionalized variable is assumed to be stationary. A stationary variable has the same mean everywhere although not all locations within a region have the same value. However, many regionalized variables are not stationary and exhibit drift such that the

mean varies with location. Another problem is that the semivariogram and cross semivariogram assume that data points are evenly spaced. If this is not the case, then the semivariogram must be modeled.

2.4.3. Model Fitting of Semivariogram Using Weighted-Least-Squares Method

The objective of semivariogram model fitting is to identify a semivariance value for the behavior of the attribute at different distances (lags) (Bailey and Gatrell, 1995). In this study, five co-regionalized models (nugget effect, exponential, Gaussian, spherical, and linear models) are used to fit the semivariogram or cross semivariogram. The best-fitting model, representing the spatial dependence of the phenomenon, would be used as input for the ordinary cokriging model. These five co-regionalized models are shown as follows:

1. Nugget effect model: $\gamma(h) = \begin{cases} 0, & \text{if} \quad h = 0 \\ 1, & \text{otherwise} \end{cases}$ 2.4

2. Exponential model defined by an effective range a and positive variance contribution or sill value c. $\gamma(h) = c \cdot Exp(\frac{h}{a}) = c \cdot \left[1 - \exp(-\frac{3h}{a}) \right]$ 2.5

3. Gaussian model defined by an effective range a and positive variance contribution or sill value c. $\gamma(h) = c \cdot \left[1 - \exp(-\frac{(3h)^2}{a^2}) \right]$ 2.6

4. Spherical model defined by an actual range a and positive variance contribution or

$$\text{sill value c. } \gamma(h) = c \cdot Sph(\frac{h}{a}) = \begin{cases} c \cdot \left[1.5\frac{h}{a} - 0.5(\frac{h}{a})^3\right], & \text{if} & 0 \le h \le a \\ c, & \text{if} & h \ge a \end{cases} \qquad 2.7$$

5. Linear model defined by w the slope at the origin. $\gamma(h) = w \cdot h$ 2.8

The nugget effect model is an apparent discontinuity at the origin of the semivariogram model, i.e., a nugget constant can be interpreted as a transition structure reaching its sill value at a very small range compared with the available distances of observation (Goovaerts, 1997; Bailey and Gatrell, 1995; Journel, 1978). The sill is the maximum level of semivariance reached by a transitive semivariogram. The range is the distance at which the maximum semivariance is attained by a transitive semivariogram.

Exponential, Gaussian, and spherical models can be classified as models with a sill and range (Journel, 1978). Exponential and spherical models present a linear behavior at the origin; Gaussian model present a parabolic behavior at the origin. Linear model can be classified as a model without a sill. For the nugget effect model, the sill is reached as soon as $h > 0$. The spherical model reaches its sill at distance a (actual range) (Goovaerts, 1997). The exponential and Gaussian models reach their sill asymptotically. A practical range a is defined as the distance at which the model value is at 95% of the sill.

The weighted-least-squares method is used to iteratively fit a linear co-regionalization model to obtain the best set of range and sill numbers for the ordinary cokriging model (Goovaerts, 1997). It starts to modify one arbitrary co-regionalized matrix at a time iteratively so as to minimize the criterion under the constraint of positive

19

semi-definiteness   of   that   matrix.   The   criterion   is

$$WSS = \sum_{k=1}^{k} \sum_{i=1}^{N_v} \sum_{j=1}^{N_v} w(h_k) \cdot \frac{[\hat{\gamma}_{ij}(h_k) - \gamma_{ij}(h_k)]^2}{\hat{\sigma}_i \cdot \hat{\sigma}_j}, \text{ where } w(h_k) \text{ is the weight of the } k\text{-}th \text{ lag}$$

and is chosen by: (1) proportional to the number $N(h_k)$ of pairs used in the estimate and (2)

proportional to the quantity $\dfrac{N(h_k)}{[\gamma_{ij}(h_k)]^2}$ to gain more weight for the first lag.

In this study, the ordinary cokriging model (Marcotte, 1991) is integrated with the weighted-least-squares method (Goovaerts, 1997) to calibrate NEXRAD rainfall surface based on rain-gage network measurements.

2.5. Artificial Neural Networks (ANNs)

ANNs are computer-based systems that are designed to emulate some of the learning and pattern recognition abilities of the human brain. The human brain is made up of billions of cells called neurons (Haykin, 1999; Bose and Liang, 1996). A general biological neuron is composed of four components: (1) a dendrite for receiving a signal, (2) a cell body or nucleus for synthesizing signals using nonlinear threshold effect, (3) an axon for transmitting signals, and (4) a synapse for transmitting weighted signals to other neurons. These neurons are all linked to each other and establish an intelligent system network (parallel complex network or information processor). This biological neural network performs various human brain abilities such as learning, analysis, prediction, or recognition.

ANNs are known as a "data-driven" modeling approach (Chakraborty et al., 1992). ANNs are well suited to solve complex problems where the relationships between the variables to be modeled are not well understood (Maren et al., 1990). ANNs use

parallel processing to learn an approximation to the underlying rules governing the relationship between inputs and output variables. However, the internal structure or topology of the best possible ANN model is generally unknown and must be developed by a trial and error process (see Figure 2.2).

ANNs can be applied in a broad range of fields, including image processing, signal processing, medical studies, financial predictions, power systems, and pattern recognition among others. Because ANN models have the ability to recursively learn from the data, they are particularly useful for applications involving complicated, nonlinear processes that are not easily modeled by traditional means. These successes have also inspired applications to water resources and environmental systems.

Shamseldin et al., (1997) merged the estimated output from various rainfall-runoff models to produce an overall combined estimated output to be used as an alternative to that obtained from a single individual rainfall-runoff model. The estimated discharges of five rainfall-runoff models for eleven catchments were used to test the performance of the three combination methods: the simple average, the weighted averaged, and the neural network methods. The results confirmed that the combined model outputs of various models performed the best discharge estimates.

Bruton et al., (2000) used a three-layer, back-propagation neural network to predict daily pan evaporation for missing data or remote areas based on easily measurable weather variables. In this study, they trained the model using 11 weather variables from three sites in Georgia collected from 1992 ~ 1996. They performed several modeling scenarios with different combinations of weather variables as inputs into the network. They found that the model performed best ($R^2 = 0.717$) with all available weather data.
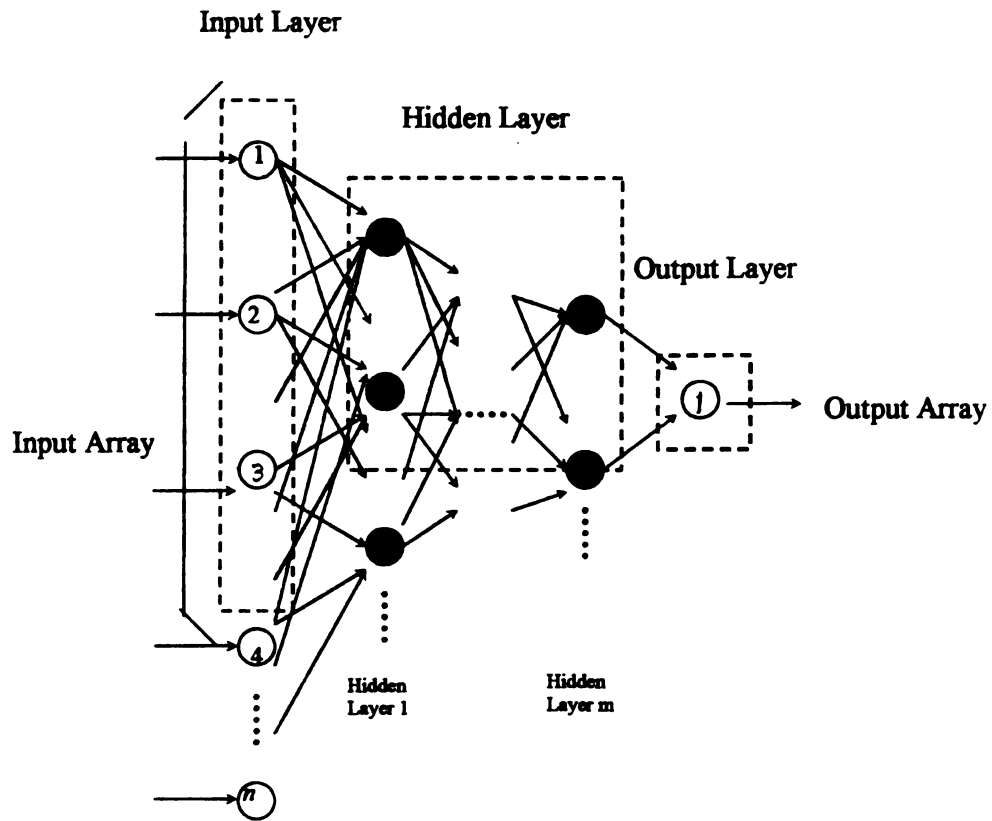
Figure 2.2. Typical Structure of A Multi-Layer Feedforward Neural Network.

Yang et al., (1996) utilized an artificial neural network to aid in land drainage engineering. They used 26 years of DRAINMOD-simulated mid-span water table depths to train a one-layer ANN. After training, they found that the ANN could simulate water table depths faster and with less input data than DRAINMOD.

Maier and Dandy (1996) trained a neural network with four years of river levels, flow rates, and salinity for the River Murray in South Australia. They used the model to provide a 14-day forecast of river salinity. Their model provided an average annual percent error in river salinity of 6.5%.

Chapter 3 STUDY AREA

3.1. SEMCOG Rain Gage Network

The SEMCOG (South Eastern Michigan Council of Governments) rain gage network is located in southeast Michigan. The SEMCOG area contains 7 counties: Livingston, Macomb, Monroe, Oakland, St. Clair, Washtenaw and Wayne Counties. The rain gage network is restricted to just 5 counties. A 108 universal weighing rain gage network used for this study is only distributed across 5 counties of the SEMCOG area, which are Livingston, Macomb, Oakland, Washtenaw, and Wayne Counties, covering an area of about 1,514 km^2 (see Figures 3.1 and 3.2). Only 66 ~ 68 rain gages are active during the study time periods, from the months of May to September from the year 1999 to 2000.

The distribution of the rain gage network was set up to reflect the population density within the five-county area. The highest density of the rain gages is in the city of Detroit, while for the least dense, the maximum spacing between the rain gages is 40km. Therefore, the rainfall patterns in the SEMCOG rain gage network are over a primarily urban setting.

The area of the SEMCOG rain gage network is covered by the overlap of four NEXRAD sites, located at Detroit-Pontiac and Grand Rapids, MI, North Webster, IN, and Cleveland, Ohio. The maximum scan range of each NEXRAD is 230km. The NEXRAD Stage III data are developed from the mean or maximum values of these four NEXRAD stations. Because of the spatial and temporal overlap of the rainfall measurements by the rain gage and NEXRAD networks, merging these two types of measurements (i.e. the high spatial resolution of NEXRAD with the measurement
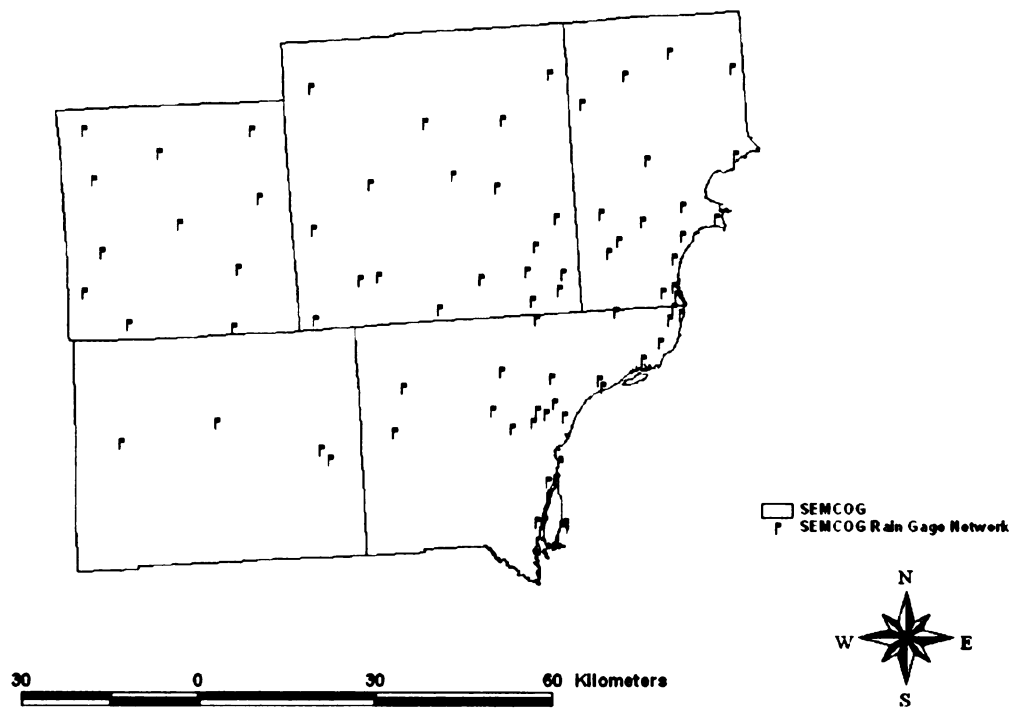
Figure 3.1. SEMCOG Rain Gage Network.
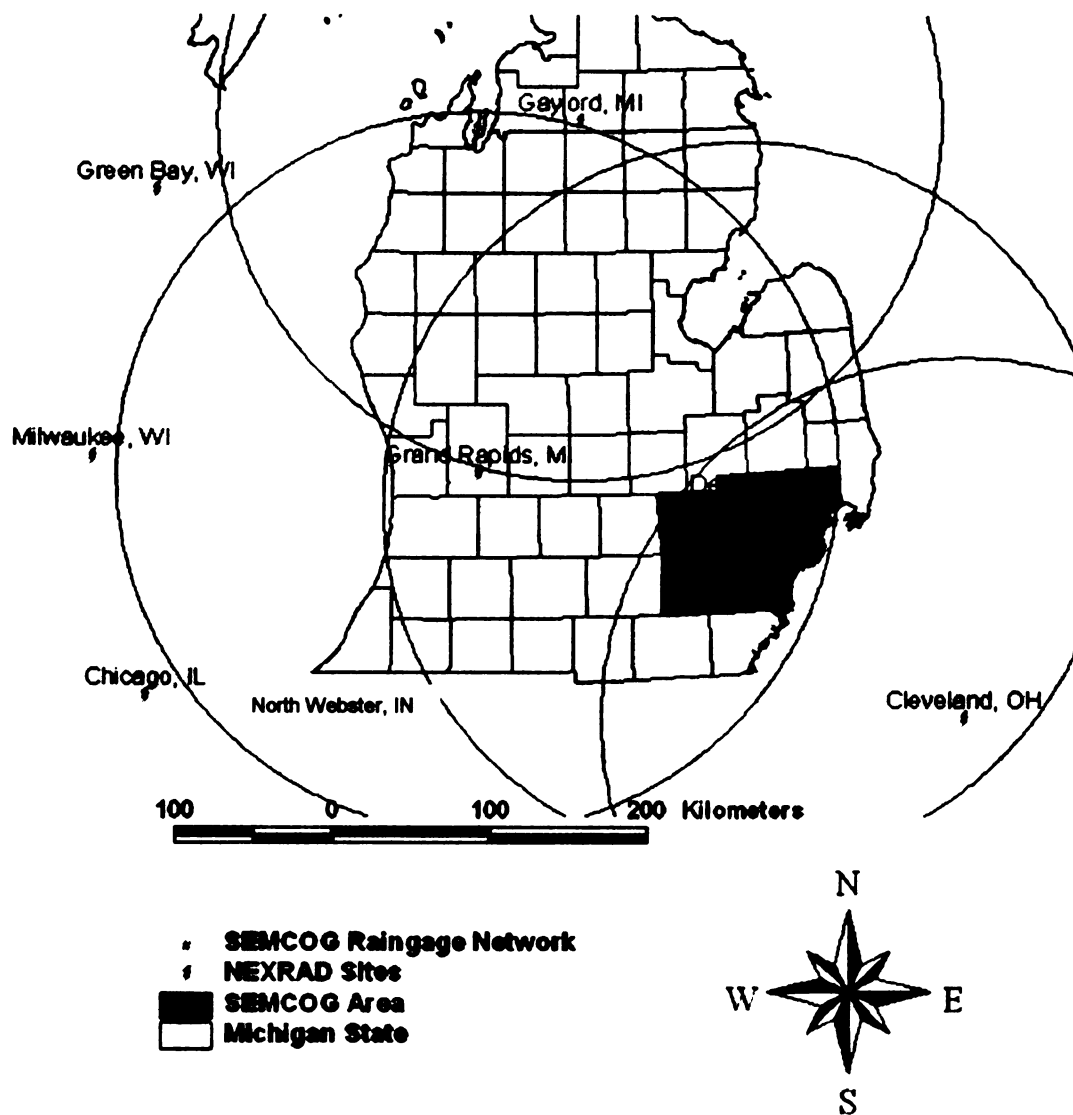
Figure 3.2. SEMCOG Rain Gage Network and the Covering NEXRAD
Stations

accuracy of the rain gages) will give estimates that are superior to estimates obtainable from each individual device alone.

3.2. National Weather Service Rain Gage Network in Michigan

The total area of Michigan is about 170,312 km^2. The land area is about 147,134 km^2 and the water area is about 103,602 km^2. The mean elevation of Michigan is 174.32m above sea level. The major lakes of Michigan are Lake Michigan, Lake Superior, Lake Huron, Lake Erie, and Lake St. Clair. The period of the study was the months of May through September for the years 1999 to 2001.

In this study, rainfall measurements 42 National Weather Service observing sites distributed across the entire state of Michigan were used to calibrate and validate the NEXRAD Stage III rainfall surface. Twelve of these sites are distributed across the Upper Peninsula and 30 are distributed across the Lower Peninsula (see Figure 3.3). Michigan is overlapped by the sweep ranges of the following ten NEXRAD radars, which are Marquette, Gaylord, Detroit-Pontiac, and Grand Rapids, MI; North Webster, IN; Cleveland, Ohio; Chicago, Illinois; Duluth, Minnesota; and Milwaukee and Green Bay, Wisconsin (see Figure 3.3). The NEXRAD Stage III data for Michigan is produced by mean or maximum values of these ten NEXRAD rainfall surfaces.
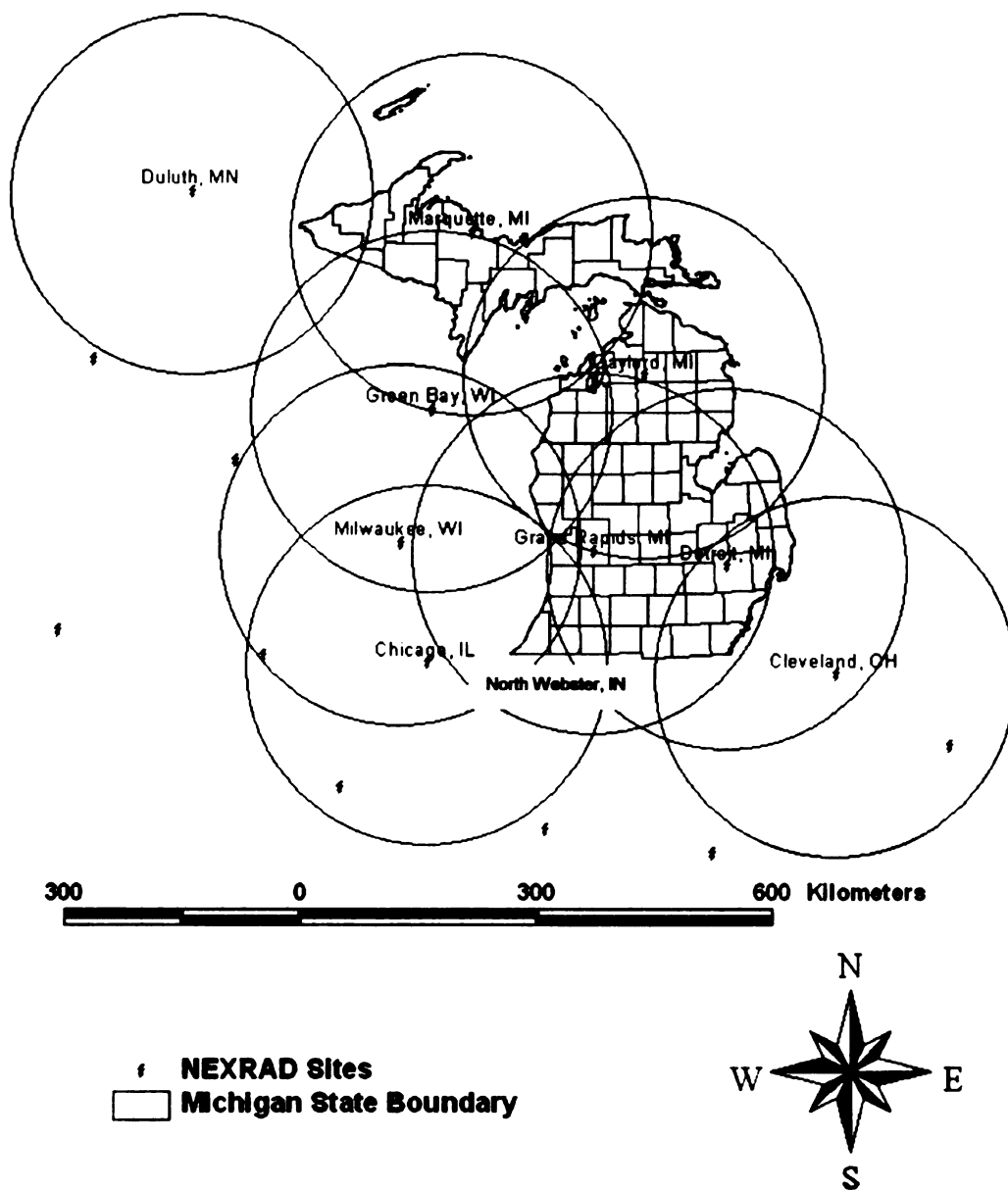
Figure 3.3. Michigan National Weather Service Rain gage Network and Covering 9 NEXRAD Radar Stations.

Chapter 4 METHODOLOGIES
PILOT STUDY: STATISTICAL ANALYSIS AND MODEL DEVELOPMENT IN THE SEMCOG RAIN GAGE NETWORK

The SEMCOG rain gage network is one of the few, large, high-density rain gage networks in the U.S. The purpose of the pilot study was to take advantage of the data from this network and to: (1) perform a statistical analysis between Stage III NEXRAD data and the ground gages to determine the frequency and type of disagreement, and the magnitude of error between radar and ground gages, and (2) use the SEMCOG network as a testing ground for developing and testing ordinary cokriging and artificial neural network models for improving spatial rainfall estimation.

4.1. Precipitation Data Sources

The hourly and daily rain gage data of the SEMCOG network used for this study were obtained from the SEMCOG web site: http://35.9.73.71/Semcog/SEM/semtable.html. The SEMCOG rain gage network consists of 108 universal weighing rain gages recording real-time rainfall information. The universal weighing rain gages in the network consist of a shelter, funnel, collection bucket, weighing device and recording chart. Precipitation falls into the universal gage receiver, where it is funneled into a collector mounted on a weighing mechanism. The weight of the precipitation compresses a spring, which is connected to a pen (ink) arm. Ink from the pen leaves a trace on a paper chart, wrapped around a clock-driven cylinder. The cylinder rotates continuously, making one revolution every 24 hours. Ink tracings on the chart provide historical precipitation rates and amounts. Charts are graduated to the nearest 1.270 mm and read to the nearest 0.254 mm by interpolation. Maximum capacity is 304.800 mm. Charts are changed once a week or within 24 hours after a precipitation

event. The time periods of the data used for this study were from the months of May through September from 1999 to 2000. During the study time periods, only about 66 to 68 universal weighing rain gages were active.

The hourly NEXRAD Stage III data of the Midwest was obtained from the Hydrology Laboratory in the Office of Hydrology Development at the National Weather Service. These data are stored in binary data format called XMRG and are mosaiced Stage II rainfall estimates from the NEXRAD radar sites located in the Midwest. The NEXRAD data are projected onto a subset of the national HRAP grid, the coordinate system that defines the locations of XMRG data values (see Figure 4.1).

4.2. Software

Since this study involves detailed spatial analysis of rainfall distribution, ArcView GIS 3.3 software with extensions made by Environmental System Research Institute (ESRI) Inc. and MATLAB 6.1 for Windows NT with toolbox made by The MathWorks Inc. were used in this study to aid in processing NEXRAD and rain gage data..

4.2.1. ArcView GIS Software and Its Extension Programs

ArcView GIS 3.3 has the ability to: (1) display spatial data, (2) query data, (3) create data, and (4) use other type of data, e.g. CAD data. ArcView GIS 3.3 displays data by creating a map in a variety of spatial data formats; e.g. the ARC/INFO spatial data formats. It can display tabular data about ground covers, land formations, and water quality to a map. The software is able to represent data on a map by symbolizing and charting the data, by labeling the map with text and graphics, and by choosing map projections. ArcView GIS 3.3 can also design and print various map layouts (ESRI, 2002).

ArcView GIS 3.3 can create new data by: (1) developing additional spatial data,
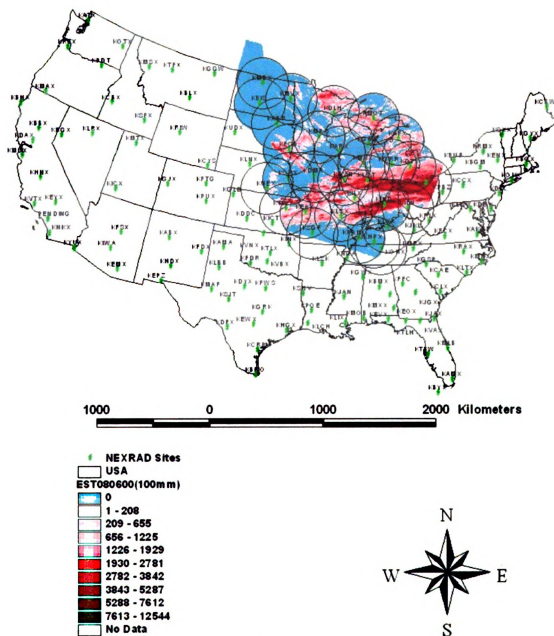
Figure 4.1. NEXRAD Stage III Data of Midwestern Area (Projected by Michigan Georef System).

(2) editing existing spatial data, and (3) digitizing a map. The software creates new spatial data either by developing a new point theme, line theme, or polygon theme, or by using a digitizing tablet to digitize a map into a point feature, a line feature, and a polygon feature. Editing spatial data can be done within certain existing themes.

ArcView GIS 3.3 data is compatible with several other data types, e.g. image-type data, Computer-Aided Design (CAD) data, Spatial Database Engine (SDE) data (ESRI, 1996). Image-type data includes scanned-map data, the aerial-photograph data, and satellite-imagery data. CAD data are a set of non-GIS graphical data for engineering or architecture design, and can be employed as if it is GIS data in ArcView GIS 3.3. With the spatial Database Themes extension of ArcView GIS 3.3, SDE data can be added to the database of a map in order to explore, query, and analyze the map data in ArcView (ESRI, 1996).

In this study, additional extension programs were used with basic ArcView GIS 3.3: (1) MI DNR Projection Extension, (2) ArcView Spatial Analyst, and (3) Grid Analyst.

4.2.2. MATLAB Software with Neural Network Toolbox

MATLAB is a high-performance language for technical computing. It is typically used in: (1) mathematics and computation, (2) algorithm development, (3) modeling, simulation, and prototyping, (4) data analysis, exploration, and visualization, (5) scientific and engineering graphics, and (6) application development, including graphical user interface building. MATLAB is an interactive system whose basic data element is an array that does not require dimensioning. This can solve the technical computing problems, especially those with matrix and vector formulations. In addition, MATLAB

features a family of application-specific solutions called toolboxes that extend the MATLAB environment to solve particular classes of problems.

In this study, MATLAB 6.1 for Windows NT software with Neural Network Toolbox was used to load and process the ordinary cokriging (Marcotte, 1991) and ANN models. For processing the ordinary cokriging model, only MATLAB 6.1 for Windows NT software was used. For processing the ANN model, MATLAB 6.1 for Windows NT software with Neural Network Toolbox was used. The Neural Network Toolbox contains the feed-forward neural network with the Levenberg-Marquardt (LM) algorithm (Demuth and Beale, 2001), which is the main algorithm used to process the ANN model in this study. The relative principles and details of ordinary cokriging and ANN approaches are described in Section 2.4 and 2.5, respectively.

4.3. Methods

4.3.1. Data Management for SEMCOG Rain Gage Measurements and NEXRAD Stage III Rainfall Estimates

ArcView with MI DNR Projection Extension, Spatial Analyst, and Grid Analyst extension programs were used to manage both the SEMCOG hourly and daily rain gage data and hourly NEXRAD Stage III data from the months of May to September from 1999 to 2000. In this study, ArcView GIS software was used to:

(1) Develop GIS precipitation maps with the same time zone (East Standard Time), time scale (Daily rainfall), and georeferenced system (Michigan Georef system) by merging SEMCOG hourly and daily rain gage measurements and hourly NEXRAD Stage III precipitation surface together.

(2) Extract corresponding NEXRAD and rain gage data for making two types of statistical analyses.

(3) Develop a MATLAB-based large matrix inputs for the OC and ANN models.

(4) Display the results after processing both the OC and ANN models.

Using ArcView, the data from both sources (rain gage and NEXRAD Stage III values) were adjusted so that they were in the same time zone, time scale, spatial projection, and coordinate system (Michigan Georef).

Initially, the SEMCOG rain gage (hourly and daily) and hourly NEXRAD Stage III data were recorded in different time zones and time scales. The SEMCOG hourly rain gage data were recorded in EST, while the NEXRAD Stage III data were recorded in Greenwich Mean Time (GMT), a difference of five hours. To bring both data sets into the same time frame, the hourly NEXRAD data were shifted back five hours. The shifted hourly data were then summed to daily totals This was accomplished by using Map Calculator in ArcView by summing up 24 initial hourly NEXRAD data from the 6th hour of the first day to the 5th hour of the second day to get the corresponding daily NEXRAD Stage III data in EST (from the 1st hour to the 24th hour).

Both the SEMCOG rain gage measurements and NEXRAD Stage III data were projected in different georeferenced systems. The SEMCOG rain gage measurements were projected in the Geographic Lat/Lon system and the NEXRAD grid themes were projected in the Michigan Georef system. Since both data must be georeferenced in the same projection in order to be compared against each other, the SEMCOG rain gage text files were converted into ArcView shape files by using the Add Event Theme and the Convert to Shapefile functions in ArcView. Then, the MI DNR Projection Extension was

used to re-project the Geographic Lat/Lon projected rain gage measurements into the Michigan Georef Projection. These techniques allowed for both data sets to be compared both spatially and temporally.

4.3.2. Statistical Analysis of SEMCOG Rain Gage Measurements and NEXRAD Stage III Rainfall Estimates

It has been previously noted that NEXRAD radar usually underestimates the convective precipitation events and overestimates stratiform precipitation events (Groisman and Legates, 1994). Many possible approaches can be taken when comparing point rain gage data to NEXRAD Stage III estimates. In this study, two types of statistical analyses were performed to describe the correlation between SEMCOG rain gage values and stage III NEXRAD. The first statistical analysis focuses on the agreement of occurrence of precipitation between the two sources and the magnitude of the differences in precipitation when there is disagreement of occurrence. The second statistical analysis simply examines the differences in magnitude between rain gage measurement and NEXRAD estimate when they both register a rainfall amount. These analyses were performed to determine the differences between rain gage measurements and the NEXRAD estimates and to provide a basis of justification for using models to improve the correlation between the two sources of rainfall measurement.

There are several possible situations during a rainfall event that can cause disagreement between rain gage and NEXRAD. These include situations such as rainfall being registered by NEXRAD, but evaporating before it reaches the rain gage, and rainfall that is measured by the rain gage, but not measured by NEXRAD due to radar beam attenuation caused by heavy precipitation. The disagreement between these two

sources is compounded by the fact that the rain gage measurement represents a point measurement, while the Stage III NEXRAD is an estimate made over a 4 km by 4 km area, i.e. within-cell rainfall variability.

To determine the correlation of rainfall occurrence between SEMCOG rain gages and NEXRAD radar estimates, hourly rainfall values for each rain gage in the network and corresponding NEXRAD estimate were extracted and separated into one of four possible classes or conditions. Each condition is described below:

Condition 1 – Both the rain gage and NEXRAD registered a precipitation event.

Condition 2 – The rain gage registered a precipitation event, but the NEXRAD did not.

Condition 3 – The rain gage did not register a precipitation event, but the NEXRAD did.

Condition 4 – Neither the rain gage nor did NEXRAD register a precipitation event.

These conditions are summarized in Table 4.1. It should be noted that throughout 1999 and 2000, there were several periods of time when either a certain rain gage in the network was not operational or NEXRAD was not available. The data used in this analysis includes all available hourly data for the more or less 10-month period, roughly 500,000 rain gage-hours.

A further analysis of these data focuses in more detail on the magnitude of difference between the SEMCOG rain gages and their corresponding NEXRAD estimate. These initial statistics consists of a set of synthetic statistical matrices used to describe the differences of each examined precipitation event between the SEMCOG daily rainfall and daily NEXRAD Stage III data. These synthetic statistical matrices consist of the

36

Table 4.1. Possible Combinations of Precipitation Occurrences between SEMCOG Rain Gages and NEXRAD Radar Estimates

Precipitation Conditions	SEMCOG Rain Gage Network	NEXRAD Stage III
1	Yes*	Yes
2	Yes	No**
3	No	Yes
4	No	No

*Yes means that the device registers precipitation information.
**No means that the device does not register precipitation information.

mean, the mean bias (*MB*), and the absolute mean bias (*AMB*).

To make these two types of statistical analyses, the hourly NEXRAD Stage III grid values where the rain gages were present were extracted and compared with the SEMCOG hourly rain gage values. The hourly NEXRAD Stage III grid values were extracted by using a function of the Grid Analyst extension named Extract X, Y, and Z Values for Point Theme from Grid Theme. The descriptive table containing the extracted hourly NEXRAD Stage III grid values was joined with the descriptive table of the SEMCOG hourly rain gage measurements by using the Join function of the ArcView GIS software, respectively.

4.3.3. Model Justification

In this study, ordinary cokriging and artificial neural network models were selected for adjusting the daily NEXRAD Stage III rainfall surfaces using the ground gage measurements. The approaches for these two models are very different from each other, but both have the potential to improve the NEXRAD estimate by incorporating ground rain gages.

Ordinary Cokriging (OC) Model

Ordinary cokriging (OC) was originally developed as geostatistical tool for the mining industry. The method can obtain the spatial correlation between two or more variables. In this study, the ordinary cokriging method was applied to spatially estimate rainfall by combining rain gage measurements and radar rainfall data. It uses the rain gage measurements and the NEXRAD-derived rainfall surface, to obtain the spatial correlation between the rain gage measurements and NEXRAD-derived rainfall. It minimizes the estimation variance, considering the statistical properties of radar rainfall data, the measurements of the rain gage network, and the dependence of each of measurements on the other (Matsoukas, 1999; Seo et al. 1990a and 1990b). It assumes second-order stationarity and ergodicity, and models the spatial dependence of each measurement of device on itself and on each other in terms of the estimations of semivariogram and cross semivariogram. However, the estimations of semivariogram and cross semivariogram are usually not well behaved for rain gage measurements. For the past two decades the ordinary cokriging approach has been used for the studies of the radar rainfall estimation and shown good results.

Artificial Neural Network (ANN) Model

Artificial neural networks are computer-based systems that are designed to emulate some of the learning and pattern recognition abilities of the human brain. The approach of the ANN is known as a "data-driven" modeling approach (Chakraborty et al., 1992). ANNs are well suited to solve complex problems where the relationships between the variables to be modeled are not well understood (Maren et al., 1990). ANNs use parallel processing to learn an approximation to the underlying rules governing the

relationship between input and output variables. However, the internal structure or topology of the ANN model is generally unknown and must be developed by a trial and error process. For the past decade ANNs have been gradually applied to problems in hydrometeorology and have shown promising results.

Selection and Classification of Examined SEMCOG Precipitation Events

In this study, twenty-two daily precipitation events from the SEMCOG network were selected for examining the performances of both the OC and ANN models. The events were divided into two types: full and partial spatial coverage. In the first type of the precipitation event, the SEMCOG network was fully covered by the precipitation. Sixteen of twenty-two events were full coverage events, in which each rain gage registered precipitation. The remaining six events were partial coverage events, where a portion of the rain gage network recorded no rain. The twenty-two daily precipitation events were further classified into three levels of daily mean rain gage values using the natural break method. The three types of precipitation events were light, moderate, and heavy precipitation events. The ranges of each level of daily precipitation events are: light (< 8.18 mm), moderate (8.18 - 18.84 mm), and heavy (> 18.84 mm).

Assignments of Model Processing Data Sets and Model Efficiency Criteria

Calibration and validation encompass accuracy, robustness, consistency, fault tolerance, and sensitivity. Standard statistical and pattern recognition techniques were used to investigate the efficiency of OC and ANNs methods.

Since rain gage values are the best estimate of precipitation at a point, they are assumed to be "ground truth." Rain gage and NEXRAD data from each event were separated into two datasets, one set for calibration and the other for validation. Figure 4.2

depicts the locations of the NEXRAD data that were used for calibration and validation in the ANN model. The assignments of the calibration or validation data sets of the rain gage measurements were the same as where their located NEXRAD grid were allocated to the calibration or validation data sets. The same calibration and validation data sets of the rain gages used in the ANN model were used in the OC model for cross validation and validation, respectively. Because of this calibration / validation process, it is possible that the split of rain gages for calibration / validation may not have been equal.

During the calibration and validation phases of the numerical processes, the model output at a grid point with a rain gage was compared to the value recorded by the rain gage values. Goodness-of-fit metrics that will be estimated are the correlation coefficient (CC), the R^2, the mean bias (MB), the absolute mean bias (AMB), the normalized mean bias (NBIAS), the normalized root-mean-square error (NRMSE), Arithmetical Averaging method (mean), and the Thiessen Polygon method ($\bar{P}$).

The holdout method was used for calibration and validation using the N extracted radar values with their N rain gage measurements. The N rain gage measurements are split into two data sets: Nd, which were used to develop the training algorithm, and Nv, which are used in validation. The l-th rain gage, which belongs in the calibration or validation subsets $l \in \{1,2,...,N\}$, has spatial coordinates $x(l)$, $y(l)$ and in reality, records rainfall $Rg(x(l),y(l))$, and the brevity of $Rg(x(l),y(l))$ is denoted as Rgl. Rgl in this location is assumed the absolute truth rainfall value, while our calibration and validation outputs are $R'l$. Then, the definitions of the comparison metrics are:

$$MB = \frac{\displaystyle\sum_{l=1}^{N,N_d,N_v}(R'_l - R_{gl})}{(N,N_d,N_v)} \qquad 4.1$$

$$AMB = Absolute\left(\frac{\sum\limits_{l=1}^{N,N_d,N_v} (R_l' - R_{gl})}{(N,N_d,N_v)}\right)$$
4.2

$$NBIAS = \frac{\sum\limits_{l=1}^{N,N_d,N_v} (R_l' - R_{gl})}{\sum\limits_{l=1}^{N,N_d,N_v} R_{gl}}$$
4.3

$$NRMSE = \sqrt{\frac{\sum\limits_{l=1}^{N,N_d,N_v} (R_l' - R_{gl})^2}{\sum\limits_{l=1}^{N,N_d,N_v} (R_{gl} - \overline{R_{gl}})^2}}$$
4.4

Arithmetical Averaging method: $mean = \dfrac{\sum\limits_{l=1}^{N,N_d,N_v} (R_{gl})}{N,N_d,N_v}$
4.5

Thiessen Polygon method: $\overline{P} = \dfrac{\sum\limits_{i=1}^{N} P_i \cdot A_i}{\sum\limits_{i=1}^{N} A_i}$
4.6

41

SEMCOG NEXRAD Grid Centroids of Calibration and Validation Used in ANN Model
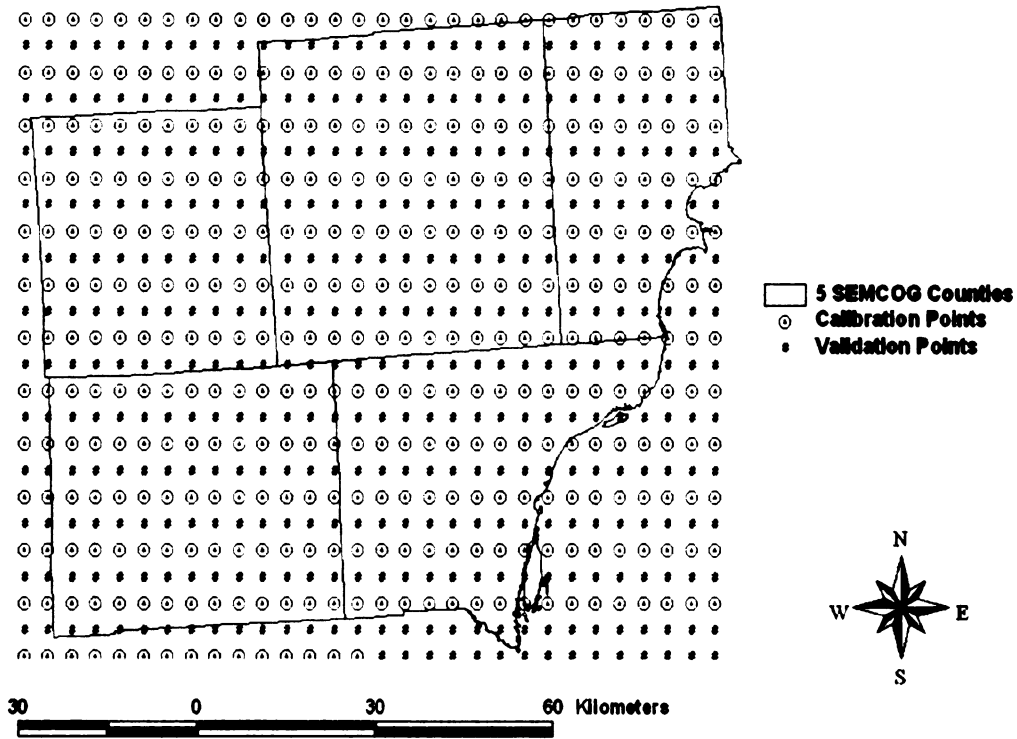
Figure 4.2. SEMCOG NEXRAD Grid Centroids of Calibration and Validation Used in ANN Model.

CC measures how well the adjusted radar values correlate with the rain gage values. Either raw radar values or adjusted radar values and rain gage values have the best correlation coefficient when $CC = 1.0$. R^2 measures how well the adjusted radar values match the rain gage values. $NBIAS$ indicates the degree of bias between either raw radar values or adjusted radar values and the ground truth values (gage values). When $NBIAS = 0$, either raw radar values or adjusted radar values and gage values are identical. NRMSE indicates the closeness of either raw radar values or adjusted radar values to the gage values and is used to measure the error between either raw radar values or adjusted radar values and gage values. A perfect $NRMSE$ means either all raw radar values or all adjusted radar values are identical to the gage values exists only if $NRMSE = 0$.

The arithmetical averaging method is performed by dividing the summed accumulation of each rain gage measurement by the number of the rain gages (N, N_d, N_v). This method is good for the region with the plain topography and small precipitation variance.

The Thiessen polygon method is a technique for approximating the distribution area around precipitation gages for the purpose of distributing average precipitation depths over an area. A Thiessen polygon network is constructed using perpendicular bisectors to lines between gages and carefully removing overlapping bisectors until an even spatial distribution is obtained. The area of polygon (A_i) is multiplied by the representative depth of rain gage (P_i) and summed over the total area of interest. This sum is divided by the total area to obtain the average depth ($\overline{P}$).

Adjusting NEXRAD Precipitation Surface Using Ordinary Cokriging and ANNs

Adjusting NEXRAD Precipitation Surface Using Ordinary Cokriging

A linear ordinary cokriging estimator combining radar-derived rainfall with rain gage measurement has the following form (Seo et al., 1990; Krajewski, 1987; Journel, 1978):

$$Z_g(U_0) = \sum_{i=1}^{N_g} \lambda_{gi} \cdot Z_g(U_i) + \sum_{i=1}^{N_g} \lambda_{rj} \cdot Z_r(U_j) \qquad 4.7$$

where

$Z_g(U_i)$: Spatial averaged gage rainfall centered at U_i;

$\lambda_{gi}, \lambda_{rj}$: Weighting coefficients to be determined;

N_g : Number of spatially averaged gage rainfall data;

$Z_r(U_j)$: Radar rainfall at the bin centered at U_j;

N_r : Number of radar rainfall data surrounding U_0;

$Z_g(U_o)$: Estimated gage rainfall averaged over A and centered at an arbitrary location

U_0.

When the mean and the covariance of the rainfall measurement fields are perfectly known, the weighting coefficients that give the unbiased, minimum-error-variance estimate are found by minimizing

$$Var\left[\varepsilon_g(U_o)\right] = E\left[\left\{\hat{Z}_g(U_o) - Z_g(U_o)\right\}^2\right] \qquad 4.8$$

where $\varepsilon_g(U_o)$ is the estimation error at the location U_0.

The solution for this problem can be obtained by the simple application of the Gauss-Markoff theorem (Liebelt, 1967) and is given by:

$$Z_g(U_o) = m_g + (Q_{og} Q_{or}) \cdot \begin{bmatrix} Q_{gg} & Q_{gr} \\ Q_{rg} & Q_{rr} \end{bmatrix}^{-1} \begin{bmatrix} Z_g - M_g \\ Z_r - M_r \end{bmatrix}$$
   4.9

$$Var[\varepsilon_g(U_o)] = \sigma_g^2 - (Q_o Q_{or}) \cdot \begin{pmatrix} Q_{gg} & Q_{gr} \\ Q_{rg} & Q_{rr} \end{pmatrix}^{-1} (Q_{go} Q_{ro})$$
   4.10

where

Q_{og} : $(1 \times Ng)$ covariance vector of the unknown gage rainfall and the sampled gage rainfall data;

Q_{or} : $(1 \times Nr)$ cross-covariance vector of the unknown gage rainfall and the sampled radar rainfall data;

Q_{gg}: $(Ng \times Ng)$ covariance matrix of the sampled gage rainfall data;

Q_{rg}: $(Nr \times Ng)$ cross-covariance matrix of the sampled radar rainfall data and the sampled gage rain fall data;

Q_{rr}: $(Nr \times Nr)$ covariance matrix of the sampled radar rainfall data;

m_g: mean of the gage rainfall;

σ_g^2: variance of the gage rainfall;

m_r: mean of the radar rainfall;

Mg: $(Ng \times 1)$ gage rainfall mean vector equal to $(m_g \dots m_g)^T$;

Mr: (Nr × 1) radar rainfall mean vector equal to *(m_r... m_r)^T*.

When the gage rainfall field and the radar rainfall field are jointly second-order homogenous, and both the mean of the gage rainfall field and the mean of the radar rainfall field are unknown but constant, and the minimization of

$$Var\left[\varepsilon_g(U_o)\right] = E\left[\left\{\hat{Z}_g(Uo) - Z_g(U_o)\right\}^2\right]$$ is made subject to the following constraints to

force unbiasedness:

$$\sum_{i=1}^{N_g} \lambda_{gi} = 1, \quad \sum_{j=1}^{N_r} \lambda_{rj} = 0,$$ 4.11

the role of the above constraints becomes:

$$E\left[\hat{Z}_g(U_o)\right] = \sum_{i=1}^{N_g} \lambda_{gi} E\left[Z_g(U_i)\right] + \sum_{j=1}^{N_r} \lambda_{rj} E\left[Z_r(U_j)\right] = m_g \cdot \sum_{i=1}^{N_g} \lambda_{gi} + m_r \sum_{j=1}^{N_r} \lambda_{rj} = m_g$$

4.12

where m_g is unknown but mean of the gage rainfall field is constant and m_r is the unknown but mean of the radar rainfall field is constant.

Process Procedures of Ordinary Cokriging

The process procedures of the OC model based on the equations are described as follows:

1. Produce a semivariogram and cross semivariogram to find the spatial surface trend of each rainfall measurement on itself and on each other.

2. Find the parameters (sill and range) from the best-fit model of semivariogram or cross semivariogram by using Nugget Effect, Exponential, Gaussian, Spherical, and Linear models. The weighted-least-square method is used to automatically model semivariograms and cross semivariogram instead of using manual operation.

3. Use the parameters (sill and range) obtained from the best-fit model to the OC model for cross validation and validation.

After finding the well-behaved semivariogram, five models and the weighted-least-square method were used to model the semivariogram and cross semivariogram in order to rapidly find the sill and range values. After finding the best set of sill and range values, these two values were used to process cross validation and validation in the OC model.

Adjusting NEXRAD Precipitation Surface Using ANNs

This study used a multi-layer feed-forward neural network with a Levenberg-Marquardt (LM) training algorithm and one single output to calibrate and validate NEXRAD rainfall surface based on rain gage measurements (Haykin, 1999; Demuth and Beale, 1997; Hagan et al., 1996). This model is a network composed of a number of interconnected artificial neurons (the hierarchy of the information processing units) organized in a series of two or more mutually exclusive sets of neurons or layers. Each neuron has an input/output (I/O) characteristic and implements a local computation or

function. The output of any artificial neural unit is determined by its I/O characteristic, its interconnection to other units, and external inputs (Wechsler, 1992).

The input layer serves as a holding site for the inputs applied to network. The output layer is the point at which the overall mapping of the network input is available. Zero or more layers of hidden units lie between these two layers as internal layers where additional re-mapping or computing takes place. Connection weights link each unit of neuron in one layer only to those in the next higher layer. There is an implied directionality in these connections, in that the output of a unit, scaled by the value of a connection weight, is fed forward to provide a portion of the activation for the units in the next higher layer.

Initially, the input data was multiplied by a randomly generated initial connection weight for each neuron connection path. The total sum of these weighted inputs plus a constant term yields the neural net input Y_{net}, that is:

$$Y_{net} = \sum_{i=1}^{N} Y_i w_i + w_0 , \qquad\qquad 4.13$$

where N is the total number of neurons in the preceding layer, Y_i is the neuron input received from the ith neuron in the preceding layer, w_i is the connection weight assigned to the path linking the neuron to that i^{th} neuron and w_0 is the neuron threshold value (Blum, 1992). The neuron threshold value provides the means of adding a constant value to the summation term, which can be used to scale this term into a useful range of values.

Next, the neuron input Y_{net} is transformed to the neuron output Y_{out} by passing through the hidden layer(s). The non-linear hyperbolic tangent transformation function was used to represent each hidden layer, that is

$$Y_{out} = f(Y_{net}) = f(\sum_{i=1}^{N} Y_i w_i + w_0) = \tanh(\sum_{i=1}^{N} Y_i w_i + w_0) \qquad 4.14$$

The topology of the multi-layer neural network belongs to the class of data driven approaches, and hence requires the specific factor (i.e. the number of hidden layers and the neuron number in a hidden layer) for keeping the network structure being minimum and obtaining maximum efficiency (Fausett, 1994). The determination of the appropriate number of hidden layers and the neural number (number of nodes) in a hidden layer are important for the success of the neural network, since it greatly enhances the performance of the neural network, i.e. the network efficiency is sensitive to these two types of numbers. If the neural network has too few hidden layers or too few neural numbers in the hidden layer i.e. the network is too parsimonious in its use of parameters (w_o and w_i), then the performance of the neural network may deteriorate below that of the appropriate number. Reversely, too many hidden layers or too many neural numbers in a hidden layer will increase the number of the parameters and cause it to over-fit the calibration (training) data set. The strategy used for selecting the appropriate number of hidden layers was done by a trial and error procedure to select the least number of hidden layers and the least neural numbers in a hidden layer for the best performance of the ANN model.

The Levenberg-Marquardt (LM) algorithm was applied to a multiplayer feed forward network for this study. The detailed presentations of LM algorithm can be found in Demuth and Beale, (2001); Hagan et al., (1996); and Marquardt, (1963) for the applications and the original description. In this section, the equations (Equation 4.15 –

4.29) of the back-propagation algorithm are briefly present (Haykin, 1999; Bose and Liang, 1996) for the purpose of introducing notation and concepts which are needed to describe the LM algorithm (equation 4.30 – 4.40).

The net input to unit i in layer k+1 is:

$$n^{k+1}(i) = \sum_{j=1}^{Sk} w^{k+1}(i,j) a^k(j) + b^{k+1}(i) \qquad 4.15$$

The output of unit i will be: $a^{K+1}(i) = f^{k+1}\left(n^{k+1}(i)\right)$ \qquad 4.16

For an M layer network the system equations in matrix form are given by

$$a^0 = P \qquad 4.17$$

$$\underline{a}^{k+1} = \underline{f}^{k+1}\left(w^{k+1}\underline{a}^k + \underline{b}^{k+1}\right), \quad k = 0,1,\cdots,M-1 \qquad 4.18$$

The task of the network is to learn associations between a specified set of input-output

pairs $\left\{\left(\underline{p}_1,\underline{t}_1\right)\left(\underline{p}_2,\underline{t}_2\right)\cdots,\left(\underline{p}_Q,\underline{t}_Q\right)\right\}$

The performance index for the network is

$$V = \frac{1}{2}\sum_{q=1}^{Q}\left(\underline{t}_q - \underline{a}_q^M\right)^T\left(\underline{t}_q - \underline{a}_q^M\right) = \frac{1}{2}\sum_{q-1}^{Q}\underline{e}_q^T\underline{e}_q \qquad 4.19$$

50

where $\underline{a}_q^M$ is the output of the network when the qth input, $\underline{P}_q$ is present and

$\underline{e}_q = \underline{t}_q - \underline{a}_q^M$ is the error for the qth input. For the standard back-propagation

algorithm we use an approximate steepest decent rule. The performance index is

approximated by

$$\hat{V} = \frac{1}{2}\underline{e}_q^T \underline{e}_q \qquad\qquad 4.20$$

where the total sum of squares is replaced by the squared errors for a single input/output

pair. The approximate steepest (gradient) descent algorithm is then

$$\Delta w^k(i, j) = -\alpha \frac{\partial \hat{V}}{\partial w^k(i, j)} \qquad\qquad 4.21$$

$$\Delta b^k(i) = -\alpha \frac{\partial \hat{V}}{\partial b^k(i)} \qquad\qquad 4.22$$

where α is the learning rate. Define $\delta^k(i) = \frac{\partial \hat{V}}{\partial n^k(i)} \qquad\qquad 4.23$

as the sensitivity of the performance index to changes in the net input of unit i in layer k.

Using 4.15, 4.20 and 4.23:

$$\frac{\partial \hat{V}}{\partial w^k(i,j)} = \frac{\partial \hat{V}}{\partial n^k(i)} \frac{\partial n^k(i)}{\partial w^k(i,j)} = \delta^k(i) \cdot a^{k+1}(j) \qquad \text{4.24}$$

$$\frac{\partial \hat{V}}{\partial b^k(i)} = \frac{\partial \hat{V}}{\partial n^k(i)} \frac{\partial n^k(i)}{\partial b^k(i)} = \delta^k(i) \qquad \text{4.25}$$

The sensitivity satisfies the following recurrence relation:

$$\underline{\delta}^k = \overset{\bullet^k}{F}\left(\underline{n}^k\right) w^{k+1^\tau} \underline{\delta}^{k+1} \qquad \text{4.26}$$

where

$$\overset{\bullet^k}{F}\left(\underline{n}^k\right) = \begin{bmatrix} \overset{\bullet^k}{f}\left(n^k(1)\right) & 0 & \cdots & 0 \\ 0 & \overset{\bullet^k}{f}\left(n^k(2)\right) & \cdots & 0 \\ \vdots & \vdots & \ddots & \vdots \\ 0 & 0 & \cdots & \overset{\bullet^k}{f}\left(n^k(s_k)\right) \end{bmatrix} \qquad \text{4.27}$$

and $\overset{\bullet^k}{f}(n) = \dfrac{df^k}{dn}$ \qquad 4.28

This recurrence relation is initialized at the finial layer:

$$\underline{\delta}^M = -\overset{\bullet}{F}^M\left(\underline{n}^M\right)\!\left(\underline{t}_q - \underline{a}_q\right)$$

4.29

The overall learning algorithm proceeds as follows:

1. Propagate the input forward using 4.17 and 4.18.

2. Propagate the sensitivities back using 4.29 and 4.26.

3. Update the weights and offsets using 4.21, 4.22, 4.24, and 4.25.

While back propagation is a steepest descent algorithm, the LM algorithm is as approximation to Newton's method. Suppose that a function $V(\underline{x})$ has to be minimized with respect to the parameter vector $\underline{x}$, and then Newton's method would be:

$$\Delta\underline{x} = -\left[\nabla^2 \cdot V(\underline{x})\right]^{-1}\nabla V(\underline{x})$$

4.30

where $\nabla^2 V(\underline{x})$ is the Hessian matrix and $\nabla V(\underline{x})$ is the gradient. If we assume that $V(\underline{x})$ is

a sum of squares function $V(\underline{x}) = \sum_{i=1}^{N} e_i^2(\underline{x})$

4.31

then it can be shown that $\nabla V(\underline{x}) = J^T(\underline{x})\underline{e}(\underline{x})$

4.32

$$\nabla^2 V(\underline{x}) = J^T(\underline{x}) \cdot J(\underline{x}) + S(\underline{x}) \qquad\qquad 4.33$$

where Jacobian matrix:

$$J(\underline{x}) = \begin{bmatrix} \dfrac{\partial e_1(x)}{\partial x_1} & \dfrac{\partial e_1(x)}{\partial x_2} & \cdots & \dfrac{\partial e_1(x)}{\partial x_n} \\ \dfrac{\partial e_2(x)}{\partial x_1} & \dfrac{\partial e_2(x)}{\partial x_2} & \cdots & \dfrac{\partial e_2(x)}{\partial x_n} \\ \vdots & \vdots & \ddots & \vdots \\ \dfrac{\partial e_N(x)}{\partial x_1} & \cdots & \cdots & \dfrac{\partial e_N(x)}{\partial x_n} \end{bmatrix} \qquad\qquad 4.34$$

and $S(\underline{x}) = \sum\limits_{i=1}^{N} e_i(x) \cdot \nabla^2 e_i(x) \qquad\qquad 4.35$

For the Gauss-Newton method:

$$S(\underline{x}) \approx 0$$

$\rightarrow (16)$ is updated: $\Delta \underline{x} = \left[J^T(\underline{x}) \cdot J(\underline{x}) \right]^{-1} J^T(\underline{x}) \cdot \underline{e}(\underline{x}) \qquad\qquad 4.36$

$\therefore$ The LM modification to the Gauss-Newton method is:

$$\Delta \underline{x} = \left[J^T(\underline{x}) \cdot J(\underline{x}) + \mu \cdot I \right]^{-1} J^T(\underline{x}) \cdot \underline{e}(\underline{x}) \qquad\qquad 4.37$$

The parameter μ is multiplied by some factor (β) whenever a step would result in an increased $V(\underline{x})$. When a step reduces $V(\underline{x})$, μ is divided by β. When μ is large the

algorithm becomes steepest descent (with step $1/\mu$). When μ is small, the algorithm becomes Gauss-Newton.

The computation of the Jacobian matrix is very important to the LM algorithm. For the neural network mapping problem, the terms in the Jacobian matrix can be computed by a simple modification to the back-propagation algorithm. The performance index for the mapping problem is given by (4.19). This is equivalent in form to (4.31), where

$$\underline{x} = [w^1(1,1)w^1(1,2)...w^1(S1,R)b^1(1)...b^1(S1)w^2(1,1)...b^M(SM)]^T, \text{ and } N = Q \times SM.$$

Standard back-propagation calculates terms like $\dfrac{\partial \hat{V}}{\partial w^k(i,j)} = \dfrac{\partial \displaystyle\sum_{m=1}^{SM} e_q^2(m)}{\partial w^k(i,j)}$ 　　　　4.38

The term needs to be calculated for the element of the Jacobian matrix that is needed for

the LM algorithm: $\dfrac{\partial e_q(m)}{\partial w^k(i,j)}$. 　　　　4.39

These terms can be calculated using the standard back-propagation algorithm with one

modification at the final layer $\Delta^M = -\dot{F}^M(\underline{n})^M$. 　　　　4.40

55

The LM algorithm modifies the back-propagation algorithm and proceeds as follows:

1. Present all inputs to the network and compute the corresponding network outputs (using 4.17 and 4.18), and errors $((\underline{e}_q = \underline{t}_q - \underline{a}_q^M)$. Compute the sum of squares of errors overall inputs $(V(\underline{x}))$.

2. Compute the Jacobian matrix (using 4.40, 4.26, 4.24, 4.25, and 4.34).

3. Solve 4.37 to obtain $\Delta \underline{x}$.

4. Re-compute the sum of squares of errors using $\underline{x} + \Delta \underline{x}$. If this new sum of squares is smaller than that computed in step 1, then reduce μ by β, let $\underline{x} = \underline{x} + \Delta \underline{x}$, and go back to step 1. If the sum of squares is not reduced, then increase μ by β and go back to step 3.

5. The algorithm is assumed to have converged when the norm of the gradient (4.32) is less than some predetermined value, or when the sum of squares has been reduced to some error goal.

Process Procedures of ANN Model

The ANN model used a feed-forward neural network with the Levenberg-Marquardt algorithm to calibrate and validate the NEXRAD Stage III data. The activation function or transformation function used for the ANN model was a hyperbolic tangent function. This network was selected because it has been shown to be a good choice for solving nonlinear relationships (Haykin, 1999; Demuth and Beal, 2000). Also, the Levenberg-Marquardt algorithm is a global search algorithm that decreases the mean square error between the actual output and estimated output much more rapidly with time.

Input data into the neural network were rescaled and the equation is shown as follows:

$$R_{\text{Re}\,scaled} = 0.1 + 0.65 \times (\frac{R_i}{R_{max}}) \qquad\qquad 4.41$$

where the $R_{\text{Re}\,scaled}$, bounded between 0.1 and 0.75, is the rescaled coordinate components (X, Y), raw NEXRAD grid values or compound training or testing data sets that rain gage and NEXRAD data are lumped together, where the Ri is the initial coordinate components (X, Y), raw NEXRAD grid values or compound training or testing data sets that rain gage and NEXRAD data are lumped together, where the $Rmax$ is the maximum value of the coordinate components (X, Y), raw NEXRAD grid values or compound training or testing data sets that rain gage and NEXRAD data are lumped together.

The available NEXRAD Stage III data were daily rainfall in a 27 x 32 grid. This data set is transformed into 27 x 32 = 864 triplets of inputs. The X and Y coordinates of each pixel form two of the three inputs; the third input is the radar-measured rainfall $Rr(x,y)$ (see Figure 4.3). The same transformation is performed on the SEMCOG rain gage data with the only difference that the third input is the gage-measured rainfall $Rg(x,y)$. The data sets of NEXRAD Stage III and rain gage triplets constitute the compound data set that is available for training and testing the feed-forward neural network. The X and Y coordinates serve as inputs to the network, $Rr(x,y)$ or $Rg(x,y)$ is the desired output, and $Rr'(x,y)$ or $Rg'(x,y)$ is the estimated radar precipitation (the actual

output of the single neuron in the output layer). Each of these triplets represents a rainfall pattern.

The neural network was trained in two phases: primary and secondary. During the primary training phase, the desired output was the radar-derived rainfall surface only. The process was repeated until the network learned a functional representation of the radar-derived rainfall surface, which was close to the original radar image. The second training phase used the same network without reinitializing its connection weights. The new patterns that the network was asked to learn consist of the gage measurements and the remaining new patterns were selected points in the radar image, with different coordinates from the rain gages. The inputs to the network will still be the coordinates X and Y. The radar- or rain gage-measured values of rainfall will be the desired output.

The optimal topologies (hidden layer number and neuron number in a hidden layer) of the feed-forward neural network were determined by the trial-and-error method. This was to test what type of the topology of the ANN model performs the best by varying with from one hidden layer to three hidden layers and various neuron numbers in each of hidden layer. The best set of the connection weight trained by the calibration of the ANN model was used to validate the validation data set. The performances of both the OC and ANN models were examined by the model efficiency criteria. The best performance of the model was used to adjust the NEXRAD Stage III data for the entire state of Michigan.

58
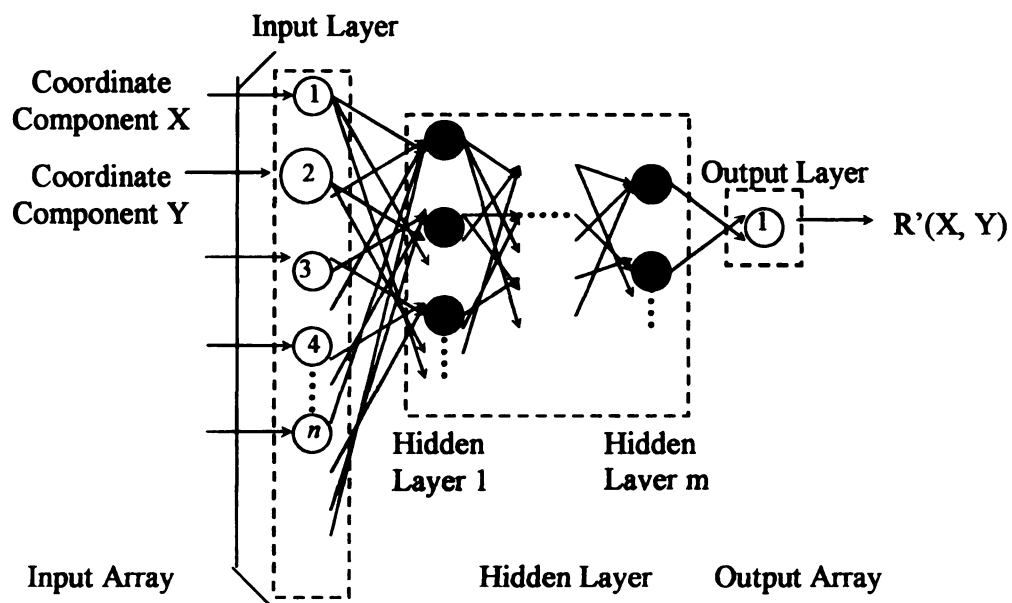
Figure 4.3. Feedforward Neural Network with Inputs (Coordinate X and Y) and
Output (R'(X, Y)).

APPLICATION OF THE MODELING METHODS IN MICHIGAN

The main purpose of modeling Michigan is to apply the ANN-based model to adjust Stage III NEXRAD data across the State of Michigan using National Weather Service gages and evaluate its performance. In this study, the ANN model is used for modeling the entire state of Michigan. Also, the performances of three types of NEXRAD grid sizes are evaluated by the improved performance of the Michigan daily Stage III NEXRAD data.

4.4. Precipitation Data Sources

Hourly rain gage observation data from Michigan used in this study were obtained from the Michigan Climatological Resources Program. Forty-two Fisher & Porter rain gages were used to record real-time rainfall information. The Fisher & Porter rain gage consisted of a collection bucket, a weighing device, an indicator dial and a paper tape for recording. Precipitation amounts were recorded at 2.54 mm increments. The maximum capacity was 495.3 mm. A machine punched holes in a paper tape on a moving scroll every 15 minutes. Around the first of the month the paper tapes were sent to Asheville, North Carolina where they were read and published. The time periods of the data used for this study were from the months of May to September from 1999 to 2000. The same hourly Stage III NEXRAD data of Midwestern area used in the pilot study is used for this study.

4.5. Methods

The methods of GIS data management used for modeling the state of Michigan are the same methods as described in Section 4.3.1. The only different one is to rescale

the 4-km NEXRAD data into 16-km resolutions and transform back to the 4-km resolution NEXRAD grids.

In this study, six daily precipitation events occurring in Michigan were selected for examining the performances of ANN model. These 6 precipitation events are divided into two types of the precipitation events: full and partial coverage. The first type of the precipitation event was that the Michigan NWS rain gage network was fully covered by the precipitation. Three of six events were full coverage events, in which each rain gage registered precipitation. The remaining three events were partial coverage events, where a portion of the rain gage network registers no rain. These six daily precipitation events were further classified into three levels of precipitation events by their daily mean rain gage values by natural break method. These three types of precipitation events were light, moderate, and heavy precipitation events. The ranges of each level of daily precipitation events are: light (< 6.73 mm), moderate (6.73 – 9.71 mm), and heavy (> 9.71 mm). These three ranges are different from the traditional one. The range of the heavy precipitation events are equivalent to that of the moderate precipitation events of the traditional classification method.

Chapter 5 RESULTS AND DISCUSSION
PILOT STUDY: MODELING SEMCOG, MICHIGAN

5.1 Results of Statistical Analyses for Pilot Study

In the pilot study, hourly precipitations were analyzed to determine the agreement of occurrence of precipitation between the two rainfall sources and the magnitude of the difference between the rain gage measurements and the NEXRAD estimate. This analysis was performed as a preliminary study to justify the use of further post processing of the NEXRAD surface with ground gages using artificial neural networks and ordinary cokriging. In the first portion of the analysis, hourly gage rainfall values and NEXRAD estimates within the SEMCOG network were compared against each other to determine if there was agreement on the occurrence of rainfall. The comparisons were grouped into one of four possible conditions (See Table 4.1). For each year in the study, the gage-hours in each condition were summed over the year. Over the 10 month time period there were approximately 500,000 gage-hours. These data are shown in Table 5.1.

Table 5.1 Hourly Precipitation Distribution Conditions from May through September.

Condition	1999		2000	
	Occurrence (Gage – hr)	Percent of Total (%)	Occurrence (Gage – hr)	Percent of Total (%)
1	4092	1.69	7895	3.17
2	11326	4.67	13442	5.40
3	5091	2.10	6368	2.56
4	221867	91.54	221247	88.87

It is obvious from Table 5.1 that for the vast majority of the time from May through September, neither the rain gages nor NEXRAD recorded rainfall events. Somewhat disturbing though, the occurrence of condition 2 is twice as frequent as condition 1. This means that during a given rainfall event, NEXRAD is twice as likely to not register a true rainfall occurrence. Similarly, condition 3 occurs roughly with the

same frequency as condition 1. This suggests that false positives are recorded by NEXRAD with roughly equal frequency as it records "true" rainfall. Further analysis was performed to examine the magnitude and significance of these errors in conditions 1 – 3. Errors between NEXRAD and gages occurring in condition 1 are shown in Table 5.2.

Table 5.2 Differences between Hourly NEXRAD and Gage Values in Condition 1.

	1999	2000
Mean Bias (mm)	-0.12	0.32
Absolute Mean Bias (mm)	3.11	3.29
Mean rainfall across gages (mm)	2.68	3.05

It can be seen from Table 5.2 that in 1999, NEXRAD on average underestimates hourly rainfall by 0.12 mm, which is in agreement with most previous studies. However, in 2000, NEXRAD overestimated hourly rainfall by 0.32 mm. The absolute magnitude of error between gages and NEXRAD is quite high, greater than 3 mm per hour in both years, which is greater than the mean hourly rainfall recorded at the gages. Additionally, the error between gages and NEXRAD during these time periods was quite variable. Figures 5.1 and 5.2 display the monthly mean bias between NEXRAD and gages for 1999 and 2000, respectively. It can be seen that across the time period NEXRAD both overestimates and underestimates monthly rainfall. These inconsistencies are most likely due to the distribution of storm types throughout the study period since NEXRAD generally underestimates convective storms and overestimates stratified storms. So for any given time period, the agreement between NEXRAD and gages will probably be depended on the distribution of storm types across the rain gage network. This adds quite a bit of uncertainty in using *raw* Stage III NEXRAD for rainfall estimation.
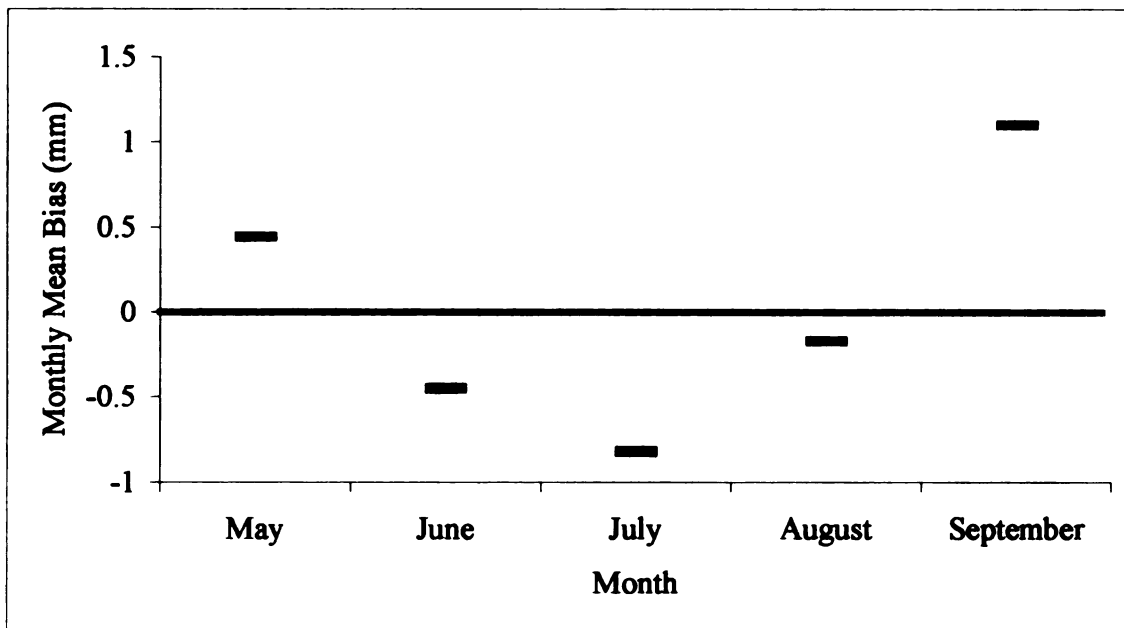
Figure 5.1 Monthly mean bias between hourly NEXRAD and rain gage network in 1999.
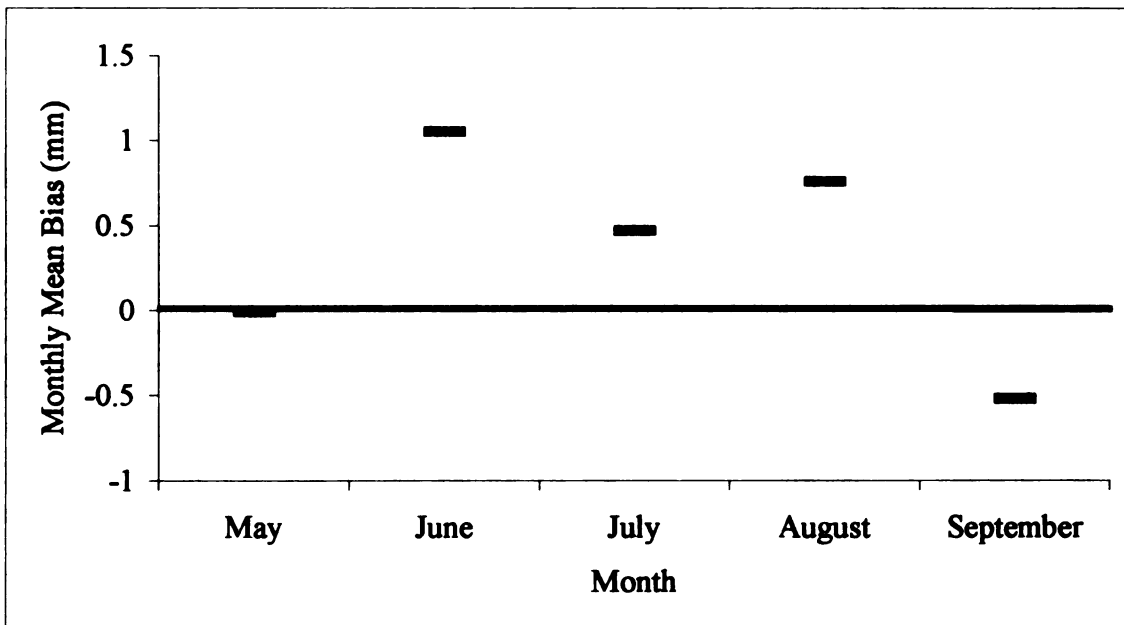
Figure 5.2 Monthly mean bias between hourly NEXRAD and rain gage network in 2000.

Table 5.3 displays the absolute mean bias between hourly gages readings and NEXRAD for conditions 2 and 3. The bias associated with condition 2 was similar between 1999 and 2000. Examining the bias in condition 2 provides some insightful information. It gives a threshold hourly rainfall rate at which NEXRAD is not able to register a true precipitation event. With the SEMCOG data, this corresponds to an hourly rainfall rate of roughly 1.25 mm/hr. This shows that while condition 2 occurs much more frequently than conditions 1, the rainfall rates involved are quite small. This suggests that condition 2 is occurring in lighter intensity rain events or is occurring during periods of light rainfall during more intense storm events. Figures 5.3 and 5.4 display the histogram of the distribution of average condition 2 error at each gage in the network for 1999 and 2000, respectively. It can be seen from these two figures that the error associated with condition 2 appears to be fairly well behaved, but slightly skewed.

Table 5.3 Hourly Errors between NEXRAD and Gage Values in Conditions 2 and 3.

	1999	2000
Condition 2 – gage value Absolute Mean Bias (mm)	1.22	1.28
Condition 3 – NEXRAD value Absolute Mean Bias (mm)	2.37	3.21
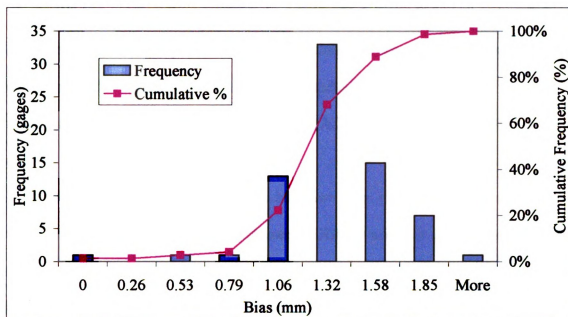
Figure 5.3 Frequency distribution of condition 2 bias averaged across SEMCOG gages for 1999.
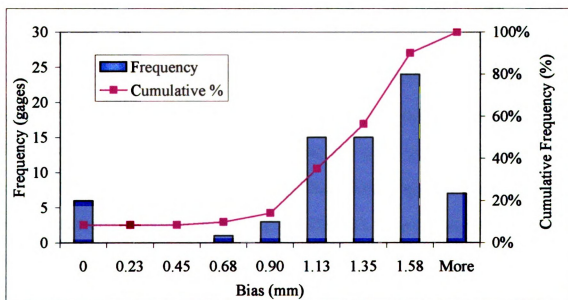
Figure 5.4 Frequency distribution of condition 2 bias averaged across SEMCOG gages for 2000.

When condition 3 occurs, hourly NEXRAD delivers a "false positive" for the occurrence of rainfall. From Table 5.1, condition 3 occurs roughly as frequent as condition 1. The magnitude of this error was quite high, 2.37 mm/hr in 1999 and 3.21 mm/hr in 2000. This condition describes NEXRAD by overestimation rainfall in a given area.

The overall conclusions that can be drawn from this analysis is that not only is there error between rainfall values between NEXRAD and rain gages, there is frequent disagreement between the two sources on whether or not it is even raining in any given hour. There are many physical explanations that have been presented in the literature review on why there is disagreement on rainfall occurrence. It has been shown in this study that NEXRAD frequently fails to register a true rainfall occurrence (condition 2), but the intensity/volume of rainfall involved in this is small (~ 1.25 mm/hr). In a spatial water balance application using NEXRAD, this most likely would not greatly affect the outcome. Conversely, when NEXRAD registers a "false positive" for rainfall occurrence (condition 3), the magnitude of error is quite high, more than twice as high as condition 2. In the same spatial water balance application, this error would probably affect the outcome by overestimating rainfall amounts. The results of this analysis suggest that it would be advantageous to try to improve the NEXRAD Stage III data using models (i.e. artificial neural networks and ordinary cokriging) to reduce the occurrence and magnitude of errors associated with conditions 1, 2, and 3.

5.2. Results of Pilot Study: Modeling SEMCOG, Michigan

The Stage III NEXRAD precipitation estimates provided excellent storm-scale information about the spatial and temporal evolution of precipitation systems; often much

better than rain gage networks. Also, Stage III NEXRAD precipitation estimates provided very valuable input as part of a comprehensive, multi-sensor precipitation system. However, many research have shown that hourly, daily, and monthly mean areal precipitation values derived from Stage III NEXRAD were generally biased low compared with gage-derived estimates, especially for convective precipitation events. Therefore, the goal of this study was to optimally combine these two types of measurements giving estimates that were superior to estimates obtainable from each individual device alone.

In this study, the rain gage measurements from the SEMCOG rain gage network were regarded as ground truth measurements used to improve the daily NEXRAD Stage III precipitation fields. Twenty-two SEMCOG daily precipitation events were used to evaluate both the OC and the ANN models by calibrating and validating the daily Stage III NEXRAD data.

Tables 5.4 – 5.7 show the results of modeling the twenty-two SEMCOG precipitation events by evaluating the performances of both the OC and the ANN models. These tables also compared with the initial synthetic statistical matrices to learn whether both models improved the initial synthetic statistical matrices of the raw Stage III NEXRAD data. Two daily precipitation events are demonstrated in details in Sections 5.2.1 and 5.2.2.

5.2.1. Results of the Precipitation Event 05/06/1999

Initial Synthetic Statistical Analysis

This precipitation event was grouped as a light precipitation event. It only covered half of the SEMCOG area. In Table 5.5, 62 SEMCOG rain gage measurements and

Table 5.4 Results of the Examined SEMCOG Light Precipitation Events (Full Coverage)

Slight Precipitation Events (Full Coverage)	5/23/1999			7/9/1999			7/31/1999			9/24/1999			9/12/2000		
Calibration	Initial	ANN	OC	Initial	ANN	OC	Initial	ANN	OC	Initial	ANN	OC	Initial	ANN	OC
	28 gages			29 gages			29 gages			28 gages			28 gages		
Mean_Gage (mm)	3.14			8.18			6.12			3.64			4.08		
Mean_NEXRAD (mm)	7.45			12.29			9.09			1.76			4.68		
Mean_ANN (mm)		4.63			9.65			6.01			2.49			4.32	
Mean_OC			3.13			12.16			9.35			1.76			4.71
CC	0.14	0.80	-0.04	0.80	0.93	0.71	0.61	0.89	0.21	0.70	0.81	0.63	0.81	0.92	0.33
R-Square	0.02	0.64	0.00	0.64	0.86	0.51	0.37	0.80	0.04	0.49	0.65	0.40	0.66	0.84	0.11
MB (mm)	-4.31	-2.82	-4.32	4.11	1.47	3.98	2.96	-0.11	3.23	-1.87	-1.15	-1.87	0.60	0.24	0.63
AMB (mm)	4.57	2.96	4.64	4.15	1.61	4.06	4.11	1.79	5.26	1.88	1.23	1.87	1.22	0.84	1.68
NBIAS	-0.58	-0.38	-0.58	0.50	0.18	0.49	0.48	-0.02	0.53	-0.52	-0.32	-0.51	0.15	0.06	0.15
NRMSE	1.01	1.07	1.70	1.74	0.75	1.64	1.00	0.45	1.26	1.44	0.97	1.49	0.72	0.44	1.04
Validation															
	34 gages			33 gages			33 gages			30 gages			35 gages		
Mean_Gage (mm)	8.02			9.36			7.48			4.29			4.01		
Mean_NEXRAD (mm)	3.37			14.02			9.80			1.89			5.93		
Mean_ANN (mm)		4.23			14.94			7.97			3.07			5.38	
Mean_OC			3.44			14.40			9.63			1.87			4.84
CC	0.25	0.32	0.19	0.60	0.55	0.53	0.31	0.56	0.04	0.51	0.61	0.39	0.79	0.78	0.63
R-Square	0.06	0.10	0.04	0.36	0.30	0.28	0.09	0.32	0.00	0.26	0.37	0.15	0.63	0.61	0.40
MB (mm)	-4.65	-3.78	-4.57	4.66	5.58	5.04	2.32	0.49	2.14	-2.40	-1.22	-2.43	1.92	1.36	0.83
AMB (mm)	4.70	4.27	4.75	4.89	5.76	5.29	5.71	3.61	5.10	2.44	1.60	2.49	2.45	2.17	1.67
NBIAS	-0.58	-0.47	-0.57	0.50	0.60	0.54	0.31	0.07	0.29	-0.56	-0.28	-0.57	0.48	0.34	0.21
NRMSE	0.99	1.56	1.68	1.15	3.44	2.89	1.21	0.90	1.19	0.95	1.00	1.52	1.07	1.26	0.94
Combination															
	62 gages			62 gages			62 gages			58 gages			63 gages		
Mean_Gage (mm)	7.76			8.81			6.85			3.98			4.04		
Mean_NEXRAD (mm)	3.27			13.21			9.47			1.83			5.38		
Mean_ANN (mm)		4.41			12.47			7.05			2.79			4.91	
Mean_OC			3.30			13.35			9.50			1.82			4.79
CC	0.21	0.49	0.11	0.72	0.69	0.63	0.43	0.72	0.14	0.58	0.69	0.49	0.77	0.80	0.50
R-Square	0.04	0.24	0.01	0.51	0.47	0.40	0.18	0.52	0.02	0.34	0.48	0.24	0.59	0.64	0.25
MB (mm)	-4.49	-3.35	-4.46	4.40	3.66	4.55	2.62	0.21	2.65	-2.15	-1.19	-2.16	1.33	0.86	0.74
AMB (mm)	4.64	3.68	4.70	4.54	3.82	4.71	4.96	2.76	5.18	2.17	1.42	2.19	1.90	1.58	1.67
NBIAS	-0.58	-0.43	-0.57	0.50	0.42	0.52	0.38	0.03	0.39	-0.54	-0.30	-0.54	0.33	0.21	0.18
NRMSE	1.68	1.37	1.68	2.12	2.16	2.15	1.17	0.72	1.21	1.44	0.98	1.48	1.12	0.95	0.99

Table 5.5 Results of the Examined SEMCOG Light Precipitation Events (Partial Coverage)

Slight Precipitation Events (Partial Coverage)	5/6/1999			5/24/1999			6/9/1999		
	Initial	ANN	OC	Initial	ANN	OC	Initial	ANN	OC
Calibration	28 gages			28 gages			29 gages		
Mean_Gage (mm)	2.36			2.16			1.19		
Mean_NEXRAD (mm)	1.96			0.18			1.45		
Mean_ANN (mm)		2.37			0.95			1.67	
Mean_OC			2.03			0.19			1.26
CC	0.72	0.79	0.51	0.04	0.81	0.08	0.90	0.96	-0.03
R-Square	0.51	0.63	0.26	0.00	0.65	0.01	0.81	0.91	0.00
MB (mm)	-0.40	0.01	-0.33	-1.98	-1.21	-1.97	0.26	0.47	0.07
AMB (mm)	0.91	0.79	1.16	1.99	1.31	2.05	0.89	0.85	1.88
NBIAS	-0.17	0.00	-0.14	-0.92	-0.56	-0.91	0.22	0.40	0.05
NRMSE	0.74	0.61	0.89	1.79	1.11	1.77	0.45	0.41	1.18
Validation	34 gages			34 gages			33 gages		
Mean_Gage (mm)	2.22			1.97			1.32		
Mean_NEXRAD (mm)	2.58			0.15			1.93		
Mean_ANN (mm)		2.57			0.27			2.02	
Mean_OC			1.75			0.28			1.56
CC	0.63	0.80	0.66	0.63	0.52	0.44	0.72	0.97	0.33
R-Square	0.41	0.63	0.43	0.40	0.27	0.19	0.52	0.95	0.11
MB (mm)	0.36	0.35	-0.47	-1.83	-1.70	-1.69	0.60	0.70	0.23
AMB (mm)	1.46	1.09	1.05	1.83	1.70	1.69	1.57	1.13	1.72
NBIAS	0.16	0.16	-0.21	-0.93	-0.86	-0.86	0.45	0.53	0.18
NRMSE	1.19	0.84	0.81	0.97	1.94	1.95	0.71	0.38	0.95
Combination	62 gages			62 gages			62 gages		
Mean_Gage (mm)	2.28			2.06			1.26		
Mean_NEXRAD (mm)	2.30			0.16			1.70		
Mean_ANN (mm)		2.48			0.58			1.85	
Mean_OC			1.88			0.24			1.42
CC	0.62	0.76	0.60	0.26	0.64	0.25	0.78	0.97	0.20
R-Square	0.38	0.58	0.36	0.07	0.42	0.06	0.60	0.94	0.04
MB (mm)	0.02	0.20	-0.41	-1.89	-1.48	-1.82	0.44	0.59	0.15
AMB (mm)	1.21	0.95	1.10	1.90	1.53	1.85	1.25	1.00	1.80
NBIAS	0.01	0.09	-0.18	-0.92	-0.72	-0.88	0.35	0.47	0.12
NRMSE	1.02	0.75	0.84	1.89	1.49	1.84	0.65	0.39	1.03

Table 5.5 Results of the Examined SEMCOG Light Precipitation Events (Partial Coverage) (Continued)

Slight Precipitation Events (Partial Coverage)	5/16/2000			5/31/2000			7/31/2000		
	Initial	ANN	OC	Initial	ANN	OC	Initial	ANN	OC
Calibration		27 gages			27 gages			26 gages	
Mean_Gage (mm)	6.59			2.42			5.51		
Mean_NEXRAD (mm)	1.08			4.53			6.98		
Mean_ANN (mm)		1.60			3.34			5.37	
Mean_OC			1.08			4.90			7.69
CC	0.49	0.61	0.57	0.85	0.88	0.43	0.50	0.93	0.57
R-Square	0.24	0.38	0.33	0.72	0.78	0.19	0.25	0.86	2.18
MB (mm)	-5.51	-4.99	-5.51	2.11	0.92	2.48	1.47	-0.14	2.06
AMB (mm)	5.51	4.99	5.51	2.23	1.31	3.25	5.14	2.37	6.03
NBIAS	-0.84	-0.76	-0.84	0.87	0.38	1.03	0.27	-0.03	0.40
NRMSE	2.31	2.08	2.27	1.14	0.64	1.60	1.11	0.41	0.91
Validation		35 gages			35 gages			34 gages	
Mean_Gage (mm)	6.83			3.51			2.82		
Mean_NEXRAD (mm)	2.20			6.73			3.05		
Mean_ANN (mm)		4.04			6.84			3.28	
Mean_OC			1.68			7.43			3.64
CC	0.14	0.76	0.37	0.76	0.82	0.61	0.88	0.78	0.77
R-Square	0.02	0.58	0.14	0.58	0.67	0.38	0.78	0.61	0.59
MB (mm)	-4.63	-2.79	-5.15	3.23	3.34	3.92	0.23	0.46	0.82
AMB (mm)	4.79	2.86	5.24	3.94	3.85	4.42	1.62	2.26	2.59
NBIAS	-0.68	-0.41	-0.76	0.92	0.95	1.12	0.08	0.16	0.29
NRMSE	1.08	1.16	2.00	1.15	1.51	1.47	0.47	0.64	0.66
Combination		62 gages			62 gages			60 gages	
Mean_Gage (mm)	6.72			3.03			3.98		
Mean_NEXRAD (mm)	1.71			5.77			4.75		
Mean_ANN (mm)		2.98			5.31			4.18	
Mean_OC			1.42			6.33			5.39
CC	0.26	0.65	0.45	0.80	0.82	0.55	0.61	0.87	0.65
R-Square	0.07	0.42	0.20	0.64	0.68	0.30	0.38	0.75	0.42
MB (mm)	-5.01	-3.75	-5.31	2.74	2.28	3.29	0.77	0.20	1.41
AMB (mm)	5.10	3.78	5.36	3.20	2.75	3.91	3.15	2.31	4.08
NBIAS	-0.75	-0.56	-0.79	0.90	0.75	1.09	0.19	0.05	0.35
NRMSE	2.13	1.57	2.10	1.37	1.23	1.50	0.92	0.50	0.82

71

Table 5.6 Results of the Examined SEMCOG Moderate Precipitation Events

Moderate Precipitation Events	5/17/1999			7/23/1999			8/13/1999		
	Initial	ANN	OC	Initial	ANN	OC	Initial	ANN	OC
Calibration	28 gages			29 gages			28 gages		
Mean_Gage (mm)	13.34			17.01			17.83		
Mean_NEXRAD (mm)	32.16			19.18			13.56		
Mean_ANN (mm)		19.76			17.30			14.98	
Mean_OC			31.71			19.27			13.73
CC	0.72	0.91	0.66	0.74	0.95	0.52	0.74	0.90	0.48
R-Square	0.51	0.82	0.43	0.54	0.91	0.27	0.55	0.81	0.23
MB (mm)	18.83	6.43	18.37	2.17	0.29	2.26	-4.27	-2.84	-4.09
AMB (mm)	18.83	6.73	18.37	5.35	2.44	6.57	6.01	4.02	7.06
NBIAS	1.41	0.48	1.38	0.13	0.02	0.13	-0.24	-0.16	-0.23
NRMSE	3.29	1.26	3.09	0.71	0.31	0.88	0.83	0.58	0.98
Validation	34 gages			33 gages			33 gages		
Mean_Gage (mm)	15.26			20.45			15.57		
Mean_NEXRAD (mm)	32.51			20.49			13.12		
Mean_ANN (mm)		28.68			22.56			13.01	
Mean_OC			30.30			19.96			12.97
CC	0.80	0.85	0.70	0.82	0.80	0.62	0.74	0.73	0.65
R-Square	0.64	0.72	0.49	0.67	0.65	0.39	0.55	0.53	0.42
MB (mm)	17.24	13.42	15.03	0.04	2.11	-0.49	-2.45	-2.56	-2.60
AMB (mm)	17.42	13.48	15.43	6.51	6.33	8.35	5.25	5.30	5.93
NBIAS	1.13	0.88	0.99	0.00	0.10	-0.02	-0.16	-0.16	-0.17
NRMSE	2.07	1.64	1.77	0.61	0.62	0.79	0.70	0.74	0.84
Combination	62 gages			64 gages			61 gages		
Mean_Gage (mm)	14.39			18.84			16.61		
Mean_NEXRAD (mm)	32.35			19.88			13.32		
Mean_ANN (mm)		24.65			20.10			13.92	
Mean_OC			30.93			19.64			13.32
CC	0.77	0.85	0.67	0.79	0.86	0.59	0.73	0.81	0.57
R-Square	0.59	0.71	0.45	0.62	0.74	0.35	0.54	0.65	0.33
MB (mm)	17.96	10.26	16.54	1.04	1.26	0.80	-3.28	-2.69	-3.28
AMB (mm)	18.05	10.43	16.76	5.97	4.51	7.52	5.60	4.71	6.45
NBIAS	1.25	0.71	1.15	0.06	0.07	0.04	-0.20	-0.16	-0.20
NRMSE	2.43	1.54	2.18	0.64	0.53	0.82	0.77	0.67	0.90

Table 5.6 Results of the Examined SEMCOG Moderate Precipitation Events (Continued)

Moderate Precipitation Events	5/28/2000 Initial	ANN	OC	8/17/2000 Initial	ANN	OC	9/14/2000 Initial	ANN	OC
Calibration	27 gages			33 gages			28 gages		
Mean_Gage (mm)	11.01			10.96			12.44		
Mean_NEXRAD (mm)	6.71			7.88			8.15		
Mean_ANN (mm)		8.42			8.38			9.64	
Mean_OC			6.53			7.90			8.12
CC	0.75	0.90	0.73	0.49	0.56	0.54	0.59	0.84	0.79
R-Square	0.56	0.81	0.54	0.24	0.31	0.29	0.34	0.71	0.62
MB (mm)	-4.30	-2.59	-4.47	-3.08	-2.58	-3.06	-4.28	-2.80	-4.32
AMB (mm)	5.29	3.12	5.25	3.08	2.76	3.06	4.59	3.05	4.52
NBIAS	-0.39	-0.24	-0.41	-0.28	-0.24	-0.28	-0.34	-0.22	-0.35
NRMSE	0.97	0.59	0.98	1.77	1.60	1.73	1.26	0.85	1.18
Validation	35 gages			28 gages			35 gages		
Mean_Gage (mm)	12.71			11.22			14.21		
Mean_NEXRAD (mm)	10.59			8.17			9.07		
Mean_ANN (mm)		10.83			9.30			12.43	
Mean_OC			10.76			7.99			8.51
CC	0.37	0.26	0.50	0.03	0.78	-0.09	0.58	0.75	0.78
R-Square	0.13	0.06	0.25	0.00	0.61	0.01	0.33	0.56	0.61
MB (mm)	-2.13	-1.88	-1.96	-3.05	-1.92	-3.23	-5.14	-1.78	-5.70
AMB (mm)	4.86	4.97	4.56	3.10	2.03	3.30	5.61	2.93	6.05
NBIAS	-0.17	-0.15	-0.15	-0.27	-0.17	-0.29	-0.36	-0.13	-0.40
NRMSE	1.34	1.60	1.28	1.08	1.10	1.90	0.91	0.74	1.23
Combination	62 gages			61 gages			63 gages		
Mean_Gage (mm)	11.97			11.10			13.42		
Mean_NEXRAD (mm)	8.90			8.04			8.66		
Mean_ANN (mm)		9.78			8.88			11.19	
Mean_OC			8.92			7.95			8.33
CC	0.57	0.57	0.61	0.23	0.64	0.20	0.59	0.77	0.78
R-Square	0.32	0.32	0.37	0.05	0.41	0.04	0.35	0.60	0.61
MB (mm)	-3.07	-2.19	-3.05	-3.06	-2.22	-3.15	-4.76	-2.23	-5.09
AMB (mm)	5.04	4.16	4.86	3.09	2.36	3.19	5.16	2.98	5.37
NBIAS	-0.26	-0.18	-0.26	-0.28	-0.20	-0.28	-0.35	-0.17	-0.38
NRMSE	1.19	1.10	1.10	1.83	1.33	1.82	1.22	0.77	1.20

Table 5.7 Results of the Examined SEMCOG Heavy Precipitation Events

Heavy Precipitation Events	7/1/1999			5/18/2000			7/28/2000			8/6/2000			9/11/2000		
	Initial	ANN	OC	Initial	ANN	OC	Initial	ANN	OC	Initial	ANN	OC	Initial	ANN	OC
Calibration		29 gages			27 gages			26 gages			33 gages			35 gages	
Mean_Gage (mm)	21.57			30.53			31.66			21.35			26.96		
Mean_NEXRAD (mm)	14.02			26.71			58.52			17.02			33.88		
Mean_ANN (mm)		17.06			28.97			40.16			20.05			30.54	
Mean OC			14.02			26.06			58.57			16.85			34.00
CC	0.74	0.95	0.64	0.69	0.92	0.66	0.54	0.89	0.11	0.76	0.96	0.72	0.66	0.93	0.62
R-Square	0.55	0.90	0.40	0.48	0.85	0.44	0.29	0.80	0.01	0.57	0.92	0.52	0.43	0.87	0.38
MB (mm)	-7.56	-4.51	-7.55	-3.82	-1.56	-4.47	26.86	8.50	26.91	-4.33	-1.29	-4.49	6.92	3.58	7.04
AMB (mm)	8.78	4.78	8.80	5.84	2.40	5.74	29.62	10.37	31.99	4.63	1.49	4.76	11.84	5.92	13.18
NBIAS	-0.35	-0.21	-0.35	-0.13	-0.05	-0.15	0.85	0.27	0.85	-0.20	-0.06	-0.21	0.26	0.13	0.26
NRMSE	0.95	0.56	1.02	1.03	0.44	0.99	2.05	0.68	2.15	1.04	0.37	1.07	0.84	0.42	0.87
Validation		33 gages			35 gages			34 gages			28 gages			28 gages	
Mean_Gage (mm)	26.27			33.06			35.95			21.67			27.35		
Mean_NEXRAD (mm)	13.91			29.92			69.26			16.84			34.25		
Mean_ANN (mm)		15.92			31.83			64.37			18.75			35.81	
Mean OC			13.52			27.81			60.91			17.47			28.35
CC	0.81	0.80	0.89	0.75	0.79	0.76	0.77	0.76	0.56	0.73	0.76	0.73	0.93	0.90	0.82
R-Square	0.66	0.64	0.80	0.57	0.62	0.58	0.59	0.57	0.31	0.53	0.58	0.53	0.86	0.81	0.67
MB (mm)	-12.36	-10.35	-12.75	-3.14	-1.22	-5.24	33.31	28.43	24.96	-4.83	-2.92	-4.19	6.90	8.46	0.99
AMB (mm)	12.97	10.94	13.23	5.01	5.03	6.01	33.77	30.92	28.90	5.45	4.96	4.93	8.30	10.77	10.44
NBIAS	-0.47	-0.39	-0.49	-0.09	-0.04	-0.16	0.93	0.79	0.69	-0.22	-0.13	-0.19	0.25	0.31	0.04
NRMSE	0.83	0.96	1.15	0.90	1.03	1.09	0.98	1.75	1.54	0.84	1.03	0.96	0.48	0.67	0.61
Combination		62 gages			62 gages			60 gages			61 gages			63 gages	
Mean_Gage (mm)	24.07			31.95			34.09			21.52			27.18		
Mean_NEXRAD (mm)	13.96			28.52			64.61			16.92			34.08		
Mean_ANN (mm)		16.45			30.58			53.88			19.35			33.47	
Mean OC			13.76			27.05			59.90			17.19			30.86
CC	0.77	0.83	0.74	0.73	0.82	0.72	0.68	0.76	0.40	0.74	0.80	0.73	0.84	0.89	0.73
R-Square	0.59	0.69	0.55	0.54	0.67	0.52	0.46	0.58	0.16	0.54	0.63	0.53	0.70	0.79	0.53
MB (mm)	-10.12	-7.62	-10.32	-3.43	-1.37	-4.90	30.51	19.79	25.81	-4.60	-2.17	-4.33	6.91	6.29	3.68
AMB (mm)	11.01	8.05	11.15	5.37	3.89	5.90	31.97	22.01	30.24	5.07	3.37	4.85	9.87	8.62	11.66
NBIAS	-0.42	-0.32	-0.43	-0.11	-0.04	-0.15	0.90	0.58	0.76	-0.21	-0.10	-0.20	0.25	0.23	0.14
NRMSE	1.03	0.82	1.09	1.00	0.78	1.02	1.87	1.46	1.77	1.05	0.84	1.01	0.65	0.59	0.72

74

corresponding NEXRAD grid values were compared by statistical analysis. The results indicated poor correlation between rain gage and radar measurements. Table 5.5 also showed the difference between the average of rain gage values and the average of Stage III NEXRAD values produced by arithmetical averaging method. This showed the precipitation patterns measured by both devices were poorly correlated, but the areal average precipitation distributions measured by both devices were very different.

The small positive MB and NBIAS showed that the radar-derived precipitation values slightly overestimated the precipitation values. Both AMB and NRMSE values were greater than 1.0 suggesting that the measurement error of NEXRAD radar was large.

Table 5.5 and Figure 5.5 depict the initial synthetic statistics of this examined precipitation event. Normally, the dependence between raw NEXRAD data and rain gage data showed up in a bivariate scatter diagram as a tendency to form an elliptical cloud along a diagonal. The cloud had a major axis along the line at 45 degree to the positive transverse axes in the case of positive correlation (CC = 1), and a major axis along the perpendicular line at 135 degree to the positive transverse axis in the case of negative correlation (CC = -1). According to the results of Section 5.1, the number and percentage of the Condition 2 by hourly, daily, monthly, and yearly were very high. Thus, most of the slopes of the trend line equations in these twenty-two bivariate diagrams were much less than one, especially the light precipitation events.

In Figure 5.5, the trend line equation showed a low slope value (0.49) and the bivariate scatter diagram depicted an elliptical shape with a wide minor axis. This showed that both measurements present many disagreements but are still slightly correlated with each other.

Figure 5.5 A Bivariate Scatter Diagram for Both Raw Stage III NEXRAD Data and
SEMCOG Rain Gage Measurements (Daily precipitation event occurred
on 05/06/1999). Light Precipitation Event.

Figure 5.6 depicted the daily raw NEXRAD Stage III precipitation surface. Approximately one half of the SEMCOG network was covered by the precipitation. Twenty-eight rain gages (yellow stars) were used for calibration (or cross validation), and thirty-four rain gages (white stars) were used for validation. The data used for calibration had higher CC and R^2 values than the data used for validation. The negative MB and NBIAS values in the calibration showed that the NEXRAD radar underestimated the precipitation. The positive MB and NBIAS values in the validation showed that the NEXRAD radar overestimated the precipitation. The AMB and NRMSE values of the validation were higher than those of the calibration showed that the radar estimation error in the validation was higher than that in the calibration.

No two or more rain gage points occupied a NEXRAD grid cell. Therefore, the percentage of the density distribution of the SEMCOG rain gages in the SEMCOG area with 27 by 32 4-km grids were calculated by the 62 gage-occupied grids divided by 864 NEXRAD grids and multiplied by 100%, which was 7.2%.

Results of OC Model

The OC approach provided an estimate of the precipitation surface assuming second-order stationarity to minimize the uncertainty associated with semivariogram estimation. It considered the statistical properties of the rain gages, the radar, and the dependence of each of the devices on each other, and eliminates the error due to point sampling of rainfall by rain gages.

The first step of processing for the OC model is to produce the semivariograms for NEXRAD radar and rain gage variates, and cross semivariogram for both variates. The two semivariograms and cross semivariogram are shown in Figure 5.7, 5.8, and 5.9,

**Raw NEXRAD Stage III Precipitation Surface
(Daily Precipitation Event Occurred on 05/06/1999)**

Figure 5.6 Daily Raw Stage III NEXRAD Precipitation Surface (Daily
precipitation event occurred on 05/06/1999). Light Precipitation Event.
*The SEMCOG area was partially covered by the precipitation event.
**The yellow and white stars were used for the calibration and
validation rain gages, respectively. They were used in the processes of
the OC and ANN models.
***Four purple rain gages were the NWS test rain gages used to
evaluate the performance of the OC and ANN models. These four
NWS rain gages were not involved in the processes of both OC and
ANN models.

Spherical model (Co = 0 ⁷⁷⁷, Co + C = 3 829, Ao = 95400 00, r2 = 0 800,
RSS = 1 20)

Figure 5.7 Isotropic Variogram of Stage III NEXRAD Data (Daily precipitation
event occurred on 05/06/1999). Light Precipitation Event.

*The best-fit model was spherical model.

**Nugget variance: $C_0 = 0.777$; structural variance: C; sill = $C_0 + C =$
3.829; range: $A_0 = 95400$.

***Active lag distance: 72,000 m and lag interval: 8,500 m.

****R^2 or Regression Coefficient was to indicate how well the model fits
the variogram data. $R^2 = 0.800$.

***** RSS or Residual Sums of Squares was used to indicate how well
the model fits the variogram data; the lower the reduced sums of
squares, the better the model fits. RSS = 1.20.

Isotropic Variogram of Raingage Measurements (05 06 1999)
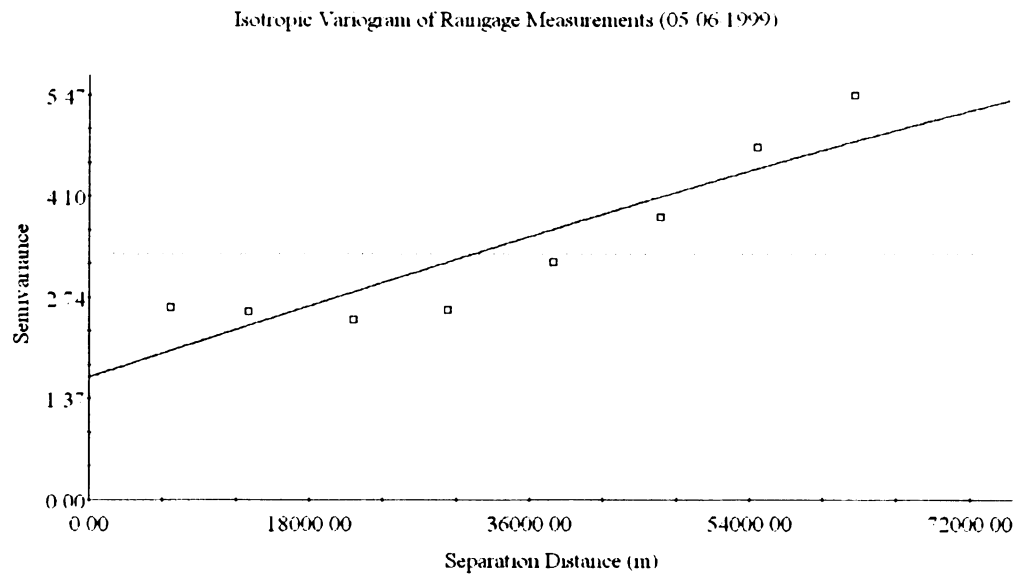
Spherical model (Co = 1 660. Co + C = 7 329, Ao = 158300 00, r2 = 0 822,
RSS = 1 67)

Figure 5.8 Isotropic Variogram of SEMCOG Rain Gage Measurements (Daily
precipitation event occurred on 05/06/1999). Light Precipitation Event.
*The best-fit model was spherical model.
**Nugget variance: C_0 = 1.660; structural variance: C; sill = C_0 + C =
7.329; range: A_0 = 158,300.
***Active lag distance: 72,000 m and lag interval: 8,400 m.
****R^2 or Regression Coefficient was to indicate how well the model fits
the variogram data. R^2 = 0.822.
***** RSS or Residual Sums of Squares was used to indicate how well
the model fits the variogram data; the lower the reduced sums of
squares, the better the model fits. RSS = 1.67.

80

Figure 5.9 Isotropic Cross Variogram of SEMCOG rain gage measurements (Daily precipitation event occurred on 05/06/1999). Light Precipitation Event.
*The best-fit model was spherical model.
**Nugget variance: C_0 = 0.450; structural variance: C; sill = C_0 + C = 4.909; range: A_0 = 129,100.
***Active lag distance: 72,000 m and lag interval: 9,000 m.
****R^2 or Regression Coefficient was to indicate how well the model fits the variogram data. R^2 = 0.765.
***** RSS or Residual Sums of Squares was used to indicate how well the model fits the variogram data; the lower the reduced sums of squares, the better the model fits. RSS = 2.52.

respectively.

The second step was to model the two semivariograms and cross semivariogram to find the best set of parameters (sill and range) for the OC model. In this case, the spherical model was the best-fit model for these semivariograms and cross semivariogram. The last step was to use the best set of parameters (sill and range) to process the OC model to derive the OC-adjusted NEXRAD precipitation surfaces. Table 5.4 shows the results by the synthetic statistic matrices. •

Range is a scalar that controls the degree of correlation between data points, usually represented as a distance. A large range value shows that more spatial continuous behavior and the variable are well correlated in space, and thus predictions resulted in fairly smooth maps of the variable of interest. Because the range values of these semivariograms and cross semivariogram are very large, the cross validation were well correlated in space. The Sill value was the maximum value of semivariogram or cross variogram. Sill value of the semivariance as the lag*(h)* goes to infinity and it was equal to the total variance of the data set. The larger the sill value is, the larger the prediction variance. Because the sill values of these semivariograms and cross semivariogram were small, the prediction variance becomes small. This will rarely affect the prediction result.

Table 5.5 shows the results after processing the OC model. Overall, the results of the cross validation were also worse than those of the initial condition. The results of the validation were slightly improved. The results of combining both cross validation and validation data were worse than those of the initial condition. Figure 5.10 depicts the OC-adjusted Stage III NEXRAD precipitation surface. Comparing with Figure 5.6, the OC-adjusted precipitation patterns degraded the valuable NEXRAD precipitation patterns.

Ordinary Cokriging-Adjusted NEXRAD Stage III Precipitation Surface
(Daily Precipitation Event Occurred on 05/06/1999)

SEMCOG
S050699_OC_mm
1
2
3
4
0

30   0   30   60 Kilometers

N
W   E
S
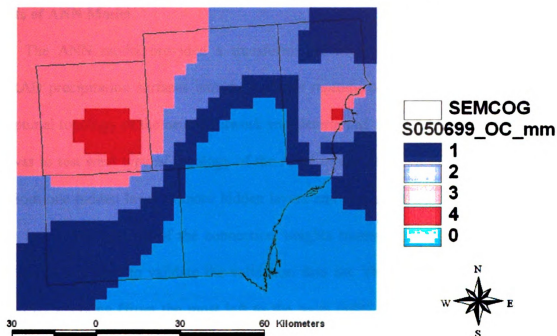
Figure 5.10 Ordinary Cokriging-Adjusted Stage III NEXRAD Precipitation Surface.
(Daily precipitation event occurred on 05/06/1999). Light Precipitation
Event.

Although OC offered a minimum variance estimate and was the best linear estimator, the semivariograms and cross semivariogram were not well behaved for both measurements, even though the model fit both semivariogram and cross semivariogram very well.

Results of ANN Model

The ANN model provided a transformation from the spatial learning of the NEXRAD precipitation surfaces into the accurate reproduction of the rain gage values. The optimal topology of the neural network was determined by a trial-and-error method. This was to test what type of topology of the ANN model performs the best by varying with from one hidden layer to more hidden layers and various neuron numbers in each hidden layer. The best set of the connection weights trained by the calibration of the ANN model was used to validate the validation data set. The neural network topology was 2-75-1 denoting (from the most left to the most right) the neuron numbers in the input layer, the first hidden layer, and the output layer, respectively. In this study, the topology of the ANN model with one hidden layer performed the best. The best set of connection weight was iteratively trained by 25 epochs per time. Over 750 times of 25 epochs were used to find the best set of connection weight. The total time spent on training and testing was about 5 hours.

Table 5.5 shows the results after processing the ANN model. Overall, the results of the calibration and validation were better than those of the initial condition. The results of combining both calibration and validation data were better than those of the initial calibration. Figure 5.11 depicts the ANN-adjusted Stage III NEXRAD precipitation surface. Comparing with Figure 5.6, the ANN-adjusted NEXRAD precipitation patterns improved the valuable NEXRAD precipitation patterns very well.

**ANN-Adjusted NEXRAD Stage III Precipitation Surface
(Daily Precipitation Event Occurred on 05/06/1999)**

SEMCOG
S050699_ANN_mm
1 - 2
3
4
5
6 - 7
8 - 9
10 - 11
12 - 13
0

30   0   30   60 Kilometers

N
W   E
S

Figure 5.11 ANN-Adjusted Stage III NEXRAD Precipitation Surface. (Daily
precipitation event occurred on 05/06/1999). Light Precipitation Event.

Performance Evaluations of Both OC and ANN Models

Two types of performance evaluations were performed by: (1) comparing the initial synthetic statistical matrices with the synthetic statistical matrices of both models, and (2) comparing the synthetic statistical matrices of both models

Table 5.5 shows that after processing the OC model, the cross validated synthetic statistical matrices did not improve the initial synthetic statistical matrices, and the validated values only slightly improved the initial synthetic statistical matrices. Both cross validated and validated values were combined together and regarded these values as the improved NEXRAD values. The adjusted NEXRAD synthetic statistical matrices were compared with the initial synthetic statistical matrices. Table 5.5 shows that the

Table 5.4 shows that after processing the ANN model both calibrated and validated synthetic statistical matrices improved the initial synthetic statistical matrices. Both calibrated and validated values were combined together and regarded these values as the improved NEXRAD values. The combined synthetic statistical matrices were compared with the initial synthetic statistical matrices. Table 5.5 shows that the calibration performance of NEXRAD precipitation surface by the ANN model improved the initial synthetic statistical matrices.

Table 5.5 shows that the synthetic statistical matrices of calibrated, validated, and combined ANN-adjusted NEXRAD precipitation were better than those of cross validated, validated, and combined OC-adjusted NEXRAD precipitation.

Figure 5.12 depicts the performances of OC- and ANN-adjusted Stage III NEXRAD data. The ANN-adjusted NEXRAD precipitation presented the best correlation with the rain gage values, because the slope of the trend line equation was very high

Figure 5.12 Performance of OC- and ANN-Adjusted Stage III NEXRAD Data
(Daily precipitation event occurred on 05/06/1999). Light Precipitation
Event.

(0.86), i.e. the difference between rain gage values and ANN-adjusted precipitation values were small. The OC-adjusted NEXRAD precipitation presented the worst correlation with the rain gage values, because the slope of the trend line equation was very low (0.4414), i.e. the difference between rain gage values and OC-adjusted precipitation values were large.

5.2.2. Results of Precipitation Event 08/06/2000

Initial Synthetic Statistical Analysis

This precipitation event was grouped as a heavy precipitation event. The SEMCOG area was fully covered by the precipitation. In Table 5.7, 61 SEMCOG rain gages measurements and NEXRAD grid values where these 61 rain gages were present were used to compare with these 61 SEMCOG rain gages measurements for the statistical analysis. The results of the combination presented that both correlation coefficient and R^2 values showed poor correlation between rain gage and radar measurements. Table 5.7 also showed difference between the average of rain gage values and the average of Stage III NEXRAD values produced by arithmetical averaging method. These show the precipitation patterns measured by both devices were poorly correlated, and the areal average precipitation distributions measured by both devices were different.

The negative MB and NBIAS showed that the radar-derived precipitation values underestimated the precipitation values. Both AMB and NRMSE values were high meaning that the measurement error of NEXRAD radar was large.

Table 5.7 and Figure 5.13 shows and depicts the initial synthetic statistics of this examined precipitation event, respectively. In Figure 5.13, the trend line equation shows a slope value (0.71) and the bivariate scatter diagram depicted a wide scattered

Raw NEXRAD Stage III Data vs. SEMCOG Raingage Measurements
(Precipitation Event Occurred on 08/06/2000)

$y = 0.7132x + 1.5703$
$R^2 = 0.5445$
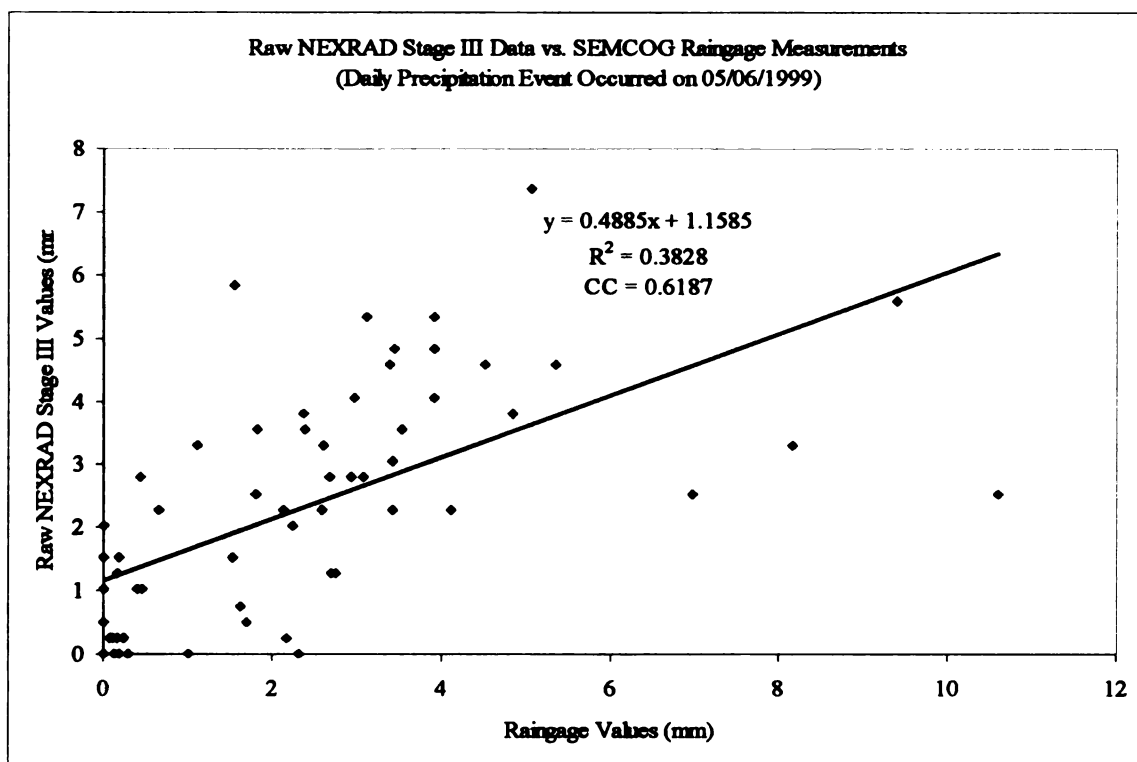
Raw NEXRAD Stage III Values (mm)

Raingage Values (mm)
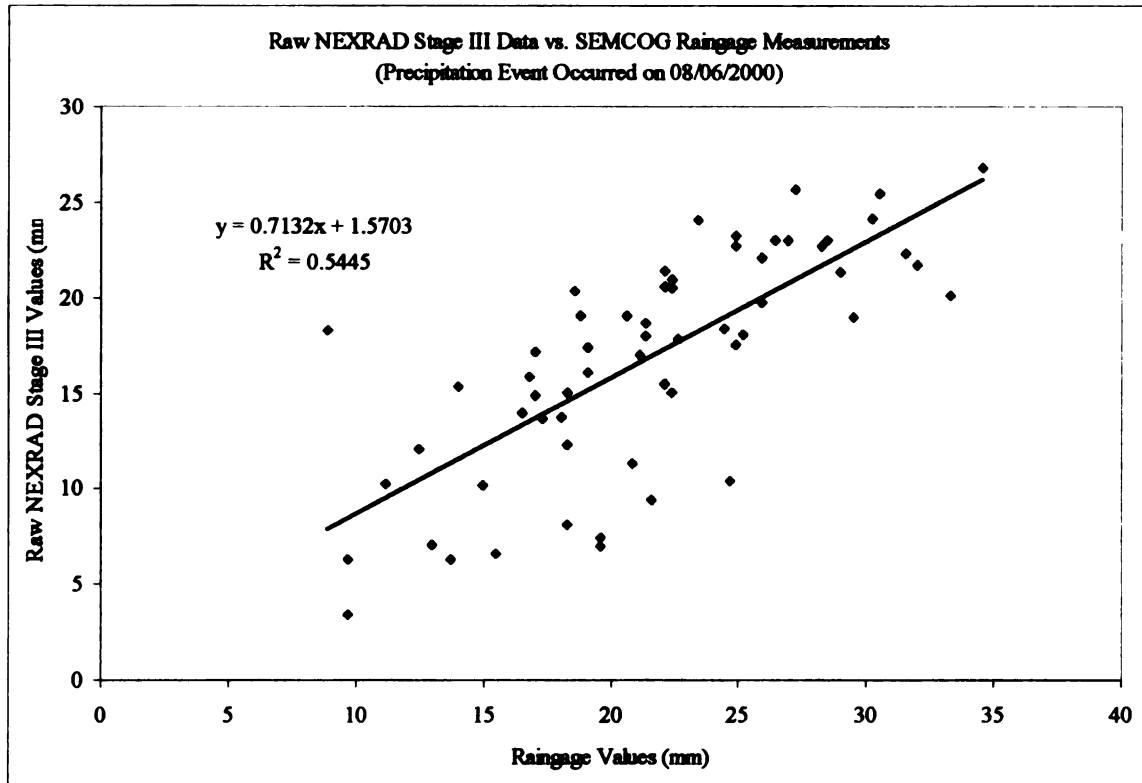
Figure 5.13 A Bivariate Scatter Diagram for Both Raw Stage III NEXRAD Data and
SEMCOG Rain Gage Measurements (Daily precipitation event occurred
on 08/06/2000).Heavy Precipitation Event.

89

distribution. This shows that both measurements presented disagreements but nicely correlated each other. These were also approved by the results of the above initial synthetic statistics.

Figure 5.14 depicts the daily raw Stage III NEXRAD precipitation surface. The SEMCOG area was fully covered by the precipitation. Thirty-three rain gages (yellow stars) were used for calibration (or cross validation), and twenty-eight rain gages (white stars) were used for validation. The data used for both calibration and validation had good CC and R^2 values. The negative MB and NBIAS values in both calibration and validation show that the NEXRAD radar underestimated the precipitation. The AMB and NRMSE values of both calibration and validation show that the radar estimation errors were large.

No two or more rain gage points occupied a NEXRAD grid cell. Therefore, the percentage of the density distribution of the SEMCOG rain gages in the SEMCOG area with 27 by 32 4-km grids were calculated by the 61 gage-occupied grids divided by 864 NEXRAD grids and multiplied by 100%, which was 7.1%.

Results of OC Model

The OC approach estimates the precipitation surface assuming second-order stationarity to minimize the uncertainty associated with semivariogram estimation. The OC approach considers the statistical properties of the rain gages, the radar, and the dependence of each of the devices on each other, and eliminates the error due to point sampling of rainfall by rain gages.

The first step of processing OC model was to produce the semivariograms for NEXRAD radar and rain gage variates, and cross semivariogram for both variates. The

**Raw NEXRAD Stage III Precipitation Surface
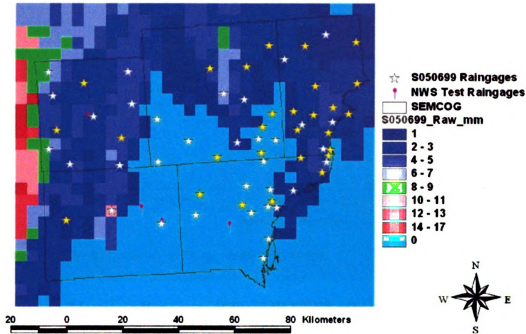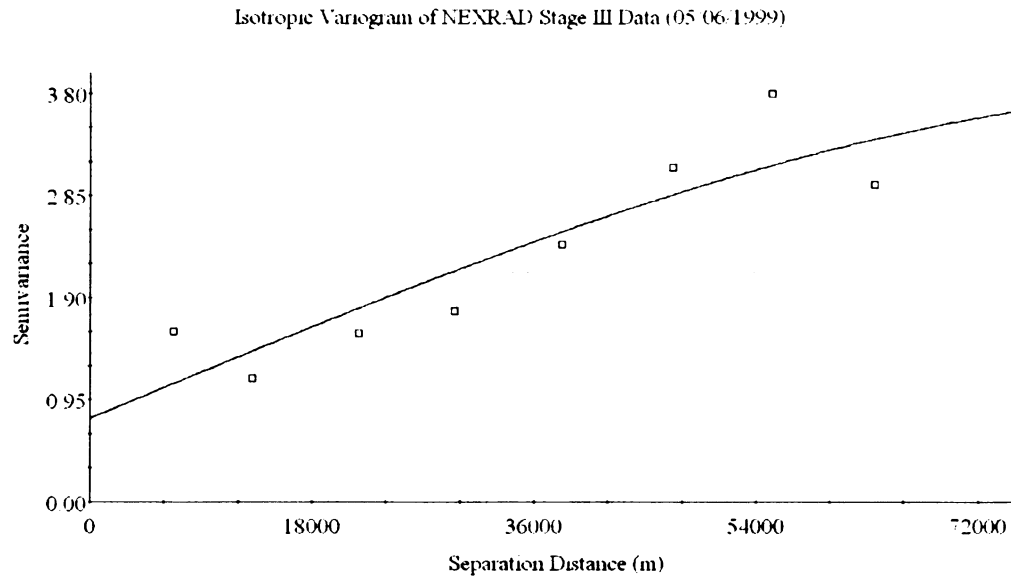(Daily Precipitation Event Occurred on 08/06/2000)**
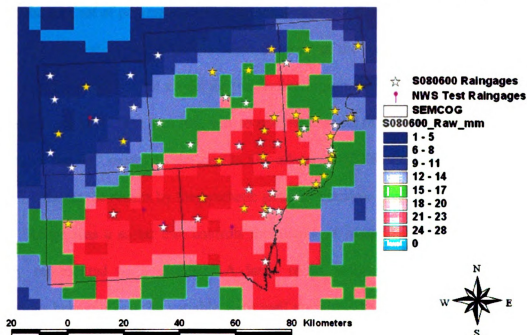
Figure 5.14 Daily Raw Stage III NEXRAD Precipitation Surface (Daily
precipitation event occurred on 08/06/2000).Heavy Precipitation Event.
*The SEMCOG area was fully covered by the precipitation event.
**The yellow and white stars were used for the calibration and
validation rain gages, respectively. They were used in the processes of
the OC and ANN models.
***Four purple rain gages were the NWS test rain gages using to
evaluate the performance of the OC and ANN models. These four
NWS rain gages were not involved in the processes of both OC and
ANN models.

two semivariograms and cross semivariogram were shown in Figures 5.15, 5.16, and 5.17, respectively.

The second step was to model the two semivariograms and cross semivariogram to find the best set of parameters (sill and range) for the OC model. In this case, spherical model was the best-fit model for the semivariogram of the Stage III NEXRAD data. The linear model was the best-fit model for the semivariogram of rain gage measurements and cross semivariogram. The last step was to use the best set of parameters (sill and range) to process the OC model to derive the OC-adjusted NEXRAD precipitation surfaces. Table 5.7 shows the results by the synthetic statistic matrices.

Range was a scalar that controls the degree of correlation between data points, usually represented as a distance. A large range value showed that more spatial continuous behavior and the variable were well correlated in space, and thus predictions resulted in fairly smooth maps of the variable of interest. Because the range values of these semivariograms and cross semivariogram were very large, the cross validation were well correlated in space. The sill value was the maximum value of semivariogram or cross variogram. Sill value of the semivariance as the lag*(h)* goes to infinity and it is equal to the total variance of the data set. The larger the sill value, the larger the prediction variance. Because the sill values of these semivariograms and cross semivariogram were large, the prediction variance becomes large. This will affect the precipitation results.

Table 5.7 shows the results after processing the OC model. Overall, the results of both cross validation and validation did not improve those of the initial condition. The results of combining both cross validation and validation data did not improve the initial
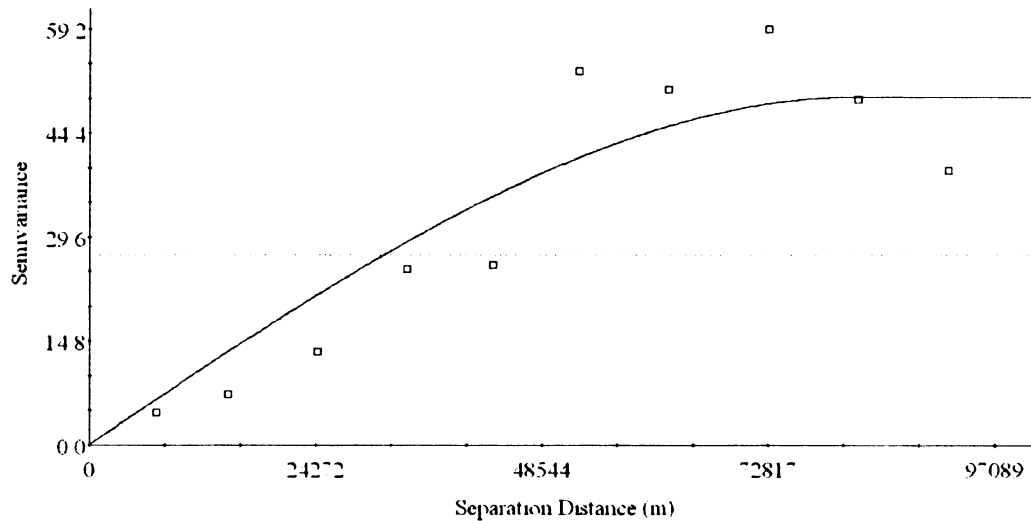
Spherical model (Co = 0.100, Co + C = 49.650, Ao = 82600.00, r2 = 0.85⁷,
RSS = 620.)

Figure 5.15 Isotropic Variogram of Stage III NEXRAD Data (Daily precipitation
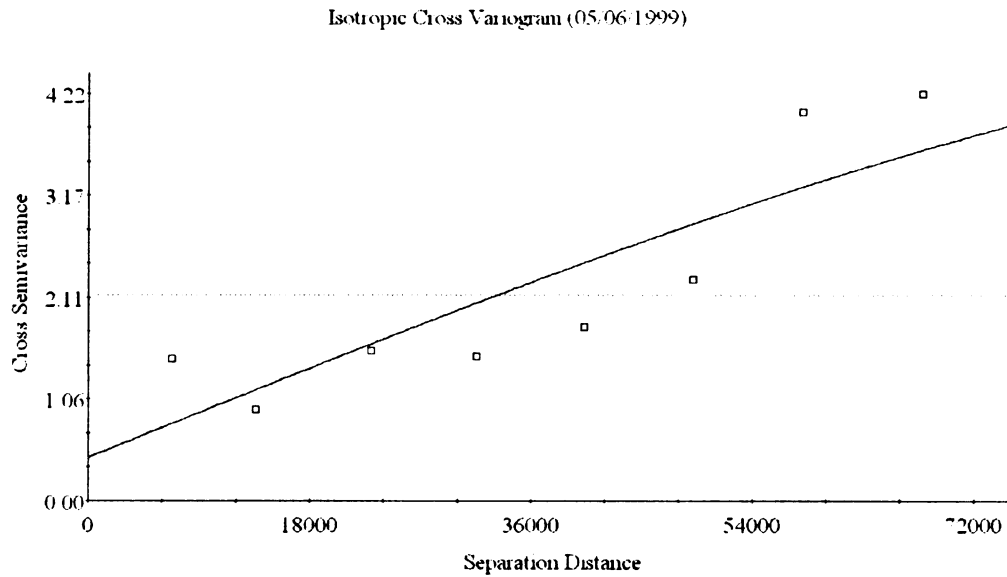event occurred on 08/06/2000). Heavy Precipitation Event.
*The best-fit model was spherical model.
**Nugget variance: $C_0 = 0.100$; structural variance: C; sill $= C_0 + C =$
49.650; range: $A_0 = 82,600.00$.
***Active lag distance: 97,088.70 m and lag interval: 9,708.87 m.
****R^2 or Regression Coefficient was to indicate how well the model fits
the variogram data. $R^2 = 0.857$.
***** RSS or Residual Sums of Squares was used to indicate how well
the model fits the variogram data; the lower the reduced sums of
squares, the better the model fits. RSS = 620.

93

Isotropic Variogram of Raingage Measurements (08/06/2000)

Linear model (Co = 0.100, Co + C = 67.980, Ao = 64400.00, r2 = 0.972,
   RSS = 244.)
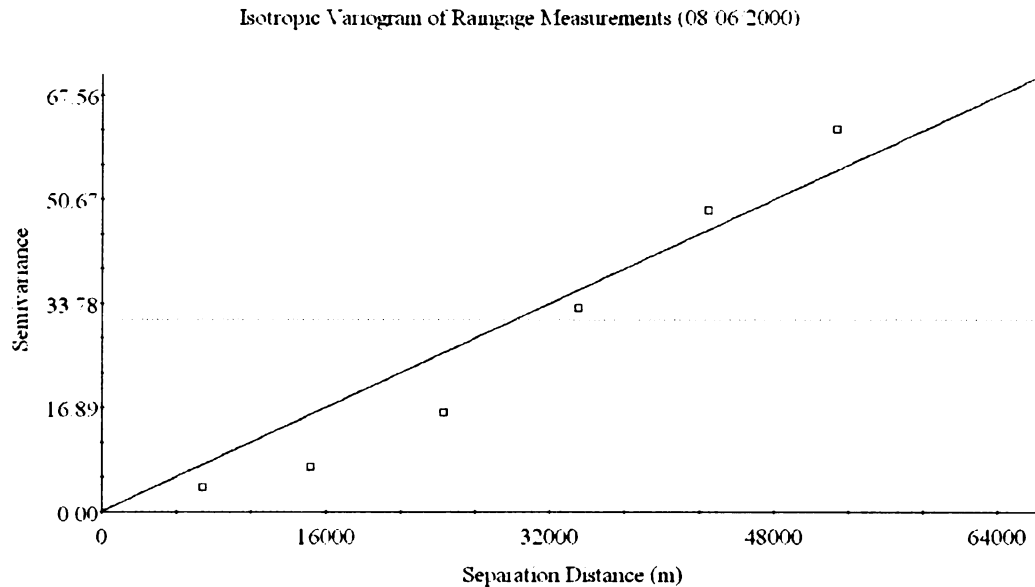
Figure 5.16. Isotropic Variogram of SEMCOG Rain Gage Measurements (Daily
   precipitation event occurred on 08/06/2000). Heavy Precipitation Event.
   *The best-fit model was linear model.
   **Nugget variance: $C_0 = 0.100$; structural variance: C; sill = $C_0 + C =$
   67.980; range: $A_0 = 64,400.00$.
   ***Active lag distance: 64,000 m and lag interval: 9,708.87 m.
   ****R^2 or Regression Coefficient was to indicate how well the model fits
   the variogram data. $R^2 = 0.972$.
   ***** RSS or Residual Sums of Squares was used to indicate how well
   the model fits the variogram data; the lower the reduced sums of
   squares, the better the model fits. RSS = 244.

94

Isotropic Cross Variogram (08/06/2000)
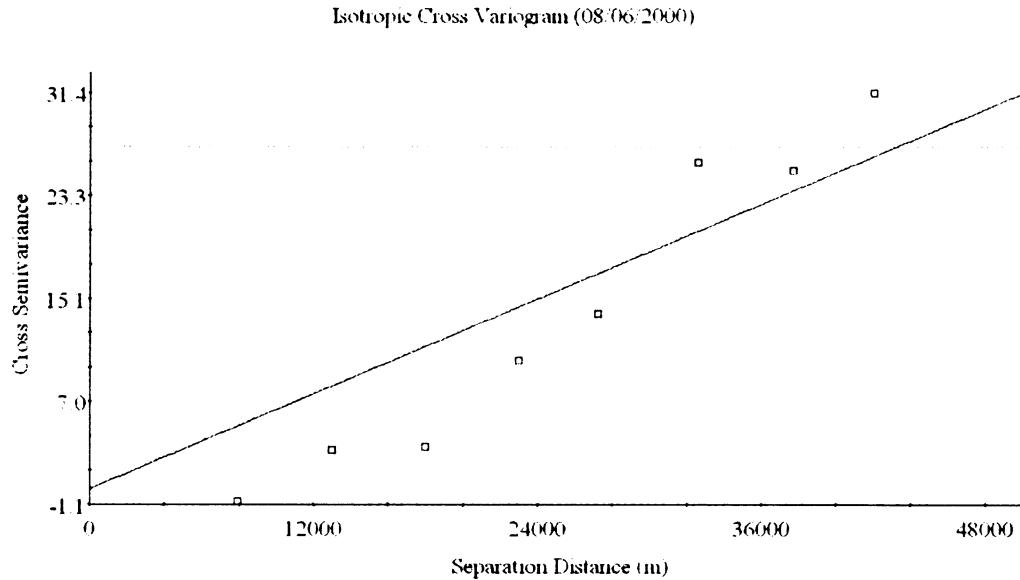
Linear model (Co = 0.100, Co + C = 40.310, Ao = 64250.00; r2 = 0.940; RSS = 219.)

Figure 5.17 Isotropic Cross Variogram of SEMCOG rain gage measurements (Daily precipitation event occurred on 08/06/2000).Heavy Precipitation Event.
*The best-fit model was linear model.
**Nugget variance: C_0 = 0.100; structural variance: C; sill = C_0 + C = 40.310; range: A_0 = 64,250.
***Active lag distance: 48,000 m and lag interval: 5,000 m.
****R^2 or Regression Coefficient was to indicate how well the model fits the variogram data. R^2 = 0.940.
***** RSS or Residual Sums of Squares was used to indicate how well the model fits the variogram data; the lower the reduced sums of squares, the better the model fits. RSS = 219.

condition. Figure 5.18 depicts the OC-adjusted Stage III NEXRAD precipitation surface. Comparing with Figure 5.14, the OC-adjusted precipitation patterns slightly degraded the valuable NEXRAD precipitation patterns.

Results of ANN Model

The ANN model provided a transformation from the spatial learning of the NEXRAD precipitation surfaces into the accurate reproduction of the rain gage values. The optimal topology of the neural network was determined by a trial-and error method. This was to test what type of the topology of the ANN model performs the best by varying with from one hidden layer to more hidden layers and various neuron numbers in each of hidden layer. The best set of the connection weight trained by the calibration of the ANN model was used to validate the validation data set. The neural network topology was 2-200-1 meaning (from the most left to the most right) the neuron numbers in the input layer, the first hidden layer, and the output layer, respectively. In this study, the topology of the ANN model with one hidden layer performed the best. The best set of connection weight was iteratively trained by 10 epochs per time. Over 650 times of 10 epochs were used find the best set of connection weight. The total time spent on training and testing was about 5.4 hours.

Table 5.7 showed the results after processing the ANN model. Overall, the results of both calibration and validation were better than those of the initial condition. The results of combining both calibration and validation data were better than those of the initial condition. Figure 5.19 depicted the ANN-adjusted Stage III NEXRAD precipitation surface. Comparing with Figure 5.14, the ANN-adjusted NEXRAD precipitation patterns improved the valuable NEXRAD precipitation patterns.

96

Ordinary Cokriging-Adjusted NEXRAD Stage III Precipitation Surface
(Daily Precipitation Event Occurred on 08/06/2000)
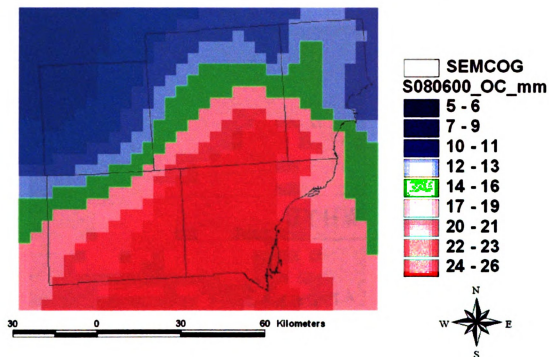
Figure 5.18 Ordinary Cokriging-Adjusted Stage III NEXRAD Precipitation Surface.
(Daily precipitation event occurred on 08/06/2000). Heavy
Precipitation Event.

**ANN-Adjusted NEXRAD Stage III Precipitation Surface
(Daily Precipitation Event Occurred on 08/06/2000)**

SEMCOG
S080600_ANN_mm
1 - 7
8 - 11
12 - 15
16 - 18
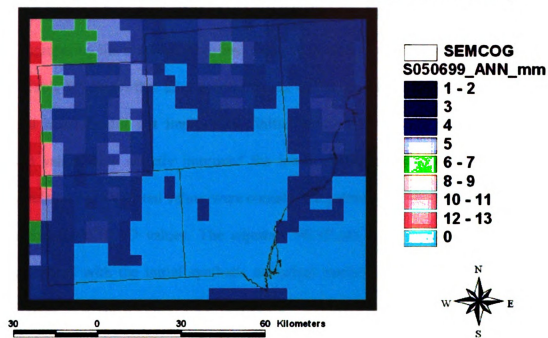19 - 21
22 - 25
26 - 29
30 - 37
0
No Data
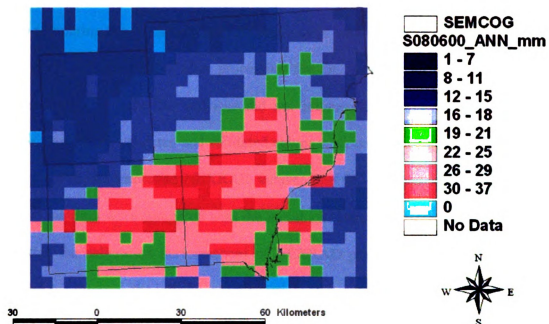
Figure 5.19 ANN-Adjusted Stage III NEXRAD Precipitation Surface. (Daily
precipitation event occurred on 08/06/2000). Heavy Precipitation Event.

Performance Evaluations of Both OC and ANN Models

Two types of performance evaluations were performed by: (1) comparing the initial synthetic statistical matrices with the synthetic statistical matrices of both models, and (2) comparing the synthetic statistical matrices of both models.

Table 5.7 shows that after processing the OC model both cross validated and validated synthetic statistical matrices did not improve the initial synthetic statistical matrices. Both cross validated and validated values were combined together and regarded these values as the improved NEXRAD values. The OC-adjusted NEXRAD synthetic statistical matrices were compared with the initial synthetic statistical matrices. Table 5.7 shows that the calibration performances of NEXRAD precipitation surface by the OC model did not improve the initial synthetic statistical matrices.

Table 5.7 shows that after processing the ANN model both calibrated and validated synthetic statistical matrices improved the initial synthetic statistical matrices. Both calibrated and validated values were combined together and regarded these values as the improved NEXRAD values. The combined synthetic statistical matrices were compared with the initial synthetic statistical matrices. Table 5.7 shows that the calibration performance of NEXRAD precipitation surface by the ANN model improved the initial synthetic statistical matrices.

Table 5.7 shows that the synthetic statistical matrices of calibrated, validated, and combined ANN-adjusted NEXRAD precipitation were better than those of cross validated, validated, and combined OC-adjusted NEXRAD precipitation.

Figure 5.20 depicts the performances of OC- and ANN-adjusted Stage III NEXRAD Data. The ANN-adjusted NEXRAD precipitation improved the correlation

Performances of OC- and ANN Adjusted NEXRAD Stage III Data
(Daily Precipitation Event Occurred on 08/06/2000)

OC Adjusted
$y = 0.6122x + 4.0147$
$R^2 = 0.526$
$CC = 0.725$

ANN Adjusted
$y = 0.9945x - 2.0529$
$R^2 = 0.634$
$CC = 0.796$

Raw NEXRAD
$y = 0.7132x + 1.5703$
$R^2 = 0.545$
$CC = 0.738$

♦ Raw NEXRAD
■ OC Adjusted
▲ ANN Adjusted
— — Linear (Raw NEXRAD)
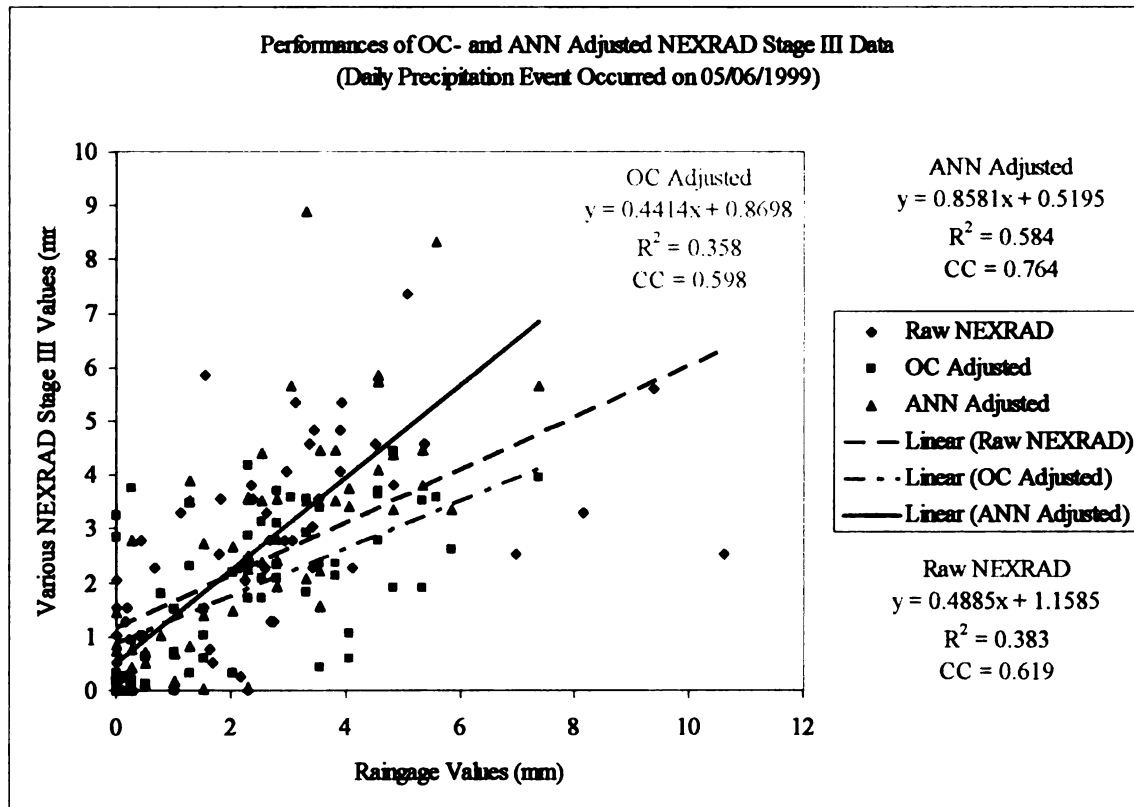— · Linear (OC Adjusted)
——— Linear (ANN Adjusted)
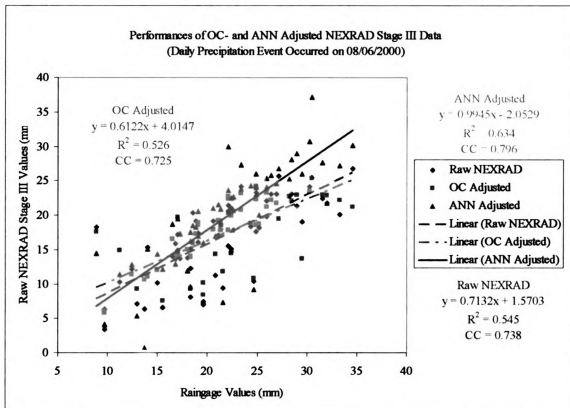
Figure 5.20 Performance of OC- and ANN-Adjusted Stage III NEXRAD Data
(Daily precipitation event occurred on 08/06/2000).Heavy Precipitation
Event.

with the rain gage values, and the slope of the trend line equation of the ANN model was the best (0.99), i.e. the difference between rain gage values and ANN-adjusted precipitation values were much improved. The OC-adjusted NEXRAD precipitation presented the worst correlation with the rain gage values, and the slope of the trend line equation was not the best (0.61), i.e. the difference between rain gage values and OC-adjusted precipitation values were not improved.

5.3. Discussion of Modeling SEMCOG, Michigan

FNN with LM algorithm considered the problem of exact interpolation in hydrological applications given a set of N input vectors x_1, x_2, ..., x_N and the corresponding desired outputs or targets y_1, y_2, ..., y_N. $F(x_i) = y_i$, $i = 1, 2, 3, ..., N$. x is a p-dimensional input vector. The exact interpolation of the generalized FNN was

$$F(x) = f(\sum_{i=1}^{N} Y_i w_i + w_O) = \tanh(\sum_{i=0}^{N} Y_i w_i), \text{ where the activation function was hyperbolic}$$

tangent function.

The goal of interpolation by Feedforward neural networks was to minimize an

$$\text{error function as } E(F) = \frac{1}{2} \sum_{q=1}^{Q} \left(t_q - a_q^M \right)^T \left(t_q - a_q^M \right) = \frac{1}{2} \sum_{q-1}^{Q} e_q^T e_q.$$

OC model was one of the popular statistical models used for interpolating spatial data in hydrological applications such as rainfall estimate based on rain gage measurements and radar estimates using ordinary cokriging model. Given a set of n spatial locations x_1, x_2, ..., x_n where a property, v, is measured as v_1, v_2, ..., v_n. OC

assumed that the value of v at some other spatial location x was given by a linear

combination of measured values as $v = \sum_{i=1}^{n} w_i v_i$.

The weights w_i, $i = 1, 2, ..., n$ depended on the spatial location x, and are

determined from the matrix equation $[C] [w] = [C_o]$, where $[C]$ is a matrix containing

covariance among v values at measured locations, $[C_o]$ is a vector of covariance of the v

values between measured locations and the interpolation point, and $[w]$ denotes the

weight vector (Journel and Huijbregts, 1978; Isaaks and Srivastava, 1989).

The similarities and differences between interpolations using FNN and OC were

as follows.

1. OC visualized the interpolation as a realization of a random field. In addition, it

   imposed second-order stationary requirements to estimate the statistics of the

   random field from a single realization. Neural networks had their origin in

   regression-based methods and were based on interpolation theory.

2. OC produced unbiased estimates so that any spatial location $\sum_{i=1}^{N_g} \lambda_{gi} = 1$ and

$\sum_{j=1}^{N_r} \lambda_{rj} = 0$ (See equation 13 in Section 3.4.4). This led to exact interpolation

when x coincides with a measurement location, just as in the case of FNN with

LM algorithm. OC was based on the idea of producing a best linear unbiased

estimate (BLUE). It was the best in the sense of minimizing the variance of

estimation error. The goal of interpolation by FNN with LM algorithm was to

minimize an error function

$$\text{as } E(F) = \frac{1}{2} \sum_{q=1}^{Q} \left(\underline{t}_q - \underline{a}_q^M \right)^T \left(\underline{t}_q - \underline{a}_q^M \right) = \frac{1}{2} \sum_{q-1}^{Q} \underline{e}_q^T \underline{e}_q \ .$$

3. A major operational difference existed between OC and FNN with LM algorithm. In OC, as the location x where an estimate was desired changes, the weight vector w_i in $v = \sum_{i=1}^{n} w_i v_i$ changes and had to be obtained from an inversion of the matrix $[C]$ in $[C][w] = [C_o]$. The linear unbiased (LU) decomposition of $[C]$ (in lieu of the inverse) for computing the inverse needed to be performed only once. In case of FNN with LM algorithm, the weight vector changed with location x.

4. Both kriging and FNN with LM algorithm were based on data exhibiting some spatial continuity. In geostatistical applications, the semivariogram or cross semivariogram function was a measure of the continuity that the quantity v possesses. The variogram is therefore crucial for OC. When using FNN with LM algorithm, smoothness was imparted to the transformation through

$$E(F) = \frac{1}{2} \sum_{q=1}^{Q} \left(\underline{t}_q - \underline{a}_q^M \right)^T \left(\underline{t}_q - \underline{a}_q^M \right) = \frac{1}{2} \sum_{q-1}^{Q} \underline{e}_q^T \underline{e}_q \ .$$

RESULTS OF MODELING STATE OF MICHIGAN

5.4. Results of Selecting the NEXRAD Grid Size

Six daily precipitation events were selected to examine the performance of the ANN model. Two factors affected the precipitation adjustment: density of rain gage network and spatial variety of a precipitation event. The grid size presented the general spatial information by distance. The density of the Michigan NWS rain gage network to the Michigan 16-km NEXRAD grid was about 3.0% and to the Michigan 32-km NEXRAD grid was about 13.8%. The density of the rain gage network used for 32-km NEXRAD grid size was much higher than that used for 16-km NEXRAD grid size.

The spatial variability of the precipitation usually was very high. This caused by many factors such as topographical feature, wind directions and speeds, spatial distribution of precipitation intensity of a precipitation event, and temporal factor.

Table 5.8 shows the results of modeling the six Michigan precipitation events by evaluating the adjusted NEXRAD performances using the ANN models. Table 5.8 also compares with the initial synthetic statistical matrices to learn whether the ANN model improves the initial synthetic statistical matrices of the raw Stage III NEXRAD data.

5.5. Results and Discussion of Precipitation Event 07/01/1999

5.5.1. Initial Synthetic Statistical Analysis

This precipitation event was grouped into the type of the heavy precipitation event. It fully covered Michigan. In Table 5.8, 28 Michigan NWS rain gages measurements and NEXRAD grid values where these 28 rain gages were present were used to compare with these 28 SEMCOG rain gage measurements for the statistical analysis. The results of the

Table 5.8 Results of the Examined Michigan Precipitation Events

Heavy/Medium/Slight Precipitation Events	7/1/1999 /Heavy		5/17/1999 /Heavy		5/6/1999/ Light		7/31/1999 /Light		5/28/2000 / Moderate		9/14/2000 / Moderate	
Calibration	Initial	ANN	Initial	ANN	Initial	ANN	Initial	ANN	Initial	ANN	Initial	ANN
	14 gages		16 gages		16 gages		16 gages		16 gages		6 gages	
Mean_Gage(mm)	26.63		13.46		6.82		5.83		4.32		13.46	
Mean_NEXRAD (mm)	13.51		12.49		7.21		7.14		6.21		5.06	
Mean_ANN (mm)		18.94		15.29		6.84		6.01		5.21		12.77
CC	0.78	0.82	0.58	0.88	0.93	0.95	0.74	0.94	0.80	0.96	0.70	0.95
R Square	0.61	0.68	0.33	0.77	0.86	0.90	0.55	0.89	0.64	0.93	0.49	0.90
MB	-13.13	-7.69	-0.97	1.83	0.39	0.02	1.32	0.18	1.89	0.90	-8.41	-0.69
AMB	13.99	8.57	6.62	3.94	2.89	1.55	2.44	1.65	2.06	1.06	8.41	2.70
NBIAS	-0.49	-0.29	-0.07	0.14	0.06	0.00	0.23	0.03	0.44	0.21	-0.62	-0.05
NRMSE	1.17	0.36	0.91	0.51	0.69	0.33	0.78	0.33	0.72	0.30	1.18	0.35
Validation												
	14 gages		14 gages		15 gages		16 gages		12 gages		12 gages	
Mean_Gage(mm)	6.62		13.41		6.64		4.32		14.16		7.83	
Mean_NEXRAD (mm)	5.50		10.79		4.24		5.03		11.26		5.94	
Mean_ANN (mm)		3.98		12.93		4.61		5.01		9.27		3.84
CC	0.33	0.54	0.47	0.77	0.72	0.70	0.99	0.95	0.87	0.96	0.47	0.61
R Square	0.11	0.29	0.22	0.59	0.52	0.49	0.98	0.90	0.76	0.92	0.22	0.37
MB	-1.12	-2.64	-2.61	-0.48	-2.40	-2.03	0.71	0.69	-2.91	-4.89	-1.89	-4.00
AMB	3.99	3.85	6.98	4.75	3.14	3.17	1.03	2.88	4.14	5.05	4.82	5.17
NBIAS	-0.17	-0.40	-0.19	-0.04	-0.36	-0.31	0.17	0.16	-0.21	-0.35	-0.24	-0.51
NRMSE	0.62	0.60	1.12	0.67	0.86	0.85	0.14	0.34	0.53	0.52	0.95	0.95
Combination												
	28 gages		30 gages		31 gages		32 gages		28 gages		18 gages	
Mean_Gage(mm)	16.63		13.44		6.73		5.07		8.54		9.71	
Mean_NEXRAD (mm)	9.51		11.70		5.77		6.09		8.37		5.65	
Mean_ANN (mm)		11.46		14.19		5.76		5.51		6.95		6.81
CC	0.75	0.89	0.53	0.83	0.81	0.84	0.93	0.95	0.84	0.93	0.47	0.75
R Square	0.56	0.79	0.28	0.68	0.65	0.70	0.87	0.90	0.71	0.87	0.22	0.56
MB	-7.12	-5.17	-1.68	0.75	-0.96	-0.97	1.01	0.44	-0.17	-1.58	-4.06	-2.90
AMB	8.99	6.21	6.57	4.32	3.01	2.33	1.74	2.27	2.95	2.77	6.01	4.35
NBIAS	-0.43	-0.31	-0.13	0.06	-0.14	-0.14	0.20	0.09	-0.02	-0.19	-0.42	-0.30
NRMSE	0.83	0.59	0.96	0.58	0.76	0.58	0.38	0.33	0.54	0.43	1.00	0.73

combination presented that both correlation coefficient and R^2 values show good correlation between rain gage and radar measurements. Table 5.8 also shows the large difference between the average of rain gage values and the average of Stage III NEXRAD values produced by arithmetical averaging method were also very different. This shows the precipitation patterns measured by both devices were nicely correlated, but the areal average precipitation distributions measured by both devices were different.

The negative MB and NBIAS shows that the radar-derived precipitation value underestimates the precipitation values. Both AMB and NRMSE values are large which means that the measurement error of NEXRAD radar is large.

Table 5.8 and Figure 5.21 shows and depicts the initial synthetic statistics of this examined precipitation event, respectively. Normally, the dependence between raw NEXRAD data and rain gage data shows up in a bivariate scatter diagram as a tendency to form an elliptical cloud along a diagonal. The cloud had a major axis along the line at 45 degree to the positive transverse axes in the case of positive correlation (CC = 1), and a major axis along the perpendicular line at 135 degree to the positive transverse axis in the case of negative correlation (CC = -1).

In Figure 5.21, the trend line equation shows a slope value (0.5644) and the bivariate scatter diagram depicted an elliptical shape with a wide minor axis. This shows that both measurements present disagreements but correlated with each other. These were also approved by the results of the above initial synthetic statistics.

Figure 5.22 depicts the daily raw Stage III NEXRAD precipitation surface. The Michigan was fully covered by the precipitation. Fourteen rain gages (yellow stars) were used for calibration (or cross validation), and fourteen rain gages (white stars) were used

Raw NEXRADStage III Data vs. Michigan NWS Raingage Measurements
(Daily Precipitation Event Occurred on 07/01/1999)

Raw NEXRAD Stage III Values (mm)

$y = 0.5644 - 0.1207$
$R^2 = 0.5631$
$CC = 0.7504$

Michigan NWS Raingage Values (mm)
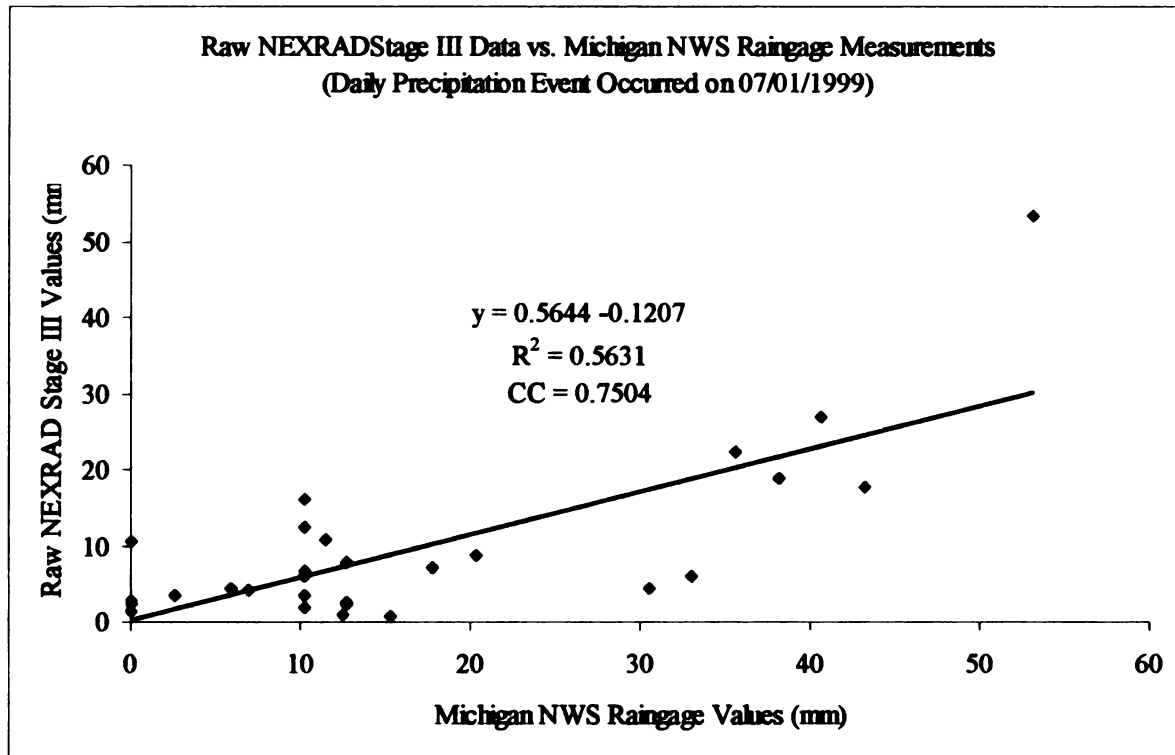
Figure 5.21 A Bivariate Scatter Diagram for Both Raw Stage III NEXRAD Data and
Michigan NWS Rain Gage Measurements (Daily precipitation event
occurred on 07/01/1999). Heavy Precipitation Event.

107

Michigan Raw NEXRAD Stage III Precipitation Surface
(Daily Precipitation Event Occurred on 07/01/1999)
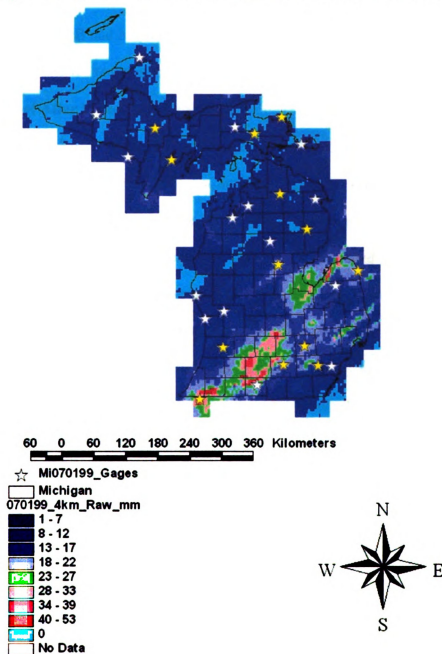
Figure 5.22 Daily Raw Stage III NEXRAD Precipitation Surface (Daily
precipitation event occurred on 07/01/1999). Heavy Precipitation Event.
*The Michigan was fully covered by the precipitation event.
**The yellow and white stars were used for the calibration and
validation rain gages, respectively.

for validation. The data used for calibration had good CC and R^2 values, but the data used for validation had poor CC and R^2 values. The negative MB and NBIAS values in the calibration and validation showed that the NEXRAD radar underestimates the precipitation. The AMB and NRMSE values of both calibration and validation were very high. This shows that the radar estimation error is very high.

5.5.2. Results of After Processing ANN Model

Figure 5.23 depicts rescaled 16-km Stage III NEXRAD precipitation surface. The precipitation patterns of the rescaled 16-km Stage III NEXRAD precipitation surface are similar with those of the raw 4-km Stage III NEXRAD precipitation surface. Comparing Figure 5.23 with Figure 5.22, the precipitation values of the rescaled one was lower than the raw one, because the rescaled one took the average value from the 16 4-km grid values of a 16-km grid as the precipitation value of that 16-km grid. If the precipitation values of the ANN-adjusted 16-km NEXRAD grids were close to the rescaled 16-km NEXRAD grid values, then the ratio would get the ANN-adjusted 16-km NEXRAD grids back to the suitable precipitation patterns. Therefore, the ratios were the most important values derived by the ANN-adjusted NEXRAD 16-km grid values divided by the rescaled 16-km NEXRAD grid values.

The ANN model provided a transformation from the spatial learning of the NEXRAD precipitation surfaces into the accurate reproduction of the rain gage values. The optimal topology of the neural network was determined by a trial-and-error method. This was to test what type of the topology of the ANN model performs the best by varying with from one hidden layer to more hidden layers and various neuron numbers in each of hidden layer. The best set of the connection weight trained by the calibration of

Rescaled Michigan 16-km NEXRAD Stage III Precipitation Surface (Daily Precipitation Event Occurred on 07/01/1999)
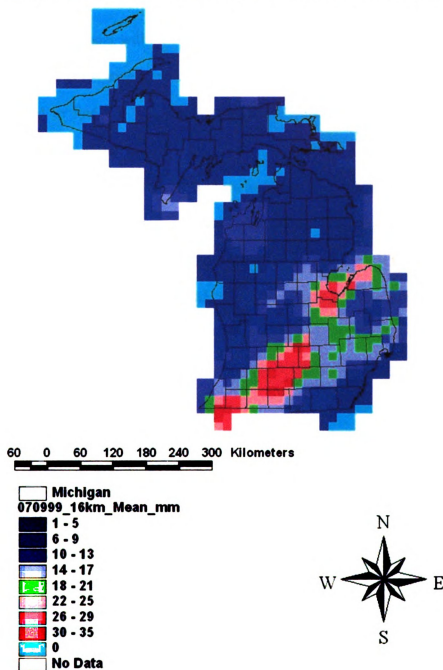
Figure 5.23 Daily Rescaled 16-km Stage III NEXRAD Precipitation Surface (Daily precipitation event occurred on 07/01/1999). Heavy Precipitation Event.

the ANN model was used to validate the validation data set. The neural network topology was 2-175-1 meaning (from the most left to the most right) the neuron numbers in the input layer, the first hidden layer, and the output layer, respectively. In this study, the topology of the ANN model with one hidden layer performed the best. The best set of connection weight was iteratively trained by 25 epochs per time. Over 550 times of 25 epochs were used to find the best set of connection weight. The total time spent on training and testing was about 5.9 hours.

Table 5.8 shows the results after processing the ANN model. Overall, the results of both calibration and validation were better than those of the initial condition. The results of combining both calibration and validation data were better than those of the initial condition. Figure 5.24 depicts the ANN-adjusted Stage III NEXRAD precipitation surface. Comparing Figure 5.24 with Figure 5.23, the ANN-adjusted NEXRAD precipitation patterns improves the valuable NEXRAD precipitation patterns. The drawback is the spatial discontinuity of precipitation patterns. Figure 5.25 depicts the transformed daily 4-km Stage III NEXRAD precipitation surface from ANN-adjusted 16-km Stage III NEXRAD precipitation surface. The same drawback, which is the spatial discontinuity of precipitation patterns depicted in the precipitation surface.

Figure 5.26 depicts the performances of the transformed 4-km Stage III NEXRAD data. It presents the better correlation with the rain gage values and the slope of the trend line equation is improved (0.69), i.e. the difference between rain gage values and ANN-adjusted precipitation values are smaller.

ANN-Adjusted Michigan 16-km NEXRAD Precipitation Surface
(Daily Precipitation Event Occurred on 07/01/1999)
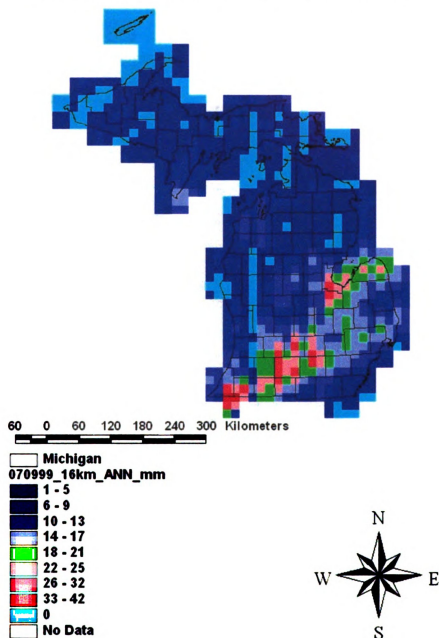
Figure 5.24 Daily ANN-Adjusted 16-km Stage III NEXRAD Precipitation Surface
(Daily precipitation event occurred on 07/01/1999). Heavy Precipitation
Event.

Transformed Michigan 4-km NEXRAD Stage III Precipitation Surface from ANN-Adjusted 16-km NEXRAD Stage III Precipitation Surface (Daily Precipitation Event Occurred in 07/01/1999)

60 0 60 120 180 240 300 360 Kilometers

Michigan
070199_4km_ANN_mm
■ 1 - 7
■ 8 - 12
■ 13 - 17
□ 18 - 22
□ 23 - 27
□ 28 - 33
□ 34 - 40
□ 41 - 52
□ 0
□ No Data

N
W — E
S
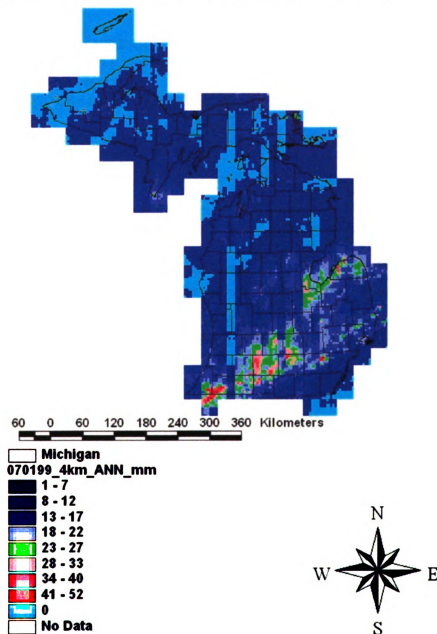
Figure 5.25 Transformed Daily 4-km Stage III NEXRAD Precipitation Surface from ANN-Adjusted 16-km Stage III NEXRAD Precipitation Surface (Daily precipitation event occurred on 07/01/1999). Heavy Precipitation Event.
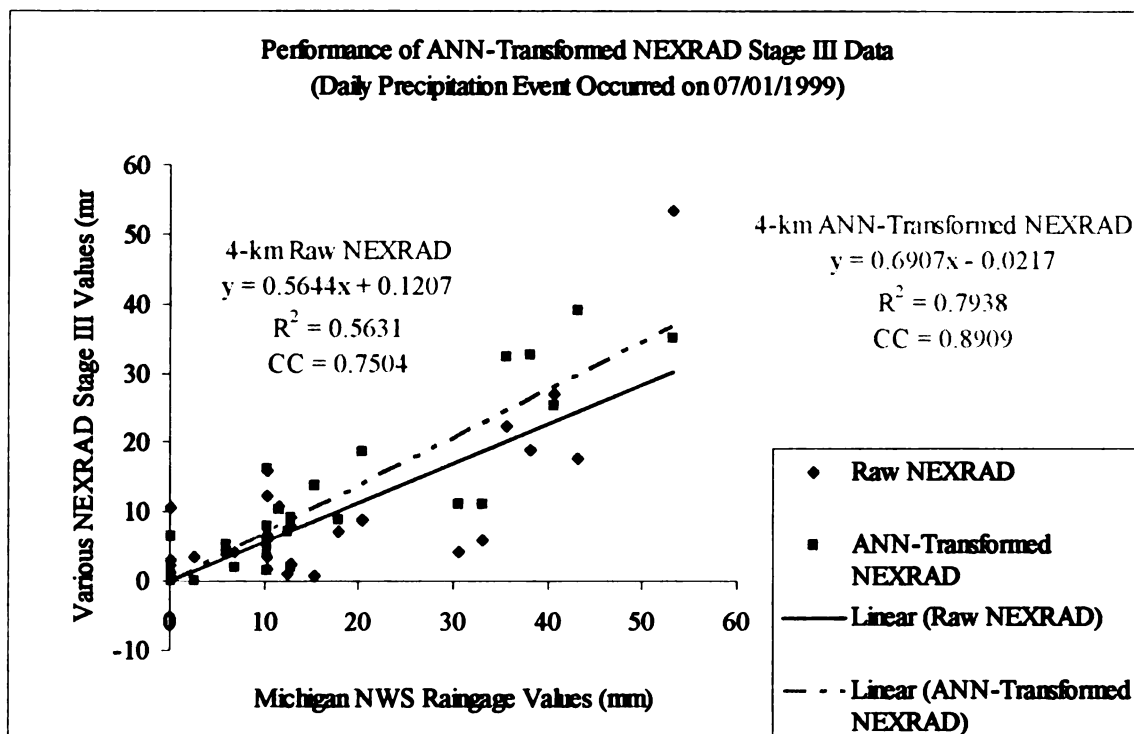
Figure 5.26 Performance of ANN-Adjusted Stage III NEXRAD Data. (Daily
precipitation event occurred on 07/01/1999). Heavy Precipitation Event.

Chapter 6 SUMMARY and CONCLUSIONS

Statistical Analysis

In the statistical analysis, the results represent the significant discrepancies between rain gage and Stage III NEXRAD data by hourly and by daily. The frequency of the difference of the most of heavy precipitation events is smaller than those of the moderate and the light precipitation events; the magnitude of the difference of the most of heavy precipitation events is greater than those of the moderate and the light precipitation events. Because the radar-derived rainfall provides valuable rainfall estimates in high spatial and temporal resolutions, it is necessary to reduce the magnitude of the considerable difference between rain gage and Stage III NEXRAD data by optimally combining both measurements to derive the more accurate rainfall surfaces.

Modeling SEMCOG Area and Entire State of Michigan

In this study, two methods, ordinary cokriging and ANNs, utilizing information from two sources of rainfall measurements are presented. A feed-forward neural network with Levenberg-Marquardt algorithm trained in two phases, primarily with daily radar precipitation data and, secondly, with rain gage data is applied to improve the radar-derived rainfall surfaces for the SEMCOG area and the entire state of Michigan. The results show a network that is able to reproduce the rainfall structure by the high spatial resolution of the radar and at the same time adjust it accordingly, so that it agrees with the more accurate ground rain gages. In the current implantation the neural network is trained and tested by the precipitation patterns and the spatial coordinates x and y. This approach generally provides much better results than the ordinary cokriging in terms of the model criteria. It is very important that the ANN model provides a robust spatial interpolation of

115

the rainfall field in high spatial resolution without rain gages, uses the fewer rain gage measurements to improve the accuracy of the rainfall estimates, and is able to well improve the accuracy of both full and partial spatial coverage.

Chapter 7 RECOMMENDATIONS FOR FUTURE STUDY

Listed below are some recommendations for future study:

1. Incorporate into an operational model to improve daily rainfall data.

2. Experiment with hourly rainfall data.

3. Statistical analysis for connection weights and biases of the ANN model using pattern classification technology to find the global connection weights and biases.

REFERENCES

Anonymous. 1984. Next Generation Weather Radar Programmatic Environmental Impact Statement. No. R400-PE201. The NEXRAD Joint System Program Office.

Anonymous. 1985. Next Generation Weather Radar Algorithm Report. No. R400-AR301. The NEXRAD Joint System Program Office.

Anonymous. 1986a. Next Generation Weather Radar Product Description Document. No. R400-PD-202. The NEXRAD Joint System Program Office.

Anonymous. 1986b. NEXRAD Technical Requirements. No. R400-SP301. The NEXRAD Joint System Program Office.

Anonymous. 1990. Federal Meteorological Handbook No. 11: Doppler Radar Meteorological Observations. Federal Coordinator for Meteorological Services and Supporting Research, Rockville, MD.

Anonymous. 1996. Hydrology Handbook. 2nd Edition. ASCE. New York, NY.

Bailey, T. C., Gatrell, A. C. 1995. Interactive Spatial Data Analysis. Longman Scientific & Technical, Harlow Essex, England; John Wiley and Sons, Inc., New York, NY.

Biswas, A.K. 1967. Development of Rain gages. Journal of the Irrigation and Drainage Division. ASCE. 93(IR3): 99 ~ 124.

Biswas, A.K. 1970. History of Hydrology. American Elsevier Pub. Co., New York, NY.

Blum, A. 1992. Neural Networks in C++: An Object-Oriented Framework for Building Connection Systems. John Wiley and Sons, Inc., New York, NY.

Bose, N.K. and Liang, P. 1996. Neural Network Fundamentals with Graphs, Algorithms, and Applications. McGraw-Hill, Inc., New York, NY.

Brandes, E. A. 1975. Optimizing Rainfall Estimates with the Aid of Radar. Journal of Applied Meteorology, 14: 1339 ~ 1344.

Chakraborty, L., Mehrotra, K., Mohan, C. K., and Ranka, S. 1992. Forecasting the Behavior of multivariate time series using neural networks. Neural Networks. 5: 961 ~ 970.

Chidley, T. R. E. and Keys, K. M. 1970. A Rapid Method of Computing Areal Rainfall. Journal of Hydrology, 12(1): 15 ~ 24.

Chua, S. and Bras, R. L. 1982. Optimatmal Estimators of Mean Areal Precipitation in Regions of Orographic Influence. Journal of Hydrology, 57(1): 23 ~ 48.

Cressie, N. A.C. 1993. Statistics for Spatial Data. John Wiley & Sons, Inc., New York, NY.

Creutin, J. D. and Obled, C. 1982. Objective Analyses and Mapping Techniques for Rainfall Fields: An Objective Comparison. Water Resource Research, 18(2):413 ~ 431.

Croley, T. E. II and Hartmann, H. C. 1985. Resolving Thiessen Polygons. Journal of Hydrology, 76(1): 363 ~ 379.

Demuth, H. and Beale, M. 2001. Neural Network Toolbox for Use with MATLAB: Computing, Visualization, and Programming. The MathWorks, Inc., Natick, MA.

Deutsch, C. V. and Journel, A. G. 1998. GSLIB: Geostatistical Software Library and User's Guide. 2nd Edition. Oxford University Press. Inc., New York, NY.

Dingman, S. L., Seely-Reynolds, D. M., and Reynolds R. C., III. 1988 Application of Kriging to Estimating Mean Annual Precipitation in a Region of Orographic influence. Water Resource Bulletin, 24 (2): 329 ~ 339.

Diskin, M. H. 1969. Thiessen Coefficients by a Monte Carlo Procedure. Journal of Hydrology. 8(3): 323 ~ 335.

Duchon, C.E., Renkevens, T.M. and Crosson, W.L. 1995. Estimation of Daily Area-Average Rainfall During the CaPE Experiment in Central Florida. Journal of Applied Meteorology, 34: 2704 ~ 2714.

Eddy, A. 1979. Objective Analysis of Convective Scale Rainfall Using Gages and Radar. Journal of Hydrology, 44: 125 ~ 134.

Fausett, L. 1994. Fundamentals of Neural Networks: Architectures, Algorithms, and Applications. Prentice-Hall International, Inc., Englewood Cliffs, NJ.

France, P. W. 1985, A Comparison of Various Techniques for Computation of Areal Rainfall. IE(I) Journ.-CI, 66: 74 ~ 78.

Goovaerts, P. 1997. Geostatistics for Natural Resources Evaluation. Oxford University Press, Inc., New York, NY.

Groisman, P. and Legates, D. 1994. The Accuracy of United States Precipitation Data. Bulletin of the American Meteorological Society. 75(3): 215 ~ 227.

Haykin, S. 1999. Neural Networks: A Comprehensive Foundation. 2nd Edition. Prentice Hall, Inc., Upper Saddle River, NJ.

Hamlin, M. J. 1983. The Significance of Rainfall in the Study of Hydrological Processes at Basin Scale. Journal of Hydrology. 65(1-3): 73 ~ 94.

Isaaks, E. H. and Srivastava, R. M. 1989. Applied Geostatistics. Oxford University Press. Inc., New York, NY.

Johnson, D., Smith, M., Koren, V., and Finnerty, B. 1999. Comparing Mean Areal Precipitation Estimates from NEXRAD and Rain Gauge Networks. Journal of Hydrological Engineering, 4(2): 117 ~ 124.

Journal, A. G. and Huijbregts, C. J. 1978. Mining Geostatistics. Academic Press Inc., New York, NY.

Joss, J. and Lee, R. 1995. The Application of Radar-Gauge Comparisons to Operational Precipitation Profile Corrections. Journal of Applied Meteorology, 34: 2612 ~ 2630.

Krajewski, W. F. 1987. Cokriging Radar-Rainfall and Rain Gage Data. Journal of Geophysical Research, 92(D8): 9,571 ~ 9,580.

Lhermitte, R. M. and Gilet, M. 1975. Dual-Doppler Radar Observation and Study of Sea Breeze Convective Storm Development. Journal of Applied Meteorology, 14: 1346 ~ 1361.

Liebelt, P.B. 1967. An Introduction to Optimal Estimation. Addison-Wesley Pub. Co., Reading, MA.

Linsley, R. K. Kohler, M. A., and Paulhus, J. L. H. 1949. Applied Hydrology. McGraw-Hill Book Co., New York, NY.

Maren, A., C. Harston, and R. Pap. 1990. Handbook of Neural Computing Applications. Academic Press. Inc., San Diego, CA.

Marquardt, D. 1963. An algorithm for Least Squares Estimation of Non-Linear Parameters. Journal of the Society for Industrial and Applied Mathematics, 431 ~ 441.

Martin, T. H., Demuth, H. B., and Beale, M. 1996. Neural Network Design. PWS Pub., Boston. MA.

Matsoukas, C., Idlam, S, and Kothari, R. 1999. Fusion of Radar and Rain Gage Measurements for an Accurate Estimation of Rainfall. Journal of Geophysical Research. 31,437 ~ 31,450.

Montmollin, F. A., Olivier, R. J., Simard, R. G., and Zwahlen, F. 1980. Evaluation of a Precipitation Map Using a Smoothed Elevation-Preciptation Relationship and Optimal Estimates (Kriging). Nordic Hydrology. 11(3-4): 113 ~ 120.

Rodriguez-Iturbe, I. and Mejia, J. M. 1974. The Design of Rainfall Networks in Time and Space. Water Resources Research. 10(4): 713 ~ 735.

Salas, J. D. 1993. Analysis and Modeling of Hydrologic Time Series. Handbook of Hydrology, D. R. Maidment, ed., McGraw-Hill, New York, NY, 19.1 ~ 19.72.

Seo, D.-J. 1998b. Real-Time Estimation of Rainfall Fields Using Radar Rainfall and Rain Gage Data. Journal of Hydrology, 208: 37 ~ 52.

Seo, D.-J., Krajewski, W. F., and Bowles, D. S. 1990a. Stochastic Interpolation of Rainfall Data from Rain Gages and Radar Using Cokriging 1: Design of Experiments. Water Resources Research, 26(3): 469 ~ 477.

Seo, D.-J., Krajewski, W. F., Azimi-Zonooz, A., and Bowles, D. S. 1990b. Stochastic Interpolation of Rainfall Data from Rain Gages and Radar Using Cokriging 2: Results. Water Resources Research, 26(5): 915 ~ 924.

Shih, S. F. and Hamrick, R. L. 1975. Modified Monte Carlo Technique to Compute Thiessen Coefficients. Journal of Hydrology, 27(3-4): 339 ~ 356.

Smith, J. A., Seo, D.-J., Baeck, M. L., and Hudlow, M. D. 1996. An Intercomparison study of NEXRAD Precipitation Estimates. Water Resource Research, 32(7), 2035 ~ 2045.

Smith, J.A. and Krajewski, W.F. 1991. Estimation of the Mean Field Bias of Radar Rainfall Estimates. Journal of Applied Meteorology, 30: 397 ~ 412.

Tabios, G. Q. and Salas, J. D. 1985. A Comparative Analysis of Techniques for Spatial Interpolation of Precipitation. Water Resource Bulletin, 21(3): 365 ~ 380.

Unwin, D. J. 1969. The Areal Extension of Rainfall Records: an Alternative Model. Journal of Hydrology. 7: 401 ~ 414.

Wackernagel, H. 1998. Multivariate Geostatistics. 2nd Edition. Springer-Verlag, Berlin, Germany.

Wechsler, H. 1992. Neural Networks for Perception Volume 1. Academic Press. Inc., San Diego, CA.

Wilson, J. W. and Brandes, E. A. 1979. Radar Measurement of Rainfall. Journal of Applied Meteorology, 60 (9): 1048 ~ 1058.

Yates, S, R, 1986, Disjunctive Kriging. 3. Cokriging. Water Resources Research 22(1): 1,371 ~ 1,376.

Yates, S. R. and Warrick, A. W. 1986 Disjuctive Kriging. 1. Overview of Estimation and Conditional Probability. Water Resources Research, 22(5): 615 ~ 621.

APPENDICES

Appendix A
Various SEMCOG Precipitation Data
(Precipitation Event 05/06/1999)

Station ID	X	Y	NEXRAD mm	Gage_mm	ANN_mm	OC_mm
A3	661857.143789	192530.880673	1.800	2.540	2.386	3.132
L3	668048.272705	241521.550493	3.440	4.826	3.364	4.432
L7	681514.971760	222057.746602	4.840	3.810	4.466	2.357
L10	658405.618120	224659.693526	3.920	5.334	4.457	3.519
M2	756937.867805	232774.056329	4.520	4.572	4.097	2.791
M4	762562.920492	230609.680239	2.170	0.254	2.797	3.760
M8	746972.860607	254820.071250	1.820	3.556	2.209	2.354
M9	742960.436068	231431.293091	1.620	0.762	1.031	1.782
M10	749986.779148	230140.273915	2.940	2.794	3.547	3.102
M12	765224.025423	256122.102610	1.540	5.842	3.364	2.615
M13	750684.183706	240383.890687	2.610	3.302	3.526	2.934
M14	765682.093654	241381.302807	3.070	2.794	1.937	2.341
M16	755400.233316	223825.771085	3.120	5.334	3.810	1.912
M17	744337.430006	224781.756367	2.130	2.286	2.509	1.696
M19	755951.048949	217610.399169	0.440	2.794	2.820	3.681
O3	735369.246078	230672.594422	0.230	0.254	0.420	0.925
O4	734168.924612	255016.775493	2.670	2.794	2.408	2.084
O5	713090.146295	246701.551082	2.750	1.270	3.898	2.309
O9	726130.235853	247275.671191	2.240	2.032	2.678	2.178
O18	731346.624696	216708.011455	0.180	0.000	0.000	0.326
O24	715654.088076	215086.283082	0.000	0.508	0.499	0.617
O25	731861.017503	225830.555575	0.170	1.270	0.813	0.319
W14	753133.344245	209696.295155	1.010	0.000	1.440	2.836
W18	745604.881900	214856.586919	1.530	1.524	2.731	1.504
W20	735298.537945	199341.859541	0.000	0.000	0.009	0.243
W23	724714.028432	197970.368012	0.000	0.000	0.314	0.000
W33	755386.272117	215582.872187	3.910	4.064	3.405	0.605
W48	709614.370019	201814.621439	0.180	1.524	1.387	0.588
A1	678039.980433	195924.936908	10.600	2.540	3.521	2.074
A2	663120.262649	212553.141409	2.690	1.270	3.519	3.460
A5	695810.135030	191348.250416	0.000	1.524	0.036	1.028
L1	656935.798800	236936.068948	3.380	4.572	5.860	3.684
L2	655307.791088	245383.380983	8.150	3.302	8.901	3.561
L5	655433.651803	217957.872282	9.390	5.588	8.333	3.580
L6	680819.554474	212103.804745	3.420	3.048	5.658	3.568
L8	683827.288566	245447.601664	5.360	4.572	5.732	3.631
L9	685117.095706	233972.632310	5.070	7.366	5.655	3.941
L11	671537.470375	229482.547174	2.590	2.286	3.588	4.173
M1	754440.159488	258799.157739	1.110	3.302	2.078	1.814
M3	753510.085060	218106.602475	3.910	4.826	4.387	1.914
M5	756874.108802	227770.456845	2.390	3.556	4.450	3.373
M7	739614.099028	250112.456291	2.360	3.810	3.532	2.141
M18	745887.802536	226750.940884	3.430	2.286	2.243	2.297
O2	730402.927052	221676.374291	0.170	0.254	0.772	0.172
O7	717831.717332	237839.089634	6.970	2.540	4.415	1.701
O8	725348.147988	235798.729758	2.970	4.064	3.762	1.061
O10	694269.889040	228610.917000	0.300	0.000	0.197	3.247
O13	705431.001880	220697.610715	0.460	1.016	0.689	1.509
O19	722772.817043	220375.078922	2.310	0.000	0.737	0.123
O22	736583.803510	221238.380171	0.400	1.016	0.702	0.724
O28	694588.732145	213376.137195	0.660	2.286	0.054	2.423
W2	708078.587107	194300.186312	0.000	2.032	1.489	0.319
W16	734607.714135	203484.977237	0.000	0.508	0.081	0.111
W22	727994.066738	195084.409450	0.000	0.000	0.048	0.000
W25	732161.441554	213556.429868	0.120	0.000	0.000	0.229
W27	726187.905777	204715.689118	0.000	1.016	0.180	0.012
W29	742838.247435	203183.487706	3.530	3.556	1.549	0.426
W35	732221.251123	179084.322024	0.070	0.254	0.008	0.116
W42	754665.813608	213426.186194	4.120	2.286	3.538	2.863
W43	733804.150235	197470.094732	0.110	0.254	0.000	0.000
W45	736867.359922	197018.994551	1.690	0.508	0.724	0.059
W46	734124.847745	185969.011278	0.000	0.000	0.860	0.091

Appendix B
Various SEMCOG Precipitation Data
(Precipitation Event 05/17/1999)

Station ID	X	Y	NEXRAD mm	Gage_mm	ANN	OC
A3	661857.143789	192530.880673	32.490	11.430	12.665	21.444
L3	668048.272705	241521.550493	12.590	6.096	9.997	13.071
L7	681514.971760	222057.746602	18.480	9.144	12.902	31.597
L10	658405.618120	224659.693526	9.850	5.588	6.403	17.038
M2	756937.867805	232774.056329	22.730	8.128	11.254	29.709
M4	762562.920492	230609.680239	22.500	8.382	14.586	25.104
M8	746972.860607	254820.071250	33.120	16.764	17.587	33.930
M9	742960.436068	231431.293091	44.400	18.034	31.760	39.076
M10	749986.779148	230140.273915	36.490	11.176	16.579	31.911
M12	765224.025423	256122.102610	34.180	13.970	21.034	30.082
M13	750684.183706	240383.890687	38.050	17.272	30.947	34.445
M14	765682.093654	241381.302807	29.160	8.636	4.352	27.814
M16	755400.233316	223825.771085	28.380	7.112	12.595	29.770
M17	744337.430006	224781.756367	28.220	12.700	24.746	36.313
M19	755951.048949	217610.399169	34.080	6.350	9.729	23.418
O3	735369.246078	230672.594422	46.810	22.606	34.658	40.567
O4	734168.924612	255016.775493	29.610	16.256	20.632	38.967
O5	713090.146295	246701.551082	34.140	14.224	17.525	38.250
O9	726130.235853	247275.671191	42.700	13.970	24.687	35.577
O18	731346.624696	216708.011455	26.650	11.430	22.830	36.434
O24	715654.088076	215086.283082	60.630	33.782	42.147	39.279
O25	731861.017503	225830.555575	37.390	21.590	29.390	40.055
W14	753133.344245	209696.295155	36.300	5.080	10.502	22.997
W18	745604.881900	214856.586919	26.580	16.256	24.487	28.632
W20	735298.537945	199341.859541	28.800	18.542	25.921	26.979
W23	724714.028432	197970.368012	27.430	15.240	26.895	40.024
W33	755386.272117	215582.872187	22.310	7.620	9.401	34.239
W48	709614.370019	201814.621439	56.460	16.002	27.134	41.049
A1	678039.980433	195924.936908	46.150	26.162	48.680	34.979
A2	663120.262649	212553.141409	19.380	10.668	14.168	18.991
A5	695810.135030	191348.250416	43.540	23.368	36.549	44.101
L1	656935.798800	236936.068948	12.070	11.684	26.236	10.028
L2	655307.791088	245383.380983	23.530	13.462	20.541	10.486
L5	655433.651803	217957.872282	13.250	2.540	11.323	13.967
L6	680819.554474	212103.804745	39.340	12.700	37.506	27.161
L8	683827.288566	245447.601664	17.720	7.366	19.276	19.967
L9	685117.095706	233972.632310	16.570	5.588	19.535	21.784
L11	671537.470375	229482.547174	7.250	10.160	12.859	13.807
M1	754440.159488	258799.157739	36.030	19.304	32.375	33.083
M3	753510.085060	218106.602475	22.310	6.350	14.085	29.437
M5	756874.108802	227770.456845	20.660	5.334	13.172	26.105
M7	739614.099028	250112.456291	40.080	16.764	28.749	35.573
M18	745887.802536	226750.940884	41.740	11.176	26.656	32.720
O2	730402.927052	221676.374291	37.390	19.812	33.877	34.085
O7	717831.717332	237839.089634	52.560	15.494	30.361	42.155
O8	725348.147988	235798.729758	56.700	37.084	54.723	44.840
O10	694269.889040	228610.917000	30.090	7.620	21.161	32.253
O13	705431.001880	220697.610715	59.720	34.290	58.775	48.973
O19	722772.817043	220375.078922	69.270	46.736	63.864	44.604
O22	736583.803510	221238.380171	41.000	10.414	30.520	29.892
O28	694588.732145	213376.137195	59.930	20.828	62.919	40.813
W2	708078.587107	194300.186312	35.820	24.892	25.045	47.673
W16	734607.714135	203484.977237	28.800	15.240	31.929	28.235
W22	727994.066738	195084.409450	34.590	16.256	25.694	28.115
W25	732161.441554	213556.429868	30.040	16.256	24.150	27.393
W27	726187.905777	204715.689118	27.430	12.192	21.909	32.503
W29	742838.247435	203183.487706	25.010	9.144	28.712	29.628
W42	754665.813608	213426.186194	24.570	6.350	5.330	27.132
W43	733804.150235	197470.094732	36.690	8.128	25.179	28.424
W44	733662.817575	179256.261133	16.470	12.954	18.657	31.920
W45	736867.359922	197018.994551	24.020	13.462	25.032	28.899
W46	734124.847745	185969.011278	15.500	9.144	25.544	30.347

Appendix C
Various SEMCOG Precipitation Data
(Precipitation Event 05/23/1999)

Station ID	X	Y	NEXRAD mm	Gage_mm	ANN	OC
A3	661857.143789	192530.880673	6.110	9.144	6.805	4.639
L3	668048.272705	241521.550493	3.440	3.810	3.464	2.866
L7	681514.971760	222057.746602	2.410	8.636	4.948	4.107
L10	658405.618120	224659.693526	4.690	6.604	5.588	4.078
M2	756937.867805	232774.056329	4.130	8.890	4.507	3.458
M4	762562.920492	230609.680239	4.050	2.794	1.431	3.975
M8	746972.860607	254820.071250	1.260	7.874	3.322	1.361
M9	742960.436068	231431.293091	2.320	10.668	6.547	2.394
M10	749986.779148	230140.273915	3.310	11.684	7.372	2.800
M12	765224.025423	256122.102610	3.080	9.906	6.107	2.803
M13	750684.183706	240383.890687	2.280	8.636	5.459	2.993
M14	765682.093654	241381.302807	4.180	10.414	7.872	3.688
M16	755400.233316	223825.771085	2.590	3.048	0.469	3.487
M17	744337.430006	224781.756367	2.410	8.128	3.757	2.562
M19	755951.048949	217610.399169	3.220	4.826	4.949	2.719
O3	735369.246078	230672.594422	1.900	11.938	6.473	2.364
O4	734168.924612	255016.775493	0.090	4.318	6.174	2.773
O5	713090.146295	246701.551082	0.780	5.588	3.998	3.764
O9	726130.235853	247275.671191	4.620	6.096	5.269	0.632
O18	731346.624696	216708.011455	3.260	13.462	6.568	2.912
O24	715654.088076	215086.283082	3.790	9.906	6.927	3.484
O25	731861.017503	225830.555575	2.210	7.874	5.507	2.454
W14	753133.344245	209696.295155	3.350	5.080	3.842	3.032
W18	745604.881900	214856.586919	2.930	5.588	0.000	2.939
W20	735298.537945	199341.859541	3.860	4.572	1.212	3.825
W23	724714.028432	197970.368012	4.130	6.096	3.294	4.206
W33	755386.272117	215582.872187	2.730	0.254	0.000	3.242
W48	709614.370019	201814.621439	4.840	12.700	7.742	4.153
A1	678039.980433	195924.936908	5.950	6.350	7.323	5.118
A2	663120.262649	212553.141409	2.410	7.874	2.232	4.768
A5	695810.135030	191348.250416	5.230	12.700	4.539	5.081
L1	656935.798800	236936.068948	3.180	6.350	2.772	4.125
L2	655307.791088	245383.380983	2.410	5.588	3.643	3.826
L5	655433.651803	217957.872282	3.510	18.034	5.323	4.983
L6	680819.554474	212103.804745	3.340	5.842	2.183	3.625
L8	683827.288566	245447.601664	3.570	5.842	5.515	2.128
L9	685117.095706	233972.632310	2.650	6.096	4.920	2.273
L11	671537.470375	229482.547174	5.160	5.842	3.267	3.315
M1	754440.159488	258799.157739	1.220	7.874	0.331	1.875
M3	753510.085060	218106.602475	2.730	4.064	0.785	2.885
M5	756874.108802	227770.456845	2.140	1.270	5.293	3.412
M7	739614.099028	250112.456291	1.920	7.366	0.735	1.282
M18	745887.802536	226750.940884	4.280	11.684	10.511	2.590
O2	730402.927052	221676.374291	2.210	9.652	5.735	2.750
O7	717831.717332	237839.089634	4.480	12.192	5.656	2.481
O8	725348.147988	235798.729758	2.850	9.652	11.378	2.894
O10	694269.889040	228610.917000	2.030	8.382	2.672	2.324
O13	705431.001880	220697.610715	1.270	8.128	2.851	3.176
O19	722772.817043	220375.078922	3.390	9.906	7.300	3.120
O22	736583.803510	221238.380171	3.670	6.604	7.405	2.595
O28	694588.732145	213376.137195	2.970	11.684	4.264	3.465
W2	708078.587107	194300.186312	4.500	13.716	10.053	4.978
W16	734607.714135	203484.977237	3.860	6.858	1.080	3.724
W22	727994.066738	195084.409450	3.480	3.810	4.555	4.128
W25	732161.441554	213556.429868	4.350	11.938	3.638	3.370
W27	726187.905777	204715.689118	4.130	10.668	0.000	3.915
W29	742838.247435	203183.487706	3.320	6.604	1.462	3.583
W35	732221.251123	179084.322024	4.400	5.842	5.177	4.339
W42	754665.813608	213426.186194	2.560	5.334	2.289	2.950
W43	733804.150235	197470.094732	3.010	3.302	2.002	3.942
W45	736867.359922	197018.994551	3.880	9.398	2.034	3.895
W46	734124.847745	185969.011278	4.520	6.096	5.014	4.199

125

Appendix D
Various SEMCOG Precipitation Data
(Precipitation Event 05/24/1999)

Station ID	X	Y	NEXRAD mm	Gage_mm	ANN	OC
A3	661857.143789	192530.880673	0.000	1.778	0.275	0.227
L3	668048.272705	241521.550493	0.000	1.524	0.367	0.000
L7	681514.971760	222057.746602	0.000	1.524	0.331	0.046
L10	658405.618120	224659.693526	0.000	1.524	0.472	0.000
M2	756937.867805	232774.056329	0.000	3.302	1.842	0.000
M4	762562.920492	230609.680239	0.000	4.064	2.232	0.207
M8	746972.860607	254820.071250	0.000	1.27	0.291	0.100
M9	742960.436068	231431.293091	0.000	1.016	0.696	0.000
M10	749986.779148	230140.273915	0.000	2.54	1.367	0.000
M12	765224.025423	256122.102610	0.380	5.842	3.468	0.161
M13	750684.183706	240383.890687	0.000	0.762	0.235	0.025
M14	765682.093654	241381.302807	0.240	3.556	2.037	0.172
M16	755400.233316	223825.771085	0.000	3.302	1.269	0.395
M17	744337.430006	224781.756367	0.000	3.048	0.995	0.000
M19	755951.048949	217610.399169	0.950	1.524	1.207	0.168
O3	735369.246078	230672.594422	0.000	1.27	0.357	0.000
O4	734168.924612	255016.775493	0.000	0.762	0.217	0.000
O5	713090.146295	246701.551082	0.000	1.524	0.444	0.000
O9	726130.235853	247275.671191	0.000	0.762	0.217	0.000
O18	731346.624696	216708.011455	0.100	4.064	1.149	0.121
O24	715654.088076	215086.283082	0.090	2.032	0.476	0.154
O25	731861.017503	225830.555575	0.000	1.016	0.557	0.000
W8	732252.968427	197942.382800	0.890	1.27	0.636	0.621
W14	753133.344245	209696.295155	1.410	1.778	0.834	0.273
W18	745604.881900	214856.586919	0.000	3.048	0.958	0.590
W23	724714.028432	197970.368012	0.500	4.572	1.542	0.684
W33	755386.272117	215582.872187	0.240	0	1.325	1.025
W48	709614.370019	201814.621439	0.350	1.778	0.695	0.252
A1	678039.980433	195924.936908	0.000	1.016	0.015	0.109
A2	663120.262649	212553.141409	0.070	2.032	-0.079	0.001
A5	695810.135030	191348.250416	0.000	0.762	0.212	0.320
L1	656935.798800	236936.068948	0.000	1.524	0.084	0.000
L2	655307.791088	245383.380983	0.000	1.016	0.000	0.000
L5	655433.651803	217957.872282	0.000	1.27	0.323	0.000
L6	680819.554474	212103.804745	0.000	2.032	0.000	0.048
L8	683827.288566	245447.601664	0.070	1.016	0.000	0.000
L9	685117.095706	233972.632310	0.000	1.27	0.000	0.000
L11	671537.470375	229482.547174	0.000	1.016	0.000	0.000
M1	754440.159488	258799.157739	0.000	1.27	0.000	0.157
M5	756874.108802	227770.456845	0.000	2.794	1.148	0.000
M7	739614.099028	250112.456291	0.000	0.762	0.138	0.000
M15	755444.220459	218949.865155	0.240	2.286	0.834	0.691
M18	745887.802536	226750.940884	0.080	1.778	0.679	0.000
O2	730402.927052	221676.374291	0.000	0.254	0.310	0.028
O7	717831.717332	237839.089634	0.000	1.778	0.010	0.008
O8	725348.147988	235798.729758	0.000	0.762	0.000	0.002
O10	694269.889040	228610.917000	0.000	2.54	0.045	0.011
O13	705431.001880	220697.610715	0.000	3.302	0.000	0.058
O19	722772.817043	220375.078922	0.000	2.794	0.169	0.051
O22	736583.803510	221238.380171	0.000	1.778	0.375	0.009
O28	694588.732145	213376.137195	0.000	0.254	0.000	0.102
W2	708078.587107	194300.186312	0.350	3.81	0.471	0.420
W16	734607.714135	203484.977237	0.890	3.048	0.350	0.675
W19	743359.844905	202028.959810	0.000	2.286	0.184	0.971
W22	727994.066738	195084.409450	0.440	3.556	0.867	0.733
W25	732161.441554	213556.429868	0.570	3.556	0.615	0.194
W27	726187.905777	204715.689118	0.500	3.556	0.694	0.419
W42	754665.813608	213426.186194	0.500	2.286	0.823	0.635
W43	733804.150235	197470.094732	0.310	2.54	0.414	0.917
W44	733662.817575	179256.261133	0.350	2.032	0.085	1.062
W45	736867.359922	197018.994551	0.270	2.794	0.188	0.972
W46	734124.847745	185969.011278	0.360	2.286	0.277	1.029

Appendix E
Various SEMCOG Precipitation Data
(Precipitation Event 06/09/1999)

Station ID	X	Y	NEXRAD mm	Gage_mm	ANN	OC
A 3	661857.143789	192530.880673	14.840	13.2080	17.024	0.408
A 4	697211.999775	189629.477045	0.940	0.2540	0.000	4.355
L 3	668048.272705	241521.550493	6.550	10.6680	10.025	0.227
L 7	681514.971760	222057.746602	0.940	0.5080	0.000	3.562
L10	658405.618120	224659.693526	0.810	2.5400	5.436	8.438
M 2	756937.867805	232774.056329	0.000	0.5080	0.931	0.175
M 4	762562.920492	230609.680239	0.000	0.2540	0.000	-0.097
M 8	746972.860607	254820.071250	3.510	0.7620	2.824	1.418
M 9	742960.436068	231431.293091	2.450	0.7620	2.111	1.498
M10	749986.779148	230140.273915	0.250	0.0000	0.000	0.721
M12	765224.025423	256122.102610	0.860	0.7620	0.000	1.565
M13	750684.183706	240383.890687	0.940	0.0000	1.254	1.621
M14	765682.093654	241381.302807	0.140	0.0000	0.124	0.353
M16	755400.233316	223825.771085	0.200	0.0000	0.036	0.000
M17	744337.430006	224781.756367	0.080	0.2540	1.657	1.140
M19	755951.048949	217610.399169	0.000	0.0000	0.706	0.022
O 3	735369.246078	230672.594422	3.480	0.2540	2.515	1.560
O 4	734168.924612	255016.775493	1.700	0.0000	0.882	2.564
O 5	713090.146295	246701.551082	1.360	0.0000	0.000	2.003
O 9	726130.235853	247275.671191	1.470	0.7620	0.000	1.924
O18	731346.624696	216708.011455	0.410	0.5080	0.000	0.233
O24	715654.088076	215086.283082	0.090	0.2540	0.000	0.493
O25	731861.017503	225830.555575	0.880	0.0000	0.324	2.092
W 8	732252.968427	197942.382800	0.000	0.7620	1.659	0.000
W14	753133.344245	209696.295155	0.000	0.0000	0.000	0.000
W18	745604.881900	214856.586919	0.000	0.0000	0.000	0.000
W23	724714.028432	197970.368012	0.000	1.0160	0.000	0.041
W33	755386.272117	215582.872187	0.000	0.0000	0.754	0.000
W48	709614.370019	201814.621439	0.200	0.5080	0.031	0.105
A 1	678039.980433	195924.936908	2.800	1.270	0.469	6.949
A 2	663120.262649	212553.141409	0.000	0.000	2.325	5.114
A 5	695810.135030	191348.250416	1.240	0.254	0.000	1.348
L 1	656935.798800	236936.068948	13.700	24.892	30.611	4.179
L 2	655307.791088	245383.380983	9.280	1.524	4.626	5.441
L 5	655433.651803	217957.872282	12.000	3.302	4.220	3.774
L 6	680819.554474	212103.804745	0.260	1.016	0.000	2.709
L 8	683827.288566	245447.601664	3.230	1.270	2.292	3.783
L 9	685117.095706	233972.632310	2.610	1.524	0.000	2.275
L11	671537.470375	229482.547174	0.000	0.762	0.824	2.752
M 1	754440.159488	258799.157739	4.150	1.270	2.022	2.323
M 5	756874.108802	227770.456845	0.350	0.000	0.000	0.047
M 7	739614.099028	250112.456291	1.040	0.762	1.860	2.469
M15	755444.220459	218949.865155	0.000	0.000	0.454	0.028
M18	745887.802536	226750.940884	1.300	0.000	0.011	0.471
O 7	717831.717332	237839.089634	2.180	0.000	2.470	1.360
O 8	725348.147988	235798.729758	2.790	0.000	3.078	1.828
O10	694269.889040	228610.917000	1.500	1.016	2.827	1.151
O13	705431.001880	220697.610715	1.840	0.508	2.485	0.533
O19	722772.817043	220375.078922	1.150	0.000	1.849	0.485
O22	736583.803510	221238.380171	0.660	0.000	0.847	0.631
O28	694588.732145	213376.137195	0.450	0.000	0.861	0.991
W 2	708078.587107	194300.186312	0.140	0.762	0.000	0.341
W16	734607.714135	203484.977237	0.000	0.762	0.000	0.016
W22	727994.066738	195084.409450	0.000	0.000	0.535	0.007
W25	732161.441554	213556.429868	0.000	0.000	0.294	0.248
W27	726187.905777	204715.689118	0.000	0.508	0.000	0.017
W29	742838.247435	203183.487706	0.440	0.508	0.000	0.000
W42	754665.813608	213426.186194	0.000	0.254	0.003	0.000
W43	733804.150235	197470.094732	0.000	0.000	0.874	0.000
W44	733662.817575	179256.261133	0.000	0.254	0.318	0.041
W45	736867.359922	197018.994551	0.400	0.508	0.391	0.000
W46	734124.847745	185969.011278	0.000	0.762	0.087	0.005

Appendix F
Various SEMCOG Precipitation Data
(Precipitation Event 07/01/1999)

Station ID	X	Y	NEXRAD mm	Gage_mm	ANN	OC
A3	661857.143789	192530.880673	19.680	34.036	22.386	13.264
L3	668048.272705	241521.550493	17.600	30.48	24.040	17.475
L7	681514.971760	222057.746602	18.030	32.766	22.796	16.056
L10	658405.618120	224659.693526	16.630	31.496	23.956	18.902
M2	756937.867805	232774.056329	20.540	19.05	18.344	19.557
M4	762562.920492	230609.680239	27.420	11.176	12.346	18.274
M8	746972.860607	254820.071250	25.640	45.466	30.243	13.559
M9	742960.436068	231431.293091	15.410	20.32	17.045	12.844
M10	749986.779148	230140.273915	12.920	20.828	20.907	13.999
M12	765224.025423	256122.102610	9.700	20.066	15.684	24.451
M13	750684.183706	240383.890687	13.160	16.002	17.894	20.252
M14	765682.093654	241381.302807	22.870	28.956	28.524	19.346
M16	755400.233316	223825.771085	10.530	11.684	8.839	12.340
M17	744337.430006	224781.756367	10.370	14.986	12.130	11.209
M19	755951.048949	217610.399169	5.260	6.35	5.531	7.500
O3	735369.246078	230672.594422	14.400	23.368	20.970	16.602
O4	734168.924612	255016.775493	16.530	39.116	31.537	25.790
O5	713090.146295	246701.551082	16.760	39.37	28.026	23.884
O9	726130.235853	247275.671191	27.340	45.72	30.106	16.150
O18	731346.624696	216708.011455	14.220	21.59	15.281	11.509
O24	715654.088076	215086.283082	13.220	23.114	18.839	13.296
O25	731861.017503	225830.555575	15.820	20.066	17.946	14.740
W8	732252.968427	197942.382800	6.990	9.144	6.587	5.592
W14	753133.344245	209696.295155	3.980	5.588	6.233	4.688
W15	750221.159860	206719.251289	3.840	5.588	4.273	4.471
W18	745604.881900	214856.586919	6.150	11.684	8.437	6.884
W23	724714.028432	197970.368012	5.890	12.954	10.619	8.198
W33	755386.272117	215582.872187	5.950	7.874	6.468	4.957
W48	709614.370019	201814.621439	9.610	16.764	8.701	10.785
A1	678039.980433	195924.936908	28.330	45.466	25.133	16.477
A2	663120.262649	212553.141409	18.070	30.988	19.053	17.853
A5	695810.135030	191348.250416	8.760	21.59	8.165	12.222
L1	656935.798800	236936.068948	14.240	41.656	15.932	17.283
L2	655307.791088	245383.380983	15.690	44.45	44.022	17.539
L5	655433.651803	217957.872282	16.280	34.29	23.207	17.439
L6	680819.554474	212103.804745	17.320	31.242	14.069	17.014
L8	683827.288566	245447.601664	17.890	36.576	19.463	17.507
L9	685117.095706	233972.632310	17.610	41.656	18.859	17.477
L11	671537.470375	229482.547174	18.950	35.306	18.605	17.570
M1	754440.159488	258799.157739	25.330	33.274	31.027	18.362
M5	756874.108802	227770.456845	19.610	11.176	19.432	16.835
M7	739614.099028	250112.456291	28.830	46.228	28.897	20.308
M15	755444.220459	218949.865155	5.950	9.906	9.121	6.385
O2	730402.927052	221676.374291	15.820	19.812	17.258	15.183
O7	717831.717332	237839.089634	18.050	46.99	20.415	19.096
O8	725348.147988	235798.729758	22.120	41.148	27.426	19.631
O10	694269.889040	228610.917000	16.230	39.37	20.034	16.793
O13	705431.001880	220697.610715	13.350	37.084	18.141	15.147
O19	722772.817043	220375.078922	13.640	21.336	16.217	15.045
O22	736583.803510	221238.380171	15.520	25.908	20.001	12.814
O26	702230.908441	220046.898222	15.190	36.068	15.578	15.229
O28	694588.732145	213376.137195	17.090	31.75	16.899	15.030
W2	708078.587107	194300.186312	8.030	16.51	10.622	9.224
W16	734607.714135	203484.977237	6.990	9.398	7.474	7.685
W19	743359.844905	202028.959810	4.800	3.302	3.774	5.241
W25	732161.441554	213556.429868	9.630	21.082	13.919	12.203
W27	726187.905777	204715.689118	5.890	14.732	8.476	8.896
W35	732221.251123	179084.322024	4.540	6.858	-0.396	4.466
W42	754665.813608	213426.186194	4.360	5.588	6.541	5.242
W43	733804.150235	197470.094732	4.430	6.35	2.788	6.643
W45	736867.359922	197018.994551	4.610	10.668	0.792	6.036
W47	731495.224830	195941.679285	5.730	9.144	4.430	6.382

128

Appendix G
Various SEMCOG Precipitation Data
(Precipitation Event 07/23/1999)

Station ID	X	Y	NEXRAD mm	Gage_mm	ANN mm	OC mm
A3	661857.143789	192530.880673	6.620	-7.620	7.503	13.970
L3	668048.272705	241521.550493	20.670	23.876	21.366	10.260
L7	681514.971760	222057.746602	9.900	3.810	2.3616	18.820
L10	658405.618120	224659.693526	8.540	6.858	9.2393	12.940
M2	756937.867805	232774.056329	26.870	20.320	22.156	23.470
M4	762562.920492	230609.680239	29.960	25.908	23.844	24.600
M8	746972.860607	254820.071250	10.530	7.112	6.9955	8.010
M9	742960.436068	231431.293091	17.990	13.970	13.632	18.410
M10	749986.779148	230140.273915	18.600	12.446	14.884	22.950
M12	765224.025423	256122.102610	8.470	5.588	6.2693	13.240
M13	750684.183706	240383.890687	13.730	14.224	15.596	17.660
M14	765682.093654	241381.302807	17.840	4.064	5.3483	20.070
M16	755400.233316	223825.771085	26.930	21.082	24.373	22.350
M17	744337.430006	224781.756367	23.340	20.320	22.667	18.230
O3	735369.246078	230672.594422	17.380	13.970	20.95	18.850
O4	734168.924612	255016.775493	7.180	8.382	6.8421	17.540
O5	713090.146295	246701.551082	24.710	23.114	26.476	21.100
O9	726130.235853	247275.671191	24.470	14.224	17.085	15.310
O18	731346.624696	216708.011455	21.960	31.242	29.442	20.970
O24	715654.088076	215086.283082	23.750	28.194	23.209	25.080
O25	731861.017503	225830.555575	18.770	16.256	21.677	19.740
W8	732252.968427	197942.382800	29.380	23.876	21.131	26.770
W14	753133.344245	209696.295155	20.240	10.414	7.3259	17.860
W15	750221.159860	206719.251289	21.420	3.556	6.9491	20.550
W18	745604.881900	214856.586919	15.350	19.050	17.912	22.480
W23	724714.028432	197970.368012	29.530	28.956	29.272	29.590
W31	756733.582014	214398.150256	13.030	16.002	15.468	19.320
W33	755386.272117	215582.872187	18.080	18.796	20.52	15.310
W48	709614.370019	201814.621439	30.940	50.038	41.267	23.460
A1	678039.980433	195924.936908	16.520	7.366	1.613	12.690
A2	663120.262649	212553.141409	9.020	4.318	6.672	7.660
A5	695810.135030	191348.250416	39.670	43.688	45.048	22.230
L1	656935.798800	236936.068948	16.760	27.178	29.589	14.400
L2	655307.791088	245383.380983	22.240	26.67	24.395	16.440
L5	655433.651803	217957.872282	13.980	4.064	14.886	7.570
L6	680819.554474	212103.804745	14.380	7.112	12.212	11.630
L8	683827.288566	245447.601664	24.990	27.686	26.892	19.830
L9	685117.095706	233972.632310	17.340	7.112	26.331	16.690
L11	671537.470375	229482.547174	5.670	2.794	4.191	13.200
M1	754440.159488	258799.157739	9.860	10.16	24.493	8.920
M5	756874.108802	227770.456845	29.670	14.224	23.159	27.260
M7	739614.099028	250112.456291	13.300	6.096	3.301	10.910
M15	755444.220459	218949.865155	18.080	23.876	30.819	21.210
O2	730402.927052	221676.374291	18.770	28.702	18.122	20.410
O7	717831.717332	237839.089634	21.260	19.558	27.946	23.730
O8	725348.147988	235798.729758	21.040	15.748	23.079	21.880
O10	694269.889040	228610.917000	11.060	6.858	3.751	18.100
O13	705431.001880	220697.610715	14.750	19.558	12.920	21.740
O19	722772.817043	220375.078922	27.030	30.988	31.685	22.030
O22	736583.803510	221238.380171	23.060	21.844	23.876	20.190
O26	702230.908441	220046.898222	12.070	17.272	15.236	21.190
O28	694588.732145	213376.137195	18.060	11.176	20.481	18.530
W2	708078.587107	194300.186312	41.630	49.784	45.969	28.800
W16	734607.714135	203484.977237	29.380	41.91	39.841	25.890
W19	743359.844905	202028.959810	28.680	21.336	30.581	23.770
W25	732161.441554	213556.429868	24.190	31.242	30.147	22.510
W27	726187.905777	204715.689118	29.530	52.07	32.815	27.100
W42	754665.813608	213426.186194	12.850	12.192	20.453	16.570
W43	733804.150235	197470.094732	22.200	16.764	19.646	28.800
W44	733662.817575	179256.261133	23.620	28.448	19.011	29.670
W45	736867.359922	197018.994551	25.420	21.59	30.830	27.660
W47	731495.224830	195941.679285	20.240	15.494	24.465	29.590

Appendix H
Various SEMCOG Precipitation Data
(Precipitation Event 07/31/1999)

Station ID	X	Y	NEXRAD mm	Gage_mm	ANN mm	OC mm
A3	661857.143789	192530.880673	9.910	7.62	7.850	15.541
L3	668048.272705	241521.550493	3.260	1.016	0.000	15.024
L7	681514.971760	222057.746602	8.850	16.764	13.025	9.416
L10	658405.618120	224659.693526	18.500	20.574	17.318	6.206
M2	756937.867805	232774.056329	3.360	1.016	1.019	4.470
M4	762562.920492	230609.680239	3.930	4.318	5.174	5.699
M8	746972.860607	254820.071250	10.540	1.016	0.000	8.683
M9	742960.436068	231431.293091	3.720	3.048	6.161	6.961
M10	749986.779148	230140.273915	2.550	1.778	0.000	5.553
M12	765224.025423	256122.102610	8.090	0.508	0.903	7.036
M13	750684.183706	240383.890687	10.450	9.398	9.468	4.448
M14	765682.093654	241381.302807	3.750	8.636	5.842	6.541
M16	755400.233316	223825.771085	7.800	8.382	6.301	9.239
M17	744337.430006	224781.756367	7.660	2.032	6.209	5.828
M19	755951.048949	217610.399169	20.150	13.716	15.702	16.809
O3	735369.246078	230672.594422	8.620	3.81	6.082	5.062
O4	734168.924612	255016.775493	7.790	1.016	0.000	11.597
O5	713090.146295	246701.551082	10.330	9.906	2.274	9.590
O9	726130.235853	247275.671191	12.060	5.334	5.394	8.676
O18	731346.624696	216708.011455	7.090	7.112	8.172	7.140
O24	715654.088076	215086.283082	6.720	4.572	6.963	7.048
O25	731861.017503	225830.555575	4.320	4.064	3.213	8.037
W14	753133.344245	209696.295155	12.020	3.302	4.644	16.993
W15	750221.159860	206719.251289	14.910	2.032	2.538	11.946
W18	745604.881900	214856.586919	11.260	11.938	10.907	11.466
W20	735298.537945	199341.859541	11.450	5.588	8.563	11.024
W23	724714.028432	197970.368012	8.850	2.032	3.897	9.677
W33	755386.272117	215582.872187	18.300	16.002	14.690	17.406
W48	709614.370019	201814.621439	7.290	1.016	2.006	7.972
A1	678039.980433	195924.936908	3.830	2.540	3.204	9.624
A2	663120.262649	212553.141409	9.350	15.494	7.489	14.183
A5	695810.135030	191348.250416	3.610	5.080	5.010	8.608
L1	656935.798800	236936.068948	1.970	0.508	0.372	10.874
L2	655307.791088	245383.380983	0.620	8.636	7.538	8.373
L5	655433.651803	217957.872282	8.980	1.016	1.736	16.806
L6	680819.554474	212103.804745	8.870	10.922	6.409	9.760
L8	683827.288566	245447.601664	3.640	2.794	15.639	5.640
L9	685117.095706	233972.632310	7.040	13.208	8.587	6.921
L11	671537.470375	229482.547174	14.510	10.160	10.478	9.551
M1	754440.159488	258799.157739	13.410	0.762	0.551	9.476
M3	753510.085060	218106.602475	18.300	3.810	5.088	14.119
M5	756874.108802	227770.456845	6.120	4.572	3.594	5.109
M7	739614.099028	250112.456291	5.160	13.970	9.574	9.443
O2	730402.927052	221676.374291	4.320	4.826	6.114	5.576
O7	717831.717332	237839.089634	19.220	20.320	16.190	9.447
O8	725348.147988	235798.729758	26.260	14.224	21.684	8.814
O10	694269.889040	228610.917000	5.520	2.286	6.533	7.540
O13	705431.001880	220697.610715	8.430	4.826	6.114	7.652
O19	722772.817043	220375.078922	6.980	1.524	6.535	6.312
O22	736583.803510	221238.380171	4.120	15.748	6.834	6.947
O26	702230.908441	220046.898222	6.150	15.748	6.834	7.426
O28	694588.732145	213376.137195	6.370	6.858	6.782	7.928
W2	708078.587107	194300.186312	4.680	2.794	0.167	8.128
W16	734607.714135	203484.977237	11.450	2.286	9.382	10.661
W25	732161.441554	213556.429868	9.260	7.620	7.762	8.058
W27	726187.905777	204715.689118	8.850	1.524	8.225	8.584
W29	742838.247435	203183.487706	14.770	9.144	13.073	12.921
W42	754665.813608	213426.186194	19.500	9.398	14.507	17.080
W43	733804.150235	197470.094732	14.930	3.556	7.794	11.188
W44	733662.817575	179256.261133	14.820	13.462	17.116	12.217
W45	736867.359922	197018.994551	17.690	7.874	9.472	11.971
W47	731495.224830	195941.679285	14.730	9.398	6.554	10.721

Appendix I
Various SEMCOG Precipitation Data
(Precipitation Event 07/09/1999)

Station ID	X	Y	NEXRAD mm	Gage_mm	ANN_mm	OC_mm
A3	661857.143789	192530.880673	23.160	13.716	16.43	15.870
L 3	668048.272705	241521.550493	14.930	9.906	12.14	19.600
L 7	681514.971760	222057.746602	19.430	9.398	13.73	17.860
L10	658405.618120	224659.693526	18.450	15.494	16.55	18.550
M 2	756937.867805	232774.056329	9.170	4.064	4.20	9.010
M 4	762562.920492	230609.680239	8.410	5.334	5.52	8.900
M 8	746972.860607	254820.071250	8.170	6.096	6.65	9.390
M 9	742960.436068	231431.293091	13.650	6.858	9.30	11.260
M10	749986.779148	230140.273915	9.750	6.35	7.70	9.980
M12	765224.025423	256122.102610	5.630	1.778	2.67	9.470
M13	750684.183706	240383.890687	9.810	6.604	6.58	10.630
M14	765682.093654	241381.302807	11.110	6.604	6.21	7.360
M16	755400.233316	223825.771085	7.150	7.112	6.51	8.250
M17	744337.430006	224781.756367	9.910	6.096	7.63	11.400
M19	755951.048949	217610.399169	7.700	7.366	7.70	7.910
O 3	735369.246078	230672.594422	13.750	7.112	11.10	14.870
O 4	734168.924612	255016.775493	11.610	7.62	8.15	14.360
O 5	713090.146295	246701.551082	22.790	11.938	18.27	18.530
O 9	726130.235853	247275.671191	19.200	10.414	13.95	16.430
O18	731346.624696	216708.011455	15.500	10.922	12.60	13.340
O24	715654.088076	215086.283082	16.110	11.43	14.07	15.230
O25	731861.017503	225830.555575	15.070	9.906	12.63	14.770
W 8	732252.968427	197942.382800	10.070	9.398	10.60	9.970
W14	753133.344245	209696.295155	8.280	6.35	6.55	7.980
W15	750221.159860	206719.251289	7.950	3.81	5.08	8.700
W18	745604.881900	214856.586919	9.600	9.144	9.32	9.740
W23	724714.028432	197970.368012	10.180	7.874	9.30	11.060
W33	755386.272117	215582.872187	8.220	8.89	7.86	7.850
W48	709614.370019	201814.621439	11.540	9.652	10.92	14.510
A 1	678039.980433	195924.936908	18.310	10.414	14.128	19.480
A 2	663120.262649	212553.141409	10.350	9.652	13.985	20.220
A 5	695810.135030	191348.250416	13.920	10.16	15.233	15.000
L 1	656935.798800	236936.068948	15.950	12.954	14.118	16.640
L 2	655307.791088	245383.380983	15.200	11.176	17.439	16.120
L 5	655433.651803	217957.872282	13.670	10.16	18.412	19.600
L 6	680819.554474	212103.804745	14.710	6.096	17.779	19.150
L 8	683827.288566	245447.601664	19.270	12.192	21.125	17.860
L 9	685117.095706	233972.632310	17.310	12.192	19.271	18.630
L11	671537.470375	229482.547174	19.760	12.7	21.908	17.770
M 1	754440.159488	258799.157739	5.090	5.842	5.323	7.080
M 3	753510.085060	218106.602475	8.220	8.636	6.292	7.970
M 5	756874.108802	227770.456845	7.220	3.302	4.187	8.010
M 7	739614.099028	250112.456291	10.520	8.128	8.646	11.200
O 2	730402.927052	221676.374291	15.070	10.16	16.717	15.460
O 7	717831.717332	237839.089634	20.500	8.89	26.493	20.420
O 8	725348.147988	235798.729758	19.430	8.128	24.480	18.000
O10	694269.889040	228610.917000	20.530	11.684	20.992	19.220
O13	705431.001880	220697.610715	18.830	10.16	21.538	17.950
O19	722772.817043	220375.078922	20.790	10.414	22.844	16.560
O22	736583.803510	221238.380171	13.270	8.89	11.839	13.400
O26	702230.908441	220046.898222	20.130	11.938	22.077	17.870
O28	694588.732145	213376.137195	18.640	7.874	18.432	17.380
W 2	708078.587107	194300.186312	12.250	9.652	13.526	11.770
W16	734607.714135	203484.977237	10.070	7.62	11.683	10.910
W25	732161.441554	213556.429868	13.360	10.668	11.012	14.210
W27	726187.905777	204715.689118	10.180	7.874	11.381	12.190
W29	742838.247435	203183.487706	8.780	6.858	8.736	9.280
W35	732221.251123	179084.322024	8.890	11.43	11.672	8.400
W42	754665.813608	213426.186194	9.770	7.366	8.833	8.240
W43	733804.150235	197470.094732	11.140	7.366	11.382	9.860
W45	736867.359922	197018.994551	10.970	9.906	10.338	9.490
W47	731495.224830	195941.679285	10.690	8.382	11.272	9.770

Appendix J
Various SEMCOG Precipitation Data
(Precipitation Event 08/13/1999)

Station ID	X	Y	NEXRAD mm	Gage_mm	ANN mm	OC mm
A 3	661857.143789	192530.880673	10.010	1.778	3.721	9.164
A 4	695810.135030	191348.250416	7.580	4.318	4.235	6.212
L 7	681514.971760	222057.746602	17.490	27.94	20.146	12.252
L10	658405.618120	224659.693526	11.210	8.636	8.874	14.724
M 2	756937.867805	232774.056329	14.670	13.716	15.786	14.126
M 4	762562.920492	230609.680239	11.020	13.208	10.292	12.804
M 8	746972.860607	254820.071250	9.300	18.796	11.475	8.103
M 9	742960.436068	231431.293091	25.730	30.734	21.956	20.064
M10	749986.779148	230140.273915	20.210	25.654	19.884	19.102
M12	765224.025423	256122.102610	5.670	17.78	15.516	7.425
M13	750684.183706	240383.890687	13.760	17.526	16.341	16.221
M14	765682.093654	241381.302807	8.890	20.32	17.298	8.991
M16	755400.233316	223825.771085	15.650	26.924	19.167	17.234
M17	744337.430006	224781.756367	19.160	18.288	18.856	20.975
O 3	735369.246078	230672.594422	21.470	34.544	26.333	20.342
O 4	734168.924612	255016.775493	6.970	19.05	12.634	13.789
O 5	713090.146295	246701.551082	15.480	20.32	16.895	17.183
O 9	726130.235853	247275.671191	17.530	24.13	17.264	13.150
O18	731346.624696	216708.011455	18.710	26.924	21.975	15.161
O24	715654.088076	215086.283082	18.790	38.608	22.950	11.948
O25	731861.017503	225830.555575	17.140	18.796	20.156	20.534
W 8	732252.968427	197942.382800	8.310	7.62	6.706	6.251
W14	753133.344245	209696.295155	7.110	4.572	6.573	14.219
W18	745604.881900	214856.586919	13.500	17.78	16.497	14.562
W23	724714.028432	197970.368012	5.170	7.112	7.502	8.265
W31	756733.582014	214398.150256	15.510	10.922	18.677	15.897
W33	755386.272117	215582.872187	18.480	17.78	16.297	15.002
W48	709614.370019	201814.621439	5.070	5.334	5.488	10.879
A 1	678039.980433	195924.936908	2.970	8.128	3.911	10.292
A 2	663120.262649	212553.141409	4.880	4.064	5.236	11.921
A 5	695810.135030	191348.250416	4.770	6.096	0.949	7.580
L 1	656935.798800	236936.068948	9.850	7.874	13.062	12.035
L 2	655307.791088	245383.380983	13.900	10.16	11.895	12.044
L 5	655433.651803	217957.872282	11.420	3.048	10.297	11.076
L 6	680819.554474	212103.804745	23.120	17.018	21.224	14.212
L 8	683827.288566	245447.601664	14.300	22.098	15.502	15.025
L 9	685117.095706	233972.632310	17.750	23.114	18.086	16.506
L11	671537.470375	229482.547174	13.980	5.334	14.329	14.689
M 1	754440.159488	258799.157739	9.130	19.812	4.711	7.050
M 5	756874.108802	227770.456845	16.170	16.002	16.586	15.103
M 7	739614.099028	250112.456291	15.350	23.368	10.649	11.334
M15	755444.220459	218949.865155	18.480	17.018	20.824	17.228
O 2	730402.927052	221676.374291	17.140	15.748	20.093	18.093
O 7	717831.717332	237839.089634	25.890	32.512	22.324	18.073
O 8	725348.147988	235798.729758	24.680	24.13	27.400	18.742
O10	694269.889040	228610.917000	21.990	26.162	20.672	17.073
O11	705431.001880	220697.610715	25.490	16.51	16.336	16.937
O13	705431.001880	220697.610715	14.660	27.686	16.277	16.937
O19	722772.817043	220375.078922	15.450	23.876	15.747	18.505
O26	702230.908441	220046.898222	16.650	32.004	19.309	16.434
O28	694588.732145	213376.137195	23.950	36.322	21.041	13.963
W 2	708078.587107	194300.186312	5.370	8.128	7.179	4.727
W16	734607.714135	203484.977237	8.310	10.668	4.794	10.349
W22	735298.537945	199341.859541	4.290	7.366	7.837	8.638
W25	732161.441554	213556.429868	11.160	23.368	18.214	16.541
W27	726187.905777	204715.689118	5.170	7.874	6.345	10.409
W29	742838.247435	203183.487706	10.230	10.414	7.316	8.642
W42	754665.813608	213426.186194	12.520	9.906	11.189	14.234
W43	733804.150235	197470.094732	5.960	4.826	7.836	8.053
W44	733804.150235	197470.094732	2.550	2.286	2.000	8.053
W45	736867.359922	197018.994551	5.450	10.922	10.309	7.613

Appendix K
Various SEMCOG Precipitation Data
(Precipitation Event 09/24/1999)

Station ID	X	Y	NEXRAD mm	Gage_mm	ANN_mm	OC_mm
A 3	661857.143789	192530.880673	0.910	2.794	0.886	1.509
A 4	695810.135030	191348.250416	1.360	3.556	1.718	0.981
L 7	681514.971760	222057.746602	3.490	5.588	3.547	1.301
L10	658405.618120	224659.693526	1.200	4.318	2.680	2.849
M 2	756937.867805	232774.056329	1.460	2.54	2.964	1.718
M 4	762562.920492	230609.680239	2.080	6.096	4.305	2.403
M 8	746972.860607	254820.071250	1.340	2.286	2.448	1.938
M 9	742960.436068	231431.293091	0.610	3.048	1.680	1.262
M10	749986.779148	230140.273915	0.880	3.302	2.144	1.600
M12	765224.025423	256122.102610	1.760	3.302	2.149	2.482
M13	750684.183706	240383.890687	0.930	5.08	2.645	1.186
M14	765682.093654	241381.302807	3.070	5.08	4.082	1.705
M16	755400.233316	223825.771085	2.860	2.794	3.032	1.902
M17	744337.430006	224781.756367	2.410	2.54	1.983	1.191
O 3	735369.246078	230672.594422	0.970	1.524	1.837	0.864
O 4	734168.924612	255016.775493	2.730	6.096	3.718	2.332
O 5	713090.146295	246701.551082	3.480	6.858	4.110	2.935
O 9	726130.235853	247275.671191	3.170	5.842	3.382	2.521
O18	731346.624696	216708.011455	0.720	1.778	1.353	1.132
O24	715654.068076	215086.283082	0.180	2.032	0.519	0.960
O25	731861.017503	225830.555575	0.480	1.27	0.604	1.018
W 8	732252.968427	197942.382800	2.100	3.302	1.903	1.706
W14	753133.344245	209696.295155	2.470	3.81	3.622	2.346
W18	745604.881900	214856.586919	2.280	4.064	2.736	2.251
W23	724714.028432	197970.368012	1.470	1.778	1.502	1.493
W31	756733.582014	214398.150256	2.320	4.318	3.371	2.371
W33	755386.272117	215582.872187	2.270	4.064	3.695	2.424
W48	709614.370019	201814.621439	0.360	2.794	0.990	1.038
A 1	678039.980433	195924.936908	0.760	2.286	1.163	1.463
A 2	663120.262649	212553.141409	1.550	3.81	2.878	1.521
A 5	695810.135030	191348.250416	1.250	3.302	2.401	1.360
L 1	656935.798800	236936.068948	1.550	9.398	5.025	1.795
L 2	655307.791088	245383.380983	2.630	4.064	1.524	2.025
L 5	655433.651803	217957.872282	1.070	2.54	4.286	1.176
L 6	680819.554474	212103.804745	1.780	3.048	3.159	2.419
L 8	683827.288566	245447.601664	1.830	5.588	3.104	3.116
L 9	685117.095706	233972.632310	1.740	5.842	2.653	3.144
L11	671537.470375	229482.547174	1.080	3.556	2.220	2.585
M 1	754440.159488	258799.157739	1.040	4.826	2.087	1.587
M 5	756874.108802	227770.456845	2.870	5.334	4.599	2.116
M 7	739614.099028	250112.456291	2.300	8.128	5.197	1.849
M15	755444.220459	218949.865155	2.270	5.588	5.197	2.542
O 2	730402.927052	221676.374291	0.480	1.524	1.303	0.569
O 7	717831.717332	237839.089634	3.160	8.636	3.493	2.391
O 8	725348.147988	235798.729758	3.080	6.604	4.827	1.747
O10	694269.889040	228610.917000	4.260	6.858	5.071	2.752
O13	705431.001880	220697.610715	1.500	4.572	3.945	1.350
O19	722772.817043	220375.078922	0.850	2.032	1.533	0.497
O28	694588.732145	213376.137195	1.520	3.302	2.713	1.893
W 2	708078.587107	194300.186312	1.420	4.064	1.536	0.861
W16	734607.714135	203484.977237	2.100	3.556	3.171	1.878
W47	736867.359922	197018.994551	1.610	2.286	2.113	2.210
W25	732161.441554	213556.429868	1.520	2.54	1.609	1.051
W27	726187.905777	204715.689118	1.470	3.81	1.540	1.207
W29	742838.247435	203183.487706	3.230	3.556	3.060	2.248
W42	754665.813608	213426.186194	2.500	3.302	5.727	2.339
W43	733804.150235	197470.094732	1.880	1.27	2.693	2.146
W44	733804.150235	197470.094732	2.420	3.556	2.275	2.146

133

Appendix L
Various SEMCOG Precipitation Data
(Precipitation Event 05/16/2000)

Station ID	X	Y	NEXRAD mm	Gage_mm	ANN mm	OC mm
A 3	661857.143789	192530.880673	0.780	5.334	1.523	1.950
L 3	668047.850000	241521.480000	2.500	10.922	1.733	2.804
L 7	681514.971760	222057.746602	0.000	7.62	1.037	2.898
L10	658405.618120	224659.693526	2.500	8.636	4.554	1.167
M 4	762562.920492	230609.680239	0.000	7.112	2.301	0.000
M 8	746972.860607	254820.071250	0.000	7.62	0.187	0.000
M 9	742960.436068	231431.293091	0.000	6.858	0.000	0.078
M10	749986.779148	230140.273915	0.000	7.366	1.898	0.000
M12	765224.025423	256122.102610	0.340	4.064	0.180	0.000
M14	765682.093654	241381.302807	0.000	4.572	0.870	0.046
M16	755400.233316	223825.771085	0.000	7.874	3.037	0.000
M17	744337.430006	224781.756367	0.000	7.874	0.000	0.000
M19	755950.630000	217610.330000	0.000	3.556	0.000	0.000
O 3	735369.246078	230672.594422	0.000	7.62	0.946	0.714
O 4	734168.924612	255016.775493	0.000	8.89	1.563	4.179
O 5	713090.146295	246701.551082	7.750	11.684	8.047	4.773
O 9	726130.235853	247275.671191	7.280	11.938	5.265	2.855
O18	731346.624696	216708.011455	0.000	3.302	0.000	0.168
O24	715654.088076	215086.283082	0.000	9.398	0.000	2.336
O25	731861.017503	225830.555575	0.000	6.858	2.829	0.233
W14	753133.344245	209696.295155	0.000	3.302	0.000	0.000
W15	750220.740000	206719.180000	0.000	3.048	0.000	0.388
W18	745604.881900	214856.586919	0.000	5.08	0.000	0.107
W20	735298.110000	199341.790000	2.270	2.794	0.000	1.243
W23	724714.028432	197970.368012	2.270	3.302	1.805	2.333
W33	755386.272117	215582.872187	0.000	5.842	1.536	0.000
W48	709614.370019	201814.621439	3.480	5.334	3.808	0.831
A 1	678039.980433	195924.936908	5.070	3.81	4.843	1.117
A 2	663120.262649	212553.141409	0.380	6.604	3.836	1.328
A 5	695810.135030	191348.250416	4.670	6.096	5.405	2.255
L 1	656935.798800	236936.068948	2.500	9.652	6.179	2.606
L 2	655307.791088	245383.380983	4.190	11.176	7.101	2.846
L 5	655433.651803	217957.872282	3.280	8.89	6.580	2.034
L 6	680819.554474	212103.804745	0.500	7.366	1.857	0.600
L 8	683827.288566	245447.601664	0.000	10.922	5.841	3.416
L 9	685117.095706	233972.632310	0.000	12.954	5.893	2.117
L11	671537.470375	229482.547174	2.500	8.128	5.103	1.570
M 1	754440.159488	258799.157739	0.000	9.398	3.135	0.124
M 5	756874.108802	227770.456845	0.000	5.842	3.033	0.000
M 7	739614.099028	250112.456291	0.000	9.906	1.793	0.563
M15	755444.220459	218949.865155	0.000	4.572	2.546	0.000
M18	745887.380000	226750.870000	0.000	6.096	2.162	0.000
O 2	730402.927052	221676.374291	0.000	7.62	4.592	0.000
O 7	717831.717332	237839.089634	7.750	9.398	9.687	5.311
O 8	725348.147988	235798.729758	7.470	10.668	7.516	3.653
O10	694269.889040	228610.917000	0.000	8.128	5.024	2.184
O13	705431.001880	220697.610715	7.320	8.382	7.639	1.737
O16	693745.730000	252604.490000	0.000	11.684	9.797	4.810
O19	722772.817043	220375.078922	7.280	7.62	5.593	0.434
O20	736063.850000	218411.640000	0.000	4.826	2.117	0.046
O26	702230.480000	220046.830000	7.300	7.874	5.105	1.728
O28	694588.732145	213376.137195	0.000	6.35	2.918	1.292
W 2	708078.587107	194300.186312	3.750	4.826	4.635	3.091
W16	734607.714135	203484.977237	2.270	3.81	1.647	1.620
W19	743359.420000	202028.890000	0.000	3.302	0.461	1.079
W25	732161.441554	213556.429868	0.000	3.302	0.433	0.321
W27	726187.905777	204715.689118	2.270	5.08	2.376	1.546
W42	754665.813608	213426.186194	0.000	4.318	2.239	0.000
W43	733803.730000	197470.030000	2.270	0.762	0.438	2.325
W44	733662.390000	179256.190000	1.530	3.302	2.483	2.325
W45	736866.940000	197018.930000	2.270	3.302	0.341	2.185
W47	731494.800000	195941.610000	2.270	3.048	1.180	2.390

Appendix M
Various SEMCOG Precipitation Data
(Precipitation Event 05/18/2000)

Station ID	X	Y	NEXRAD mm	Gage_mm	ANN mm	OC mm
A 3	661857.143789	192530.880673	48.600	39.370	41.675	27.861
L 3	668047.850000	241521.480000	38.840	32.004	33.085	26.648
L 7	681514.971760	222057.746602	22.800	33.274	28.889	33.505
L10	658405.618120	224659.693526	28.420	37.084	36.614	38.974
M 4	762562.920492	230609.680239	25.210	22.606	21.610	23.264
M 8	746972.860607	254820.071250	45.300	51.816	44.240	37.296
M 9	742960.436068	231431.293091	25.040	24.130	22.525	25.192
M10	749986.779148	230140.273915	28.870	29.972	25.811	25.355
M12	765224.025423	256122.102610	40.220	38.100	39.345	33.624
M14	765682.093654	241381.302807	22.810	19.812	22.727	32.676
M16	755400.233316	223825.771085	23.200	25.400	24.340	22.352
M17	744337.430006	224781.756367	22.120	21.844	21.430	22.371
M19	755950.630000	217610.330000	17.740	26.670	24.011	20.077
O 3	735369.246078	230672.594422	19.690	26.162	24.097	23.388
O 4	734168.924612	255016.775493	38.190	39.116	38.754	35.675
O 5	713090.146295	246701.551082	29.820	32.766	34.356	26.581
O 9	726130.235853	247275.671191	25.360	38.608	37.093	31.701
O18	731346.624696	216708.011455	18.130	26.670	21.034	21.079
O24	715654.088076	215086.283082	20.690	40.132	32.437	26.166
O25	731861.017503	225830.555575	21.240	29.210	29.047	19.101
W14	753133.344245	209696.295155	17.260	25.400	24.356	17.811
W15	750220.740000	206719.180000	17.260	22.352	22.658	18.533
W18	745604.881900	214856.586919	17.690	26.162	23.723	19.223
W20	735298.110000	199341.790000	26.550	26.416	28.333	22.864
W23	724714.028432	197970.368012	28.220	29.464	25.101	27.885
W33	755386.272117	215582.872187	19.200	29.210	24.938	17.518
W48	709614.370019	201814.621439	32.610	30.480	29.891	26.946
A 1	678039.980433	195924.936908	44.770	33.528	54.167	39.065
A 2	663120.262649	212553.141409	42.850	43.434	43.273	33.490
A 5	695810.135030	191348.250416	39.140	33.782	38.901	36.455
L 1	656935.798800	236936.068948	30.000	41.656	36.081	34.898
L 2	655307.791088	245383.380983	41.740	47.498	47.224	37.902
L 5	655433.651803	217957.872282	39.530	42.418	44.440	32.471
L 6	680819.554474	212103.804745	32.750	31.496	28.264	28.688
L 8	683827.288566	245447.601664	39.570	39.37	43.660	33.220
L 9	685117.095706	233972.632310	37.790	39.878	40.287	27.913
L11	671537.470375	229482.547174	24.400	31.496	26.990	29.514
M 1	754440.159488	258799.157739	40.790	39.624	45.893	43.843
M 5	756874.108802	227770.456845	22.650	25.908	34.790	25.344
M 7	739614.099028	250112.456291	38.950	43.434	44.916	37.196
M15	755444.220459	218949.865155	19.200	29.464	26.431	18.908
M18	745887.380000	226750.870000	28.550	24.384	22.063	24.088
O 2	730402.927052	221676.374291	21.240	29.464	25.486	19.724
O 7	717831.717332	237839.089634	24.140	28.448	24.542	24.414
O 8	725348.147988	235798.729758	21.270	26.67	19.553	22.754
O10	694269.889040	228610.917000	19.060	33.782	23.876	25.196
O13	705431.001880	220697.610715	23.090	32.512	23.694	23.582
O16	693745.730000	252604.490000	43.390	43.688	56.795	34.173
O19	722772.817043	220375.078922	23.390	27.686	25.996	20.274
O20	736063.850000	218411.640000	21.690	28.956	24.620	18.949
O26	702230.480000	220046.830000	23.000	35.56	27.896	24.318
O28	694588.732145	213376.137195	30.280	29.972	25.761	27.136
W 2	708078.587107	194300.186312	35.260	35.814	33.504	34.183
W16	734607.714135	203484.977237	26.550	32.512	22.491	24.087
W19	743359.420000	202028.890000	21.860	28.194	20.910	21.412
W25	732161.441554	213556.429868	17.670	24.384	21.995	19.270
W27	726187.905777	204715.689118	28.220	27.178	27.318	24.875
W42	754665.813608	213426.186194	16.520	23.876	20.370	18.406
W43	733803.730000	197470.030000	28.860	25.908	26.946	27.010
W44	733662.390000	179256.190000	31.790	32.766	27.104	27.010
W45	736866.940000	197018.930000	33.560	32.258	24.630	26.161
W47	731494.800000	195941.610000	33.690	29.972	33.253	27.591

Appendix N
Various SEMCOG Precipitation Data
(Precipitation Event 05/28/2000)

Station ID	X	Y	NEXRAD mm	Gage_mm	ANN mm	OC mm
A 3	661857.143789	192530.880673	23.840	33.020	27.618	17.773
L 3	668047.850000	241521.480000	20.440	18.034	18.067	13.186
L 7	681514.971760	222057.746602	15.290	20.828	19.050	15.408
L10	658405.618120	224659.693526	16.390	16.764	15.237	21.479
M 4	762562.920492	230609.680239	1.520	4.318	2.949	2.022
M 8	746972.860607	254820.071250	1.850	3.048	2.287	2.944
M 9	742960.436068	231431.293091	1.990	6.858	6.078	1.570
M10	749986.779148	230140.273915	0.850	5.334	2.596	1.879
M12	765224.025423	256122.102610	0.600	3.302	0.000	2.121
M14	765682.093654	241381.302807	2.340	3.048	2.186	0.934
M16	755400.233316	223825.771085	2.330	7.112	3.263	1.268
M17	744337.430006	224781.756367	1.930	8.636	5.333	1.996
M19	755950.630000	217610.330000	1.720	7.620	5.993	1.822
O 3	735369.246078	230672.594422	2.200	10.668	6.595	3.132
O 4	734168.924612	255016.775493	4.940	8.636	5.427	4.132
O 5	713090.146295	246701.551082	4.900	5.842	4.687	8.087
O 9	726130.235853	247275.671191	6.260	3.556	5.393	4.470
O18	731346.624696	216708.011455	3.400	16.002	5.508	5.433
O24	715654.088076	215086.283082	3.730	14.732	8.371	9.684
O25	731861.017503	225830.555575	3.400	11.938	6.118	2.467
W14	753133.344245	209696.295155	4.750	14.478	9.491	4.914
W15	750220.740000	206719.180000	7.050	13.208	9.555	6.510
W18	745604.881900	214856.586919	3.960	13.462	7.876	4.231
W20	735298.110000	199341.790000	14.450	10.414	12.403	10.950
W23	724714.028432	197970.368012	14.450	11.684	13.553	13.717
W33	755386.272117	215582.872187	1.710	11.176	6.756	2.432
W48	709614.370019	201814.621439	14.920	13.462	14.891	11.847
A 1	678039.980433	195924.936908	26.460	0.508	30.378	20.371
A 2	663120.262649	212553.141409	13.000	14.224	17.050	18.713
A 5	695810.135030	191348.250416	16.130	12.7	15.353	18.764
L 1	656935.798800	236936.068948	15.350	17.526	12.885	18.854
L 2	655307.791088	245383.380983	9.710	19.812	11.350	19.355
L 5	655433.651803	217957.872282	20.060	17.78	14.890	18.115
L 6	680819.554474	212103.804745	19.990	18.034	17.835	16.707
L 8	683827.288566	245447.601664	12.610	13.97	14.796	14.523
L 9	685117.095706	233972.632310	20.770	18.796	17.061	14.049
L11	671537.470375	229482.547174	17.520	23.622	22.454	17.241
M 1	754440.159488	258799.157739	0.760	3.048	0.584	1.393
M 5	756874.108802	227770.456845	0.380	4.826	2.372	1.702
M 7	739614.099028	250112.456291	4.750	5.588	3.990	3.513
M15	755444.220459	218949.865155	1.710	8.382	3.087	1.832
M18	745887.380000	226750.870000	2.160	7.874	4.416	1.655
O 2	730402.927052	221676.374291	3.400	13.208	2.489	3.249
O 7	717831.717332	237839.089634	7.280	9.398	4.325	4.772
O 8	725348.147988	235798.729758	4.980	11.684	5.712	4.160
O10	694269.889040	228610.917000	13.440	14.732	13.807	11.065
O13	705431.001880	220697.610715	6.020	12.954	4.988	7.625
O16	693745.730000	252604.490000	10.850	10.16	23.905	11.267
O19	722772.817043	220375.078922	2.800	13.716	2.458	3.458
O20	736063.850000	218411.640000	3.740	11.938	6.517	3.592
O26	702230.480000	220046.830000	7.740	13.462	9.088	9.083
O28	694588.732145	213376.137195	11.820	13.97	11.152	13.224
W 2	708078.587107	194300.186312	15.240	15.24	14.739	17.088
W16	734607.714135	203484.977237	14.450	13.462	7.393	11.686
W29	742837.820000	203183.420000	5.890	15.748	3.740	10.148
W25	732161.441554	213556.429868	3.330	15.24	5.151	5.175
W27	726187.905777	204715.689118	14.450	13.97	14.152	10.832
W42	754665.813608	213426.186194	3.200	8.89	6.585	2.775
W43	733804.150235	197470.094732	14.420	9.906	12.738	14.754
W35	732220.830000	179084.250000	17.220	16.256	16.677	16.307
W45	736866.940000	197018.930000	14.450	11.938	11.900	14.389
W47	731494.800000	195941.610000	14.450	12.446	13.069	15.028

Appendix O
Various SEMCOG Precipitation Data
(Precipitation Event 05/31/2000)

Station ID	X	Y	NEXRAD mm	Gage_mm	ANN_mm	OC_mm
A 3	661857.143789	192530.880673	1.680	0.508	3.722	18.507
L 3	668047.850000	241521.480000	0.420	0.508	0.000	13.062
L 7	681514.971760	222057.746602	15.920	5.334	9.469	5.436
L10	658405.618120	224659.693526	14.690	12.954	11.141	4.197
M 4	762562.920492	230609.680239	0.500	0	0.000	0.020
M 8	746972.860607	254820.071250	0.000	0	0.583	0.000
M 9	742960.436068	231431.293091	0.000	0	0.000	1.090
M10	749986.779148	230140.273915	0.000	0.254	0.000	1.036
M12	765224.025423	256122.102610	0.000	0.508	0.000	0.000
M14	765682.093654	241381.302807	0.000	0.508	0.000	0.027
M16	755400.233316	223825.771085	0.800	0.508	0.743	1.392
M17	744337.430006	224781.756367	5.040	0	0.291	2.154
M19	755950.630000	217610.330000	1.840	1.524	1.219	2.191
O 3	735369.246078	230672.594422	0.000	0.254	0.196	1.137
O 4	734168.924612	255016.775493	0.000	0	0.000	0.327
O 5	713090.146295	246701.551082	1.190	0.762	0.000	1.509
O 9	726130.235853	247275.671191	1.040	0.762	0.170	0.173
O18	731346.624696	216708.011455	8.110	3.048	5.191	5.971
O24	715654.088076	215086.283082	3.340	2.032	4.476	9.385
O25	731861.017503	225830.555575	1.910	0	0.868	2.977
W14	753133.344245	209696.295155	6.590	1.524	3.612	5.687
W15	750220.740000	206719.180000	7.440	4.064	5.081	7.829
W18	745604.881900	214856.586919	7.200	5.08	5.360	6.261
W20	735298.110000	199341.790000	10.920	10.668	11.049	15.637
W23	724714.028432	197970.368012	20.310	8.89	13.441	10.725
W33	755386.272117	215582.872187	2.590	2.54	2.798	3.141
W48	709614.370019	201814.621439	10.680	3.048	10.649	12.443
A 1	678039.980433	195924.936908	14.220	6.35	19.704	8.233
A 2	663120.262649	212553.141409	5.580	6.604	10.024	11.472
A 5	695810.135030	191348.250416	20.950	16.764	25.376	10.931
L 1	656935.798800	236936.068948	0.000	0.254	0.000	6.734
L 2	655307.791088	245383.380983	0.000	1.27	0.614	3.327
L 5	655433.651803	217957.872282	13.350	9.398	13.994	12.298
L 6	680819.554474	212103.804745	12.340	1.27	17.866	13.069
L 8	683827.288566	245447.601664	0.000	0.254	0.000	2.946
L 9	685117.095706	233972.632310	0.520	0.254	0.268	8.102
L11	671537.470375	229482.547174	4.860	0.762	1.470	10.369
M 1	754440.159488	258799.157739	0.000	0.508	0.000	0.000
M 5	756874.108802	227770.456845	0.610	0.254	0.221	0.316
M 7	739614.099028	250112.456291	0.000	0.508	0.000	0.000
M 3	753509.660000	218106.530000	2.590	3.556	0.620	2.687
M18	745887.380000	226750.870000	0.000	0	0.000	2.967
O 2	730402.927052	221676.374291	1.910	0	1.819	4.577
O 7	717831.717332	237839.089634	0.000	1.27	5.342	1.339
O 8	725348.147988	235798.729758	1.150	1.778	2.444	0.751
O10	694269.889040	228610.917000	8.250	0	2.920	8.269
O13	705431.001880	220697.610715	1.830	4.572	2.462	5.978
O16	693745.730000	252604.490000	0.000	0.254	0.000	0.998
O19	722772.817043	220375.078922	1.320	0	0.000	4.046
O20	736063.850000	218411.640000	0.590	2.032	1.266	6.873
O26	702230.480000	220046.830000	2.930	4.318	3.581	7.135
O28	694588.732145	213376.137195	5.900	4.826	12.236	10.499
W 2	708078.587107	194300.186312	16.950	4.318	13.062	12.800
W16	734607.714135	203484.977237	10.920	5.588	12.209	11.197
W29	742837.820000	203183.420000	15.640	5.334	12.612	9.392
W25	732161.441554	213556.429868	9.000	3.302	9.532	9.102
W27	726187.905777	204715.689118	20.310	5.08	14.937	13.855
W42	754665.813608	213426.186194	5.950	1.27	3.857	4.108
W43	733804.150235	197470.094732	17.350	8.382	13.507	12.922
W35	732220.830000	179084.250000	11.530	4.572	8.791	15.763
W45	736866.940000	197018.930000	13.570	10.16	13.145	11.644
W47	731494.800000	195941.610000	15.510	7.62	15.546	15.169

Appendix P
Various SEMCOG Precipitation Data
(Precipitation Event 07/28/2000)

Station ID	X	Y	NEXRAD mm	Gage_mm	ANN mm	OC mm
A 3	661857.143789	192530.880673	74.040	45.720	52.422	64.179
L 3	668047.850000	241521.480000	103.720	55.880	71.512	88.484
L 7	681514.971760	222057.746602	134.800	56.896	86.268	65.930
L10	658405.618120	224659.693526	70.310	37.084	46.501	109.255
M 2	756937.449154	232773.992790	133.970	39.116	44.957	77.421
M 4	762562.920492	230609.680239	88.820	27.686	38.802	99.972
M 8	746972.860607	254820.071250	74.340	22.860	38.145	55.000
M 9	742960.436068	231431.293091	51.470	19.304	41.638	59.743
M10	749986.779148	230140.273915	60.950	13.970	36.763	80.872
M14	765682.093654	241381.302807	62.300	23.876	32.041	102.127
M16	755400.233316	223825.771085	73.130	67.564	80.997	58.781
M17	744337.430006	224781.756367	35.310	13.208	31.777	47.935
M19	755950.630000	217610.330000	29.790	21.590	15.484	62.191
O 3	735369.246078	230672.594422	70.040	45.212	54.022	51.320
O 4	734168.924612	255016.775493	38.470	17.526	23.242	67.790
O 5	713090.146295	246701.551082	50.110	36.068	50.005	71.591
O 9	726130.235853	247275.671191	62.440	32.766	39.139	49.098
O24	715654.088076	215086.283082	45.610	35.052	39.811	36.322
O25	731861.017503	225830.555575	51.140	52.578	43.006	56.357
W20	735298.119300	199341.796003	41.590	75.692	70.994	18.437
W14	753133.344245	209696.295155	15.840	15.240	13.100	43.728
W15	750220.740000	206719.180000	35.330	17.018	20.574	19.278
W18	745604.881900	214856.586919	33.200	16.510	30.432	35.262
W23	724714.028432	197970.368012	14.150	3.810	10.435	32.647
W33	755386.272117	215582.872187	59.280	19.304	22.256	25.791
W48	709614.370019	201814.621439	11.340	11.684	9.925	43.363
A 1	678039.980433	195924.936908	57.160	30.480	81.760	71.542
A 2	663120.262649	212553.141409	71.880	8.128	90.572	84.560
A 5	695810.135030	191348.250416	31.860	12.446	20.102	40.366
L 1	656935.798800	236936.068948	98.370	39.878	56.464	85.651
L 2	655307.791088	245383.380983	66.540	29.464	58.139	88.476
L 5	655433.651803	217957.872282	104.000	67.056	84.064	73.630
L 6	680819.554474	212103.804745	123.670	64.262	135.333	102.653
L 8	683827.288566	245447.601664	120.150	56.134	128.582	97.336
L 9	685117.095706	233972.632310	118.640	56.134	110.850	109.981
L11	671537.470375	229482.547174	90.290	53.340	118.818	108.168
M 1	754440.159488	258799.157739	83.380	48.260	73.325	69.612
M 5	756874.108802	227770.456845	92.390	72.390	48.492	93.855
M 7	739614.099028	250112.456291	48.640	35.814	33.924	60.294
M 3	753509.666411	218106.538937	59.280	32.258	90.793	42.035
M18	745887.380000	226750.870000	44.360	11.176	43.894	43.249
O 2	730402.927052	221676.374291	51.140	12.954	41.424	46.401
O 7	717831.717332	237839.089634	55.930	25.654	42.101	58.634
O 8	725348.147988	235798.729758	50.250	35.814	53.682	61.145
O10	694269.889040	228610.917000	75.160	34.544	67.083	96.552
O13	705431.001880	220697.610715	86.300	57.658	83.062	64.621
O16	693745.730000	252604.490000	130.970	58.166	106.338	80.287
O19	722772.817043	220375.078922	36.550	12.954	34.559	47.406
O20	736063.850000	218411.640000	27.730	22.606	17.480	38.314
O28	694588.732145	213376.137195	95.560	72.390	143.297	78.729
W 2	708078.587107	194300.186312	10.090	8.382	10.281	17.167
W16	734607.714135	203484.977237	41.590	49.022	54.561	37.570
W22	727993.648094	195084.345910	44.520	14.986	36.953	24.892
W25	732161.441554	213556.429868	68.850	14.478	22.411	37.457
W27	726187.905777	204715.689118	14.150	4.064	7.010	28.490
W19	743359.426259	202028.896272	81.740	82.042	104.934	36.671
W42	754665.813608	213426.186194	42.650	11.430	0.000	43.193
W43	733804.150235	197470.094732	87.950	27.432	71.131	40.479
W35	732220.832480	179084.258487	34.770	11.430	23.411	22.756
W45	736866.940000	197018.930000	108.300	49.022	93.903	38.886

Appendix Q
Various SEMCOG Precipitation Data
(Precipitation Event 07/31/2000)

Station ID	X	Y	NEXRAD mm	Gage_mm	ANN mm	OC mm
A 3	661857.143789	192530.880673	0	0.508	1.126	3.269
L 3	668047.850000	241521.480000	0	0	0.000	0.988
L 7	681514.971760	222057.746602	3.980	3.048	2.001	0.830
L10	658405.618120	224659.693526	0.000	0.508	0.928	0.600
M 2	756937.449154	232773.992790	10.350	2.54	5.567	17.183
M 4	762562.920492	230609.680239	2.170	1.778	2.520	10.411
M 8	746972.860607	254820.071250	1.360	2.286	3.560	2.483
M 9	742960.436068	231431.293091	1.190	0	5.753	15.234
M10	749986.779148	230140.273915	43.340	0.508	8.119	5.519
M14	765682.093654	241381.302807	0.920	1.016	0.000	4.363
M16	755400.233316	223825.771085	11.730	12.446	13.148	20.879
M17	744337.430006	224781.756367	0.000	1.778	2.316	10.947
W31	756733.163365	214398.086719	36.660	31.75	29.843	20.905
O 3	735369.246078	230672.594422	0.790	0.254	0.000	0.000
O 4	734168.924612	255016.775493	0.000	0.508	0.000	0.361
O 5	713090.146295	246701.551082	0.000	0.508	1.564	0.000
O 9	726130.235853	247275.671191	0.000	0	0.591	0.156
O24	715654.088076	215086.283082	1.480	4.318	2.385	0.572
O25	731861.017503	225830.555575	0.000	0	0.000	0.000
W 8	732252.549782	197942.319261	0.660	0	0.709	3.172
W14	753133.344245	209696.295155	26.070	6.604	10.341	21.253
W15	750220.740000	206719.180000	14.950	8.128	7.070	18.986
W18	745604.881900	214856.586919	0.000	0.254	2.516	8.519
W23	724714.028432	197970.368012	0.840	0.508	0.000	1.691
W33	755386.272117	215582.872187	19.900	33.528	23.516	30.258
W48	709614.370019	201814.621439	5.120	30.48	16.099	1.426
A 1	678039.980433	195924.936908	7.390	4.318	10.445	2.361
A 2	663120.262649	212553.141409	0.000	0	0.000	0.964
A 5	695810.135030	191348.250416	0.490	1.016	0.000	4.145
L 1	656935.798800	236936.068948	0.000	0	0.000	0.000
L 2	655307.791088	245383.380983	0.000	0	0.662	0.000
L 5	655433.651803	217957.872282	0.920	0	0.000	0.067
L 6	680819.554474	212103.804745	10.670	2.032	3.275	3.359
L 8	683827.288566	245447.601664	1.160	1.524	1.845	0.845
L 9	685117.095706	233972.632310	1.750	5.08	0.000	2.173
L11	671537.470375	229482.547174	0.000	0.508	0.705	1.558
M 1	754440.159488	258799.157739	0.750	0.762	0.000	0.740
M 5	756874.108802	227770.456845	3.390	6.35	4.339	14.244
M 7	739614.099028	250112.456291	0.930	0.254	1.091	1.991
M15	755443.801809	218949.801618	19.900	31.75	16.963	16.532
M18	745887.380000	226750.870000	3.510	0	12.523	10.815
O 2	730402.927052	221676.374291	0.000	0.254	0.000	0.000
O 7	717831.717332	237839.089634	0.000	1.524	0.000	0.285
O 8	725348.147988	235798.729758	0.000	0.508	1.778	0.293
O10	694269.889040	228610.917000	0.310	0.254	0.468	2.635
O13	705431.001880	220697.610715	0.000	0	0.000	2.110
O16	693745.730000	252604.490000	1.050	0	1.140	0.000
O19	722772.817043	220375.078922	0.000	0	1.956	0.000
O22	736583.384861	221238.316631	0.000	0.508	0.000	0.000
O28	694588.732145	213376.137195	7.010	7.366	4.288	3.736
W 2	708078.587107	194300.186312	8.950	8.128	17.896	4.641
W16	734607.714135	203484.977237	0.660	0	0.407	0.511
W22	727993.648094	195084.345910	1.010	0	0.857	1.645
W25	732161.441554	213556.429868	0.250	0	1.227	0.000
W27	726187.905777	204715.689118	0.840	0	0.000	0.000
W19	743359.426259	202028.896272	6.530	0	3.526	7.133
W42	754665.813608	213426.186194	23.980	21.59	25.061	26.673
W43	733804.150235	197470.094732	0.730	0.254	0.406	1.675
W44	733662.398932	179256.197595	0.800	1.778	0.145	8.796
W45	736866.940000	197018.930000	0.640	0	0.379	3.720

Appendix R
Various SEMCOG Precipitation Data
(Precipitation Event 08/06/2000)

Station ID	X	Y	NEXRAD mm	Gage_mm	ANN mm	OC mm
A 3	661857.143789	192530.880673	18.980	29.464	26.065	13.680
L 3	668047.850000	241521.480000	6.580	15.494	12.100	7.500
L 7	681514.971760	222057.746602	11.290	20.828	16.903	14.362
L10	658405.618120	224659.693526	7.020	19.558	15.903	10.213
M 2	756937.449154	232773.992790	13.670	17.272	17.264	13.919
M 4	762562.920492	230609.680239	12.290	18.288	17.487	13.909
M 8	746972.860607	254820.071250	15.330	13.97	15.085	11.086
M 9	742960.436068	231431.293091	18.710	21.336	20.882	17.820
M10	749986.779148	230140.273915	15.470	22.098	20.490	17.832
M12	765223.606768	256122.039071	12.080	12.446	12.818	11.367
M14	765682.093654	241381.302807	10.200	14.986	14.266	11.999
M16	755400.233316	223825.771085	20.320	18.542	18.505	15.910
M17	744337.430006	224781.756367	20.470	22.352	20.940	19.937
M19	755950.630299	217610.335632	17.050	21.082	21.552	19.276
O 3	735369.246078	230672.594422	19.730	25.908	24.016	21.214
O 4	734168.924612	255016.775493	10.230	11.176	11.408	14.908
O 5	713090.146295	246701.551082	14.870	17.018	14.702	13.959
O 9	726130.235853	247275.671191	15.040	18.288	16.192	13.949
O18	731346.206049	216707.947915	22.090	25.908	25.400	23.287
O24	715654.088076	215086.283082	22.360	31.496	27.650	22.990
O25	731861.017503	225830.555575	24.100	23.368	23.782	20.731
W 8	732252.549782	197942.319261	23.050	26.924	24.587	21.706
W14	753133.344245	209696.295155	17.550	24.892	24.030	18.633
W15	750220.740000	206719.180000	18.370	24.384	24.235	18.764
W18	745604.881900	214856.586919	21.000	22.352	22.471	20.268
W23	724714.028432	197970.368012	22.700	24.892	24.287	24.149
W33	755386.272117	215582.872187	19.090	18.796	18.274	17.255
W48	709614.370019	201814.621439	26.790	34.544	30.143	21.241
A 1	678039.980433	195924.936908	25.680	27.178	26.743	19.478
A 2	663120.262649	212553.141409	9.400	21.59	7.277	11.856
A 5	695810.135030	191348.250416	24.160	30.226	30.706	23.497
L 1	656935.798800	236936.068948	6.290	9.652	4.195	6.157
L 2	655307.791088	245383.380983	3.390	9.652	4.091	5.795
L 5	655433.651803	217957.872282	8.110	18.288	9.671	9.293
L 6	680819.554474	212103.804745	13.770	18.034	11.950	14.955
L 8	683827.288566	245447.601664	7.060	12.954	5.324	9.244
L 9	685117.095706	233972.632310	10.400	24.638	9.232	10.793
L11	671537.470375	229482.547174	7.440	19.558	7.428	8.378
M 5	756874.108802	227770.456845	13.950	16.51	18.698	16.489
M 7	739614.099028	250112.456291	15.840	16.764	12.872	13.538
M15	755443.801809	218949.801618	19.090	20.574	20.998	17.959
M18	745887.380000	226750.870000	17.970	21.336	18.728	19.174
O 2	730402.927052	221676.374291	24.100	23.368	27.331	23.220
O 7	717831.717332	237839.089634	18.300	8.89	14.411	17.566
O 8	725348.147988	235798.729758	16.110	19.05	16.924	18.931
O10	694269.889040	228610.917000	15.050	22.352	14.995	14.456
O13	705431.001880	220697.610715	17.160	17.018	19.405	19.625
O16	693745.730000	252604.490000	6.290	13.716	0.783	10.579
O19	722772.817043	220375.078922	21.420	22.098	23.635	22.355
O22	736583.384861	221238.316631	23.240	24.892	25.989	22.340
O28	694588.732145	213376.137195	18.090	25.146	20.037	18.680
W 2	708078.587107	194300.186312	25.450	30.48	37.151	25.400
W16	734607.714135	203484.977237	23.050	26.416	25.788	22.176
W19	743359.426259	202028.896272	17.850	22.606	22.642	20.550
W25	732161.441554	213556.429868	23.040	28.448	28.120	22.086
W27	726187.905777	204715.689118	22.700	28.194	25.213	22.778
W35	732220.832480	179084.258487	21.730	32.004	21.729	22.852
W42	754665.813608	213426.186194	17.420	19.05	20.556	18.582
W43	733804.150235	197470.094732	20.600	22.098	29.953	22.745
W45	736866.940000	197018.930000	20.140	33.274	27.168	22.135
W47	731494.806185	195941.615746	21.330	28.956	28.995	22.945

Appendix S
Various SEMCOG Precipitation Data
(Precipitation Event 08/17/2000)

Station ID	X	Y	NEXRAD mm	Gage_mm	ANN mm	OC mm
A 3	661857.143789	192530.880673	7.210	14.732	7.263	8.406
L 3	668047.850000	241521.480000	5.970	10.668	6.858	7.608
L 7	681514.971760	222057.746602	8.110	11.430	7.923	7.962
L10	658405.618120	224659.693526	7.030	14.478	10.252	6.562
M 2	756937.449154	232773.992790	10.050	11.430	12.323	9.161
M 4	762562.920492	230609.680239	9.640	13.208	12.643	9.477
M 8	746972.860607	254820.071250	7.820	11.176	6.582	8.313
M 9	742960.436068	231431.293091	7.630	10.160	7.539	7.917
M10	749986.779148	230140.273915	8.140	11.938	8.706	8.282
M12	765223.606768	256122.039071	7.490	10.922	7.666	9.082
M14	765682.093654	241381.302807	9.860	11.430	9.927	8.954
M16	755400.233316	223825.771085	8.200	12.192	8.486	7.462
M17	744337.430006	224781.756367	6.480	10.668	6.598	7.208
O 3	735369.246078	230672.594422	8.540	10.414	7.404	7.704
O 4	734168.924612	255016.775493	8.270	8.636	6.411	8.072
O 5	713090.146295	246701.551082	9.030	12.700	9.670	8.073
O 9	726130.235853	247275.671191	8.250	10.668	6.835	8.659
O18	731346.206049	216707.947915	8.370	11.684	10.912	7.670
O24	715654.088076	215086.283082	9.480	16.002	10.500	9.463
O25	731861.017503	225830.555575	7.840	10.160	10.775	8.386
W 8	732252.549782	197942.319261	8.540	8.890	9.851	8.507
W14	753133.344245	209696.295155	4.750	7.366	5.766	6.135
W15	750220.740000	206719.180000	6.460	7.620	5.987	5.251
W18	745604.881900	214856.586919	5.660	8.890	5.325	6.354
W23	724714.028432	197970.368012	9.370	10.414	10.477	9.192
W31	756733.163365	214398.086719	6.020	9.144	5.629	6.464
W33	755386.272117	215582.872187	5.900	8.382	5.462	5.646
W48	709614.370019	201814.621439	10.560	11.430	10.853	9.253
A 1	678039.980433	195924.936908	10.060	12.192	11.348	8.304
A 2	663120.262649	212553.141409	8.410	13.970	10.99	7.373
A 5	695810.135030	191348.250416	11.330	11.430	10.702	9.427
L 1	656935.798800	236936.068948	6.770	16.256	11.605	6.329
L 2	655307.791088	245383.380983	6.740	12.446	9.3419	6.114
L 5	655433.651803	217957.872282	7.420	14.224	10.688	7.047
L 6	680819.554474	212103.804745	7.400	12.192	8.2915	8.355
L 8	683827.288566	245447.601664	8.700	11.938	9.2444	7.275
L 9	685117.095706	233972.632310	6.260	16.002	11.486	7.767
L11	671537.470375	229482.547174	6.620	14.478	11.2	7.084
M 5	756874.108802	227770.456845	10.470	10.414	10.173	9.025
M 7	739614.099028	250112.456291	7.140	9.652	6.8871	8.188
M3	753509.666411	218106.538937	5.900	9.652	7.2586	6.141
M18	745887.380000	226750.870000	7.800	10.414	8.6041	7.006
O 2	730402.927052	221676.374291	7.840	11.938	9.3049	8.135
O 7	717831.717332	237839.089634	7.940	9.652	9.0595	8.815
O 8	725348.147988	235798.729758	7.860	9.906	8.7815	8.625
O10	694269.889040	228610.917000	8.540	12.954	10.029	8.579
O13	705431.001880	220697.610715	11.590	11.684	11.223	9.326
O16	693745.730000	252604.490000	7.980	8.890	8.5565	7.763
O19	722772.817043	220375.078922	9.890	9.906	8.506	8.858
O22	736583.384861	221238.316631	6.100	10.414	9.3504	7.308
O28	694588.732145	213376.137195	7.600	11.684	8.7439	9.222
W 2	708078.587107	194300.186312	10.720	11.176	10.145	10.030
W16	734607.714135	203484.977237	8.540	10.668	9.1103	8.067
W47	731494.806185	195941.615746	9.330	11.176	9.1818	8.662
W25	732161.441554	213556.429868	9.940	12.192	9.4018	8.174
W27	726187.905777	204715.689118	9.370	11.176	9.9609	9.017
W19	743359.426259	202028.896272	7.220	7.874	6.3459	7.189
W42	754665.813608	213426.186194	4.550	7.366	5.5561	5.445
W43	733804.150235	197470.094732	7.850	7.112	8.5817	8.379
W35	732220.832480	179084.258487	8.160	8.890	9.1281	8.719
W45	736866.940000	197018.930000	7.610	10.414	8.1222	8.065

141

Appendix T
Various SEMCOG Precipitation Data
(Precipitation Event 09/11/2000)

Station ID	X	Y	NEXRAD mm	Gage_mm	ANN mm	OC mm
A 3	661857.143789	192530.880673	33.950	21.844	20.587	19.254
L 3	668047.850000	241521.480000	3.680	1.524	1.412	8.290
L 7	681514.971760	222057.746602	15.220	13.462	13.649	17.761
L10	658405.618120	224659.693526	4.000	6.096	8.419	12.835
M 2	756937.449154	232773.992790	40.290	30.734	30.764	43.449
M 4	762562.920492	230609.680239	34.110	23.876	26.925	43.404
M 8	746972.860607	254820.071250	26.300	11.938	24.058	31.834
M 9	742960.436068	231431.293091	33.790	10.16	17.412	41.274
M10	749986.779148	230140.273915	53.230	21.336	36.096	41.067
M12	765223.606768	256122.039071	25.630	9.144	23.231	30.299
M14	765682.093654	241381.302807	34.790	26.924	34.984	30.776
M16	755400.233316	223825.771085	55.740	43.18	42.189	45.250
M17	744337.430006	224781.756367	34.280	25.4	33.306	39.080
M19	755950.630299	217610.335632	46.180	30.988	31.599	48.465
O 3	735369.246078	230672.594422	36.180	24.638	30.831	24.965
O 4	734168.924612	255016.775493	32.290	27.432	23.341	35.981
O 5	713090.146295	246701.551082	30.370	5.08	16.899	32.281
O 9	726130.235853	247275.671191	44.420	40.894	38.784	31.587
O18	731346.206049	216707.947915	11.760	6.096	9.548	25.837
O24	715654.088076	215086.283082	26.790	13.716	20.500	26.193
O25	731861.017503	225830.555575	16.030	17.018	16.443	26.490
W 8	732252.549782	197942.319261	41.390	91.44	75.493	47.495
W14	753133.344245	209696.295155	46.720	39.116	45.002	43.512
W15	750220.740000	206719.180000	41.440	44.958	49.982	44.444
W18	745604.881900	214856.586919	38.740	50.546	43.408	36.456
W23	724714.028432	197970.368012	53.920	54.356	58.750	38.939
W33	755386.272117	215582.872187	46.680	44.196	43.537	46.133
W48	709614.370019	201814.621439	40.740	18.796	37.855	38.744
A 1	678039.980433	195924.936908	27.240	24.13	39.955	32.941
A 2	663120.262649	212553.141409	15.350	9.398	5.456	15.855
A 5	695810.135030	191348.250416	77.980	44.196	94.181	41.047
L 1	656935.798800	236936.068948	3.570	1.27	0.896	2.805
L 2	655307.791088	245383.380983	2.740	3.81	8.034	2.988
L 5	655433.651803	217957.872282	9.520	10.16	6.054	9.784
L 6	680819.554474	212103.804745	14.100	7.366	18.038	21.836
L 8	683827.288566	245447.601664	6.340	7.62	5.231	12.134
L 9	685117.095706	233972.632310	4.330	3.302	10.602	13.746
L11	671537.470375	229482.547174	3.220	2.286	3.928	7.898
M 1	754439.740000	258799.090000	25.460	10.922	10.922	25.719
M 5	756874.108802	227770.456845	41.390	32.258	31.951	48.131
M 7	739614.099028	250112.456291	35.960	14.732	27.828	33.082
M18	745887.380000	226750.870000	27.700	23.368	26.869	40.017
M3	753509.666411	218106.538937	46.680	57.658	47.284	47.142
O 2	730402.927052	221676.374291	16.030	12.192	21.386	13.947
O 7	717831.717332	237839.089634	34.910	38.608	50.312	30.919
O 8	725348.147988	235798.729758	30.700	20.574	46.791	32.530
O10	694269.889040	228610.917000	24.140	20.066	29.211	19.570
O13	705431.001880	220697.610715	45.670	42.418	43.930	24.883
O16	693745.730000	252604.490000	3.610	2.54	4.623	17.977
O19	722772.817043	220375.078922	27.140	11.176	20.274	18.778
O22	736583.384861	221238.316631	19.700	8.128	19.790	21.168
O26	702230.480000	220046.830000	41.340	32.004	46.360	24.871
O28	694588.732145	213376.137195	39.540	18.034	37.641	26.255
W 2	708078.587107	194300.186312	62.030	55.118	47.247	44.691
W16	734607.714135	203484.977237	41.390	38.354	49.032	35.561
W22	727993.648094	195084.345910	77.760	84.582	84.049	49.804
W25	732161.441554	213556.429868	19.140	8.128	10.536	18.740
W27	726187.905777	204715.689118	53.920	39.116	28.489	37.703
W29	742837.828788	203183.424168	52.970	43.18	61.474	38.445
W35	732220.832480	179084.258487	68.160	48.514	77.127	51.435
W42	754665.813608	213426.186194	46.030	35.56	46.272	46.573
W43	733804.150235	197470.094732	79.150	74.422	95.990	41.513
W45	736866.940000	197018.930000	73.780	72.136	95.579	41.617

Appendix U
Various SEMCOG Precipitation Data
(Precipitation Event 09/12/2000)

Station ID	X	Y	NEXRAD mm	Gage_mm	ANN mm	OC mm
A 3	661857.143789	192530.880673	0.890	1.778	0.989	3.296
L 3	668047.850000	241521.480000	2.230	0.762	1.492	1.865
L 7	681514.971760	222057.746602	3.560	2.794	2.455	5.072
L10	658405.618120	224659.693526	1.310	1.016	2.183	1.598
M 2	756937.449154	232773.992790	4.950	5.08	4.608	5.504
M 4	762562.920492	230609.680239	6.220	6.35	5.768	5.354
M 8	746972.860607	254820.071250	1.390	2.286	0.911	2.194
M 9	742960.436068	231431.293091	6.900	4.318	4.031	3.839
M10	749986.779148	230140.273915	5.080	5.842	5.053	5.122
M12	765223.606768	256122.039071	1.890	2.032	0.969	3.730
M14	765682.093654	241381.302807	5.740	3.81	4.075	4.366
M16	755400.233316	223825.771085	4.540	6.35	6.180	5.529
M17	744337.430006	224781.756367	3.600	3.556	3.664	5.282
M19	755950.630299	217610.335632	6.050	4.572	6.373	5.317
O 3	735369.246078	230672.594422	3.490	3.556	4.912	5.031
O 4	734168.924612	255016.775493	1.170	2.794	2.039	2.279
O 5	713090.146295	246701.551082	3.480	2.032	2.974	4.222
O 9	726130.235853	247275.671191	3.140	2.032	1.781	2.688
O18	731346.206049	216707.947915	3.400	0.762	3.680	6.651
O24	715654.088076	215086.283082	15.160	11.938	12.326	5.351
O25	731861.017503	225830.555575	4.380	4.318	4.586	4.044
W 8	732252.549782	197942.319261	6.690	8.128	7.365	4.782
W14	753133.344245	209696.295155	5.880	5.842	6.064	6.021
W15	750220.740000	206719.180000	6.300	5.842	7.611	5.748
W18	745604.881900	214856.586919	4.830	4.826	5.426	4.481
W23	724714.028432	197970.368012	4.870	2.54	1.679	7.563
W33	755386.272117	215582.872187	5.550	6.35	8.354	5.974
W48	709614.370019	201814.621439	8.460	2.794	3.362	9.025
A 1	678039.980433	195924.936908	7.100	2.54	9.737	3.305
A 2	663120.262649	212553.141409	0.740	2.54	1.577	1.629
A 5	695810.135030	191348.250416	7.540	2.032	5.497	5.565
L 1	656935.798800	236936.068948	1.610	2.286	0.000	1.420
L 2	655307.791088	245383.380983	1.320	1.27	0.645	1.337
L 5	655433.651803	217957.872282	0.930	0.254	1.877	1.114
L 6	680819.554474	212103.804745	10.450	5.842	7.632	4.008
L 8	683827.288566	245447.601664	2.910	3.556	2.793	3.181
L 9	685117.095706	233972.632310	1.570	2.54	2.846	4.046
L11	671537.470375	229482.547174	0.850	0.00	1.765	2.483
M 1	754439.740000	258799.090000	0.710	1.524	1.524	1.445
M 5	756874.108802	227770.456845	6.580	4.572	4.600	5.025
M 7	739614.099028	250112.456291	4.290	3.556	2.074	2.190
M18	745887.380000	226750.870000	6.890	3.302	7.014	4.527
M3	753509.666411	218106.538937	5.550	4.064	6.328	5.357
O 2	730402.927052	221676.374291	4.380	4.572	3.497	4.575
O 7	717831.717332	237839.089634	4.800	4.064	5.667	5.359
O 8	725348.147988	235798.729758	7.190	3.556	6.868	4.784
O10	694269.889040	228610.917000	4.830	3.81	3.642	6.187
O13	705431.001880	220697.610715	7.430	7.62	10.201	10.293
O16	693745.730000	252604.490000	1.160	2.794	0.000	2.954
O19	722772.817043	220375.078922	12.150	7.62	14.407	8.686
O22	736583.384861	221238.316631	5.170	4.572	4.153	3.463
O26	702230.480000	220046.830000	11.220	5.588	11.431	9.481
O28	694588.732145	213376.137195	8.140	3.556	8.625	7.376
W 2	708078.587107	194300.186312	7.880	3.302	1.670	6.736
W16	734607.714135	203484.977237	6.690	4.826	3.287	5.899
W22	727993.648094	195084.345910	15.590	8.128	10.800	5.651
W25	732161.441554	213556.429868	4.890	3.048	3.960	4.263
W27	726187.905777	204715.689118	4.870	1.27	3.783	6.484
W19	743359.426259	202028.896272	12.470	6.35	7.347	6.049
W35	732220.832480	179084.258487	1.800	2.032	1.698	6.094
W42	754665.813608	213426.186194	5.330	7.366	9.513	5.650
W43	733804.150235	197470.094732	10.870	7.874	9.276	6.563
W45	736866.940000	197018.930000	11.780	8.636	12.480	6.398

Appendix V
Various SEMCOG Precipitation Data
(Precipitation Event 09/14/2000)

Station ID	X	Y	NEXRAD mm	Gage_mm	ANN mm	OC mm
A 3	661857.143789	192530.880673	10.730	15.24	13.990	10.068
L 3	668047.850000	241521.480000	10.320	19.558	13.502	13.738
L 7	681514.971760	222057.746602	9.400	17.78	12.027	11.049
L10	658405.618120	224659.693526	13.260	18.034	14.443	10.217
M 2	756937.449154	232773.992790	8.420	10.668	9.228	7.817
M 4	762562.920492	230609.680239	7.600	9.144	8.084	7.656
M 8	746972.860607	254820.071250	7.070	17.272	9.307	8.574
M 9	742960.436068	231431.293091	6.890	13.208	11.867	7.726
M10	749986.779148	230140.273915	8.540	13.462	10.172	7.185
M12	765223.606768	256122.039071	8.640	11.176	9.369	7.488
M14	765682.093654	241381.302807	7.920	13.716	12.865	8.259
M16	755400.233316	223825.771085	5.970	8.636	7.322	7.101
M17	744337.430006	224781.756367	6.790	11.684	7.922	6.483
O 3	735369.246078	230672.594422	6.960	16.256	10.112	7.312
O 4	734168.924612	255016.775493	8.720	17.78	11.060	11.802
O 5	713090.146295	246701.551082	18.090	18.796	17.212	12.521
O 9	726130.235853	247275.671191	14.830	17.018	11.889	11.819
O18	731346.206049	216707.947915	5.820	7.112	7.749	5.832
O24	715654.088076	215086.283082	5.380	17.526	10.073	7.504
O25	731861.017503	225830.555575	6.190	14.478	9.681	6.838
W 8	732252.549782	197942.319261	5.350	7.112	5.160	5.596
W14	753133.344245	209696.295155	7.710	5.334	6.139	7.131
W15	750220.740000	206719.180000	7.880	6.35	6.480	7.272
W18	745604.881900	214856.586919	6.410	9.144	6.888	6.590
W23	724714.028432	197970.368012	4.860	7.62	5.653	5.618
W31	756733.163365	214398.086719	6.440	6.096	7.986	5.975
W33	755386.272117	215582.872187	5.550	7.112	5.883	6.439
W48	709614.370019	201814.621439	6.520	10.922	7.829	5.638
A 1	678039.980433	195924.936908	10.460	12.192	12.640	9.246
A 2	663120.262649	212553.141409	14.690	16.764	18.059	11.595
A 5	695810.135030	191348.250416	8.220	9.906	10.778	7.511
L 1	656935.798800	236936.068948	10.650	23.622	12.779	12.024
L 2	655307.791088	245383.380983	8.750	22.098	12.085	11.902
L 5	655433.651803	217957.872282	11.780	15.748	15.041	12.744
L 6	680819.554474	212103.804745	9.450	17.78	15.787	9.336
L 8	683827.288566	245447.601664	9.450	20.066	10.759	12.285
L 9	685117.095706	233972.632310	10.680	23.622	13.466	11.048
L11	671537.470375	229482.547174	13.210	17.526	15.151	10.873
M 1	754439.740000	258799.090000	8.950	19.05	19.050	7.881
M 5	756874.108802	227770.456845	6.070	8.89	12.123	7.244
M 7	739614.099028	250112.456291	7.670	19.558	14.735	8.311
M18	745887.380000	226750.870000	6.970	13.97	13.433	7.142
M3	753509.666411	218106.538937	5.550	10.16	7.555	5.788
O 2	730402.927052	221676.374291	6.190	16.002	10.679	6.008
O 7	717831.717332	237839.089634	16.400	21.844	24.460	13.645
O 8	725348.147988	235798.729758	14.450	17.018	17.656	11.025
O10	694269.889040	228610.917000	8.740	20.32	16.768	10.674
O13	705431.001880	220697.610715	14.670	16.764	18.590	8.614
O16	693745.730000	252604.490000	9.470	19.304	15.480	14.321
O19	722772.817043	220375.078922	16.720	14.478	16.299	6.382
O20	736063.852221	218411.644446	6.370	11.176	11.692	6.106
O26	702230.480000	220046.830000	14.500	16.764	16.973	8.699
O28	694588.732145	213376.137195	7.010	15.494	10.729	8.326
W 2	708078.587107	194300.186312	7.250	10.16	9.458	6.456
W16	734607.714135	203484.977237	5.350	9.652	7.936	5.745
W22	727993.648094	195084.345910	5.580	6.858	5.755	5.152
W25	732161.441554	213556.429868	5.930	12.954	9.046	5.786
W27	726187.905777	204715.689118	4.860	9.906	6.704	5.253
W29	742837.828788	203183.424168	8.690	6.604	8.161	6.741
W35	732220.832480	179084.258487	3.430	2.794	4.214	5.954
W42	754665.813608	213426.186194	6.230	7.112	8.125	6.470
W43	733804.150235	197470.094732	6.120	2.794	5.549	5.531
W45	736866.940000	197018.930000	6.920	8.382	7.350	5.884

Appendix W
Various Michigan Precipitation Data
(Precipitation Event 05/06/1999)

Station Name	NEXRAD_mm	Gage_mm	ANN_mm
Kenton	20.320	15.000	16.162
SSMarie	4.572	4.340	4.688
Newberry	12.700	11.780	12.769
Iron Moutain	43.180	27.390	31.194
Bellaire	0.000	2.670	4.465
Alpena	2.794	1.960	3.187
TravCity	5.080	3.100	3.219
Gladwin	10.160	16.600	8.999
Cass City	2.540	2.120	2.702
Montague	7.620	7.020	7.729
Vassar	0.000	4.700	3.510
Grand Rapids	2.286	2.160	0.803
Jackson	0.000	6.160	4.549
Ypsilanti	0.000	0.000	1.831
Detroit Met	0.254	0.250	0.000
South Bend	3.810	3.790	3.616
Copper Harbor	11.100	20.320	7.091
Wakefield	5.370	12.700	5.461
Gwinn	3.510	15.240	9.515
Trout Lake	3.130	7.620	2.045
Glennie Alcona	4.420	7.620	3.644
Houghton Lake	5.350	6.350	6.266
Muskegon	5.040	6.858	5.623
Kent City	0.380	0.000	2.193
Grand Haven	3.620	5.080	6.488
Owosso	6.180	5.080	5.311
Flint	5.320	5.334	4.609
Lansing	3.550	3.556	4.132
Howell	2.590	2.540	4.205
Coldwater	4.060	0.000	2.459
Toledo	0.000	1.270	0.114

Appendix X
Various Michigan Precipitation Data
(Precipitation Event 05/17/1999)

Station Name	NEXRAD_mm	Gage_mm	ANN_mm
Kenton	30.480	10.830	20.797
SSMarie	5.842	2.550	5.884
Newberry	10.160	4.290	5.491
Iron Mountain	38.100	22.030	28.669
Bellaire	2.540	5.080	4.701
Alpena	3.810	3.540	6.975
TravCity	5.080	6.860	6.721
Gladwin	17.780	23.310	20.431
Cass City	15.240	20.210	22.678
Montague	10.160	13.950	11.707
Vassar	12.700	19.260	19.888
Grand Rapids	0.000	4.540	6.376
Jackson	7.620	15.380	21.009
Ypsilanti	20.320	43.540	32.963
Detroit Met	14.986	14.960	25.960
South Bend	5.080	5.070	4.459
Copper Harbor	3.250	20.320	26.383
Wakefield	6.810	0.000	0.000
Gwinn	7.120	33.020	21.461
Trout Lake	5.390	10.160	4.487
Glennie Alcona	4.860	7.620	9.772
Houghton Lake	21.770	18.542	16.395
Muskegon	4.380	3.556	3.768
Kent City	9.690	17.780	10.078
Grand Haven	4.510	10.160	3.649
Flint	6.590	6.604	11.013
Lansing	9.380	9.398	8.513
Howell	7.250	10.160	16.702
Coldwater	20.720	12.700	23.228
Toledo	39.390	27.686	25.538

Appendix Y
Various Michigan Precipitation Data
(Precipitation Event 05/28/1999)

Station Name	NEXRAD_mm	Gage_mm	ANN_mm
SSMarie	0.000	0.000	0.127
Newberry	0.000	0.000	0.000
Detour Village	0.000	0.000	0.000
Iron Mountain	7.000	0.000	0.942
Vanderbilt	0.000	0.000	0.000
Bellaire	0.000	0.000	0.623
Alpena	0.390	0.000	0.322
TravCity	0.000	0.000	0.000
Gladwin	0.000	0.000	0.443
Cass City	0.000	0.000	0.000
Vassar	0.000	0.000	0.000
Grand Rapids	23.090	23.114	23.390
Jackson	20.730	0.000	8.026
Ypsilanti	16.130	12.700	16.877
Detroit Met	14.450	14.986	13.696
South Bend	17.500	18.288	18.985
Wakefield	1.540	2.540	0.550
Gwinn	0.000	0.000	0.000
Trout Lake	0.000	0.000	0.000
Glennie Alcona	0.000	0.000	0.361
Houghton Lake	0.000	0.000	0.302
Harbor Beach	0.000	0.000	0.297
Muskegon	19.930	27.178	12.866
Grand Haven	22.170	33.020	19.584
Lansing	16.470	16.510	11.791
Howell	17.520	17.780	14.469
Coldwater	15.240	38.100	21.744
Toledo	42.190	34.798	29.259

147

Appendix Z
Various Michigan Precipitation Data
(Precipitation Event 07/01/1999)

Station Name	NEXRAD_mm	Gage_mm	ANN_mm
Gwinn	4.280	30.480	11.089
SSMarie	1.020	12.446	7.151
Trout Lake	0.800	15.240	13.839
Escanaba	5.940	33.020	11.069
Vanderbilt	3.560	10.160	5.941
Glennie Alcona	2.350	12.700	8.149
Gladwin	16.000	10.160	16.276
Harbor Beach	17.660	43.180	38.899
Allegan	7.210	17.780	8.953
Howell	18.950	38.100	32.574
Jackson	22.360	35.560	32.395
Ypsilanti	8.760	20.320	18.644
South Bend	53.310	53.086	35.027
Coldwater	26.900	40.640	25.189
Copper Harbor	2.850	0.000	0.058
Kenton	7.810	12.700	2.003
Newberry	2.450	12.700	8.980
Detour Village	2.240	0.000	1.869
Iron Mountain	6.580	10.160	1.615
Bellaire	1.820	10.160	4.221
Alpena	4.240	6.858	2.039
TravCity	12.360	10.160	5.056
Houghton Lake	4.420	5.842	5.199
Montague	1.380	0.000	0.000
Cass City	10.550	0.000	6.519
Kent City	3.440	2.540	0.000
Grand Haven	6.020	10.160	7.887
Detroit Met	10.890	11.430	10.312

Appendix AA
Various Michigan Precipitation Data
(Precipitation Event 07/31/1999)

Station Name	NEXRAD_4km	Gage	ANN_mm
Ontonago	0.000	2.540	0.491
Kenton	0.000	0.000	0.941
SSMarie	12.170	15.748	10.072
Newberry	21.250	17.780	18.464
Detour Village	20.190	0.000	0.000
Iron Moutain	0.640	0.000	0.000
Bellaire	16.700	17.780	14.051
Alpena	4.620	0.508	4.416
TravCity	13.290	12.700	13.725
Cass City	0.000	0.000	1.404
Montague	0.000	0.000	0.923
Grand Rapids	0.000	0.000	0.341
Jackson	8.370	10.160	12.413
Ypsilanti	3.610	2.540	5.522
Detroit Met	12.180	12.192	11.896
South Bend	1.250	1.270	1.474
Copper Harbor	0.000	2.540	0.000
Wakefield	0.000	0.000	2.475
Trout Lake	54.760	53.340	45.692
Escanaba	4.760	0.000	0.000
Glennie Alcona	0.790	0.000	0.568
Houghton Lake	0.750	0.508	4.222
Harbor Beach	0.000	0.000	0.000
Muskegon	0.000	0.000	2.188
Kent City	0.000	0.000	2.306
Grand Haven	0.000	0.000	2.080
Flint	0.000	0.000	0.000
Lansing	0.000	0.000	0.008
Allegan	0.980	0.000	0.000
Howell	14.510	12.700	5.376
Coldwater	3.940	0.000	11.937
Toledo	0.000	0.000	3.299

Appendix AB
Various Michigan Precipitation Data
(Precipitation Event 09/14/2000)

Station Name	NEXRAD_mm	Gage_mm	ANN_mm
SSMarie	0.000	0.000	0.000
Newberry	19.380	15.240	3.100
Detour Village	0.000	0.000	1.433
Vanderbilt	0.000	5.080	4.436
Bellaire	1.480	10.160	0.000
Alpena	3.070	2.540	1.766
TravCity	3.030	0.000	0.000
Gladwin	8.790	7.620	11.189
Grand Rapids	14.940	17.780	6.443
Jackson	8.110	2.540	4.609
Ypsilanti	8.220	5.080	3.284
South Bend	4.300	27.940	9.765
Copper Harbor	0.000	0.000	0.000
Muskegon	11.610	22.860	16.717
Grand Haven	2.520	10.160	13.698
Allegan	8.040	12.700	10.895
Coldwater	2.950	7.112	9.584
Toledo	5.220	27.940	25.712